Mechanisms of Efferent Postsynaptic Assembly in Cochlear Hair Cells

A thesis

submitted by

Elizabeth Kathryn Storer

In partial fulfillment of the requirements
for the degree of

Doctor of Philosophy

in

Neuroscience

TUFTS UNIVERSITY

Sackler School of Graduate Biomedical Sciences

February, 2012

Adviser: Michele H. Jacob, Ph.D.

Abstract

Sensory hair cells in the cochlea are innervated by efferent olivocochlear neurons that originate in the superior olivary complex of the brainstem. These cholinergic synapses regulate auditory sensitivity and frequency selectivity by suppressing the electromotile activity of hair cells that amplifies sound signals transmitted to the brain. Cholinergic signals in the postsynaptic hair cell are inhibitory, mediated by Ca^{2+}-permeable α9/10 nicotinic acetylcholine receptors (α9/10-nAChRs) that are functionally coupled to small-conductance Ca^{2+}-activated potassium (SK2) channels. Ca^{2+} influx through α9/10-nAChRs rapidly activates nearby SK2 channels, resulting in hair cell hyperpolarization and suppression of electromotile sound amplification. Olivocochlear synapse activity in hair cells is critical for normal responses to sound and provides protection against noise overexposure.

The processes that direct the assembly and function of nicotinic synapses in hair cells are not well understood. The goal of the studies presented here is to identify novel proteins and mechanisms that underlie the development of hair cell synapses and the proper localization and functional coupling of α9/10-nAChRs and SK2 channels. We first characterize the protein composition of postsynaptic sites in hair cells and show that this unusual nicotinic synapse shares common components with nicotinic synapses elsewhere in the nervous system. We also explore mechanisms and protein interactions that direct the co-localization of α9/10-nAChRs and SK2 channels at the postsynaptic membrane. Phenotypic

comparison of mice lacking α9 or α10-nAChR subunits or SK2 channels has previously suggested that the SK2 channel is particularly important for the functional synaptic localization of α9/10-nAChRs. In support of these prior studies, we show that α9/10-nAChRs and SK2 channels interact with one another in a heterologous cell expression system and demonstrate that the membrane expression of α9/10-nAChRs is correlated with the presence and membrane expression of SK2 channels. We also identify α-actinin-1 as a binding partner of SK2 channels in hair cells.

We present evidence of two novel mechanisms by which hair cells may regulate the nAChR-SK2 postsynaptic complex. We first demonstrate that alternative splicing of the SK2 channel alters its protein interactions and surface expression. We further show that Ca^{2+} differentially affects the interactions of SK2 splice variants with α9/10-nAChRs and α-actinin-1, suggesting that postsynaptic Ca^{2+} signaling represents another mechanism to modulate the function or localization of nAChRs and SK2 channels. Finally, we identify two additional binding partners of SK2 channels and α9/10-nAChRs that may serve as adapter protein linkages to the postsynaptic protein complex. Overall, our studies provide new insights into the molecular organization of nicotinic synapses in cochlear hair cells and indicate that multiple protein interactions and processes contribute to the coupling and regulation of α9/10-nAChRs and SK2 channels.

Table of Contents

Table of Figures

Chapter 1

Introduction

The mammalian organ of Corti

Hair cells and auditory transduction

The organ of Corti is the functional unit of hearing in the mammalian inner ear. This sensory epithelium rests on the basilar membrane that extends in a spiral shape from the base to the apex of the coiled, fluid-filled cochlear duct (Figure 1.1a, b). Sound waves transmitted from the environment into the fluid within the cochlea displace the basilar membrane and organ of Corti at a frequency-specific location, with high-frequency sounds detected at the base of the cochlear spiral and low-frequencies detected at the apex. The frequency mapping of the organ of Corti is due, in part, to a stiffness gradient along the length of the basilar membrane, such that specific sound frequencies elicit maximal vibration of the basilar membrane at specific locations (Emadi et al., 2004; Fettiplace and Hackney, 2006). Motion of the basilar membrane causes the depolarization of inner hair cells (IHCs) and outer hair cells (OHCs) within the organ of Corti. Stereocilia bundles at the apical end of OHCs are embedded in the tectorial membrane above the organ of Corti, creating a shearing motion that rhythmically deflects the hair bundles as the basilar membrane and organ of Corti vibrate with the traveling sound wave (Figure 1.1c). These frequency-driven hair bundle deflections open and close cation-permeable mechanoelectric transduction channels, generating cyclic depolarizations in the hair cell and thereby translating fluid sound waves into electrical fluctuations across the hair cell membrane. (Dallos, 1992; Fettiplace and Hackney, 2006)

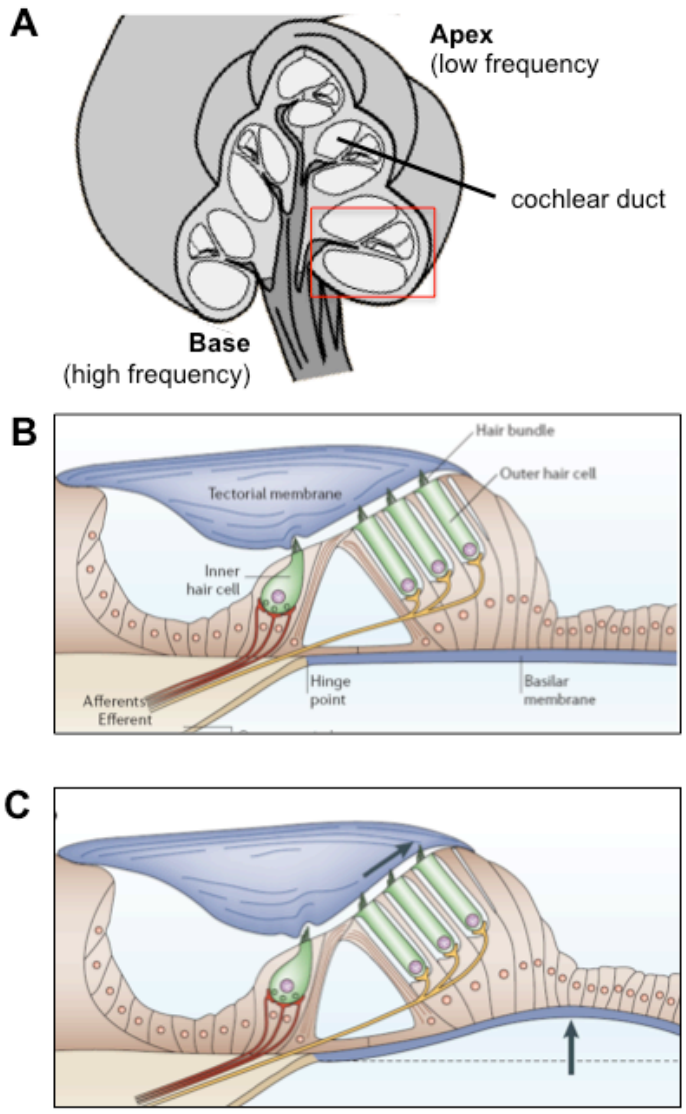

Figure 1.1: The mammalian organ of Corti.
(A) Schematic cross-section of the mammalian cochlea. Modified from http://hyperphysics.phy-astr.gsu.edu/hbase/sound/cochlea.html. Boxed region: cross section of the organ of Corti (B) showing inner and outer hair cells with afferent and efferent innervation. (C) Sound wave-induced basilar membrane motion causes deflection of hair bundles embedded in the tectorial membrane and opening of mechanoelectric transduction channels. Modified from (Fettiplace and Hackney, 2006)

Outer hair cells and the cochlear amplifier

The two types of hair cells within the organ of Corti serve distinct functions in sound detection, transmission, and amplification. IHCs communicate sound signals to the brain through voltage-dependent glutamate release onto dendrites of afferent spiral ganglion neurons. OHCs, by contrast, receive few afferent contacts and do not participate significantly in sound detection. Whereas hair bundle-driven voltage fluctuations in IHCs are translated into synaptic signals, in OHCs these fluctuations drive active mechanisms that enhance sound detection by IHCs. Force generated from these active processes can be detected as acoustic signals, or otoacoustic emissions, retrogradely transmitted from the cochlea to the middle ear and ear canal (Kemp, 1978; Wilson, 1980). One mechanism of amplification occurs through OHC electromotility. Isolated OHCs change their shape in response to voltage changes, shortening when depolarized and lengthening when hyperpolarized (Ashmore, 1987; Brownell et al., 1985). OHC somatic motility requires prestin, a voltage-sensitive protein expressed at high levels in the hair cell lateral membrane (Belyantseva et al., 2000; Zheng et al., 2000). Prestin binds and releases chloride ions in a voltage-dependent manner, triggering conformational changes in the surface area of prestin within the hair cell membrane that elongate or contract the cell on a cycle-by-cycle basis with hair bundle-driven periodic voltage fluctuations (Oliver et al., 2001a; Song and Santos-Sacchi, 2010). These expansion-contraction cycles amplify basilar membrane vibrations (Brownell et al., 1985).

A second mechanism of sound amplification by OHCs is derived from active forces generated by the hair bundle. When hair bundles are deflected and mechanoelectric transduction channels are opened, the resulting Ca^{2+} influx triggers the re-closing of the channels, which in turn causes stereocilia to “twitch” back to their original position (Benser et al., 1996; Ricci et al., 2000). Active hair bundle movement has been observed spontaneously in isolated hair cells, or in response to mechanical bundle deflection or current application (Brix and Manley, 1994; Crawford and Fettiplace, 1985; Kennedy et al., 2005; Ricci et al., 2000). Although these hair bundle-derived forces are thought to be small relative to forces generated by hair cell electromotility, they are believed to contribute to active mechanical sound amplification in mammalian species and be the primary source of active amplification in non-mammalian vertebrates , which do not demonstrate hair cell somatic electromotility (Chan and Hudspeth, 2005; He et al., 2003; Kennedy et al., 2005).

In summary, voltage-dependent somatic and hair bundle motility mechanisms in mammalian OHCs generate forces that amplify the local vibrations within the organ of Corti and, consequently, amplify frequency-specific sound signal detection by IHCs. Ablation of OHCs or genetic knockdown of prestin dramatically reduces hearing sensitivity and frequency tuning, underscoring the importance of OHC-derived amplification for normal sound detection (Dallos and Harris, 1978; Liberman et al., 2002; Ryan and Dallos, 1975).

Olivocochlear inhibition of hair cells

Mechanism

Cochlear hair cells are innervated by olivocochlear neurons located in the superior olivary complex of the brainstem. Efferent fibers originating in the medial and rostral superior olivary complex (MOC) neurons directly innervate OHCs (Figure 1.1), and lateral area of the superior olivary complex (LOCs) innervate the afferent spiral ganglion neuron dendrites that contact IHCs (Warr and Guinan, 1979). Olivocochlear inputs to hair cells are mainly cholinergic (Norris and Guth, 1974). Cholinergic transmission in hair cells is inhibitory, mediated by a unique, rapid coupling mechanism between heteromeric, Ca^{2+}-permeable α9/10 nicotinic acetylcholine receptors (nAChRs) and Ca^{2+}-sensitive small-conductance potassium (SK2) channels (Elgoyhen et al., 1994; Elgoyhen et al., 2001; Oliver et al., 2000). Acetylcholine (ACh) release from efferent terminals elicits biphasic responses in hair cells, consisting of a brief, nAChR-derived depolarization followed by a larger, SK2-mediated hyperpolarization (Glowatzki and Fuchs, 2000; Oliver et al., 2000).

Olivocochlear development

The development of mature olivocochlear innervation occurs during the first 12-16 days of postnatal development in rodents. Although efferent olivocochlear fibers form direct contacts almost exclusively with OHCs in the mature cochlea, developing efferents form temporary synapses directly onto IHCs shortly after birth, before the onset of hearing (Bruce et al., 2000; Simmons et al., 1996).

Immature IHCs express α9/10-nAChRs and SK2 channels and respond to efferent stimulation or exogenous acetylcholine application with biphasic responses characteristic of functionally coupled α9/10-nAChRs and SK2 channels (Glowatzki and Fuchs, 2000; Morley and Simmons, 2002; Simmons and Morley, 1998). These responses can be detected at P1-P3 and continue through the onset of hearing at approximately P12 (Uziel et al., 1981), at which time responses to acetylcholine begin to decline; by P14-P16, IHCs display a complete loss of cholinergic sensitivity (Katz et al., 2004; Marcotti et al., 2004). This change coincides both with the loss of axosomatic efferent contacts and with the loss of α10-nAChR and SK2 channel expression from IHCs, though α9-nAChRs continue to be expressed in adulthood (Katz et al., 2004; Morley and Simmons, 2002; Simmons and Morley, 1998). Meanwhile, efferent fibers contact OHCs beginning at approximately P4, and cholinergic sensitivity can be observed beginning at P6 (Bruce et al., 2000; Dulon and Lenoir, 1996; He and Dallos, 1999; Roux et al., 2011; Simmons et al., 1996).

Transient IHC innervation from olivocochlear contacts seems to contribute to the developmental regulation of temporary Ca^{2+}-mediated action potentials in immature IHCs that are essential for the development of mature vesicle exocytosis and afferent innervation patterns (Glowatzki and Fuchs, 2000; Johnson et al., 2007; Johnson et al., 2011; Marcotti et al., 2004). Sectioning the olivocochlear bundle shortly after birth has been reported to result in abnormal spiking patterns in pre-hearing auditory nerve fibers, disruption of afferent innervation to both OHCs and IHCs, and elevated auditory detection thresholds

in the adult animal (Elgoyhen et al., 2009; Pujol and Carlier, 1982; Walsh et al., 1998).

Functional effects of olivocochlear inhibition

Sensitivity and frequency selectivity

Hyperpolarization of OHCs by olivocochlear signaling provides an inhibitory feedback mechanism that modulates frequency-specific sound sensitivity by regulating the OHC-based cochlear amplifier. OHC hyperpolarization resulting from stimulation of efferent fibers suppresses their inherent electromotile responses to sound and their amplification of basilar membrane vibration (Brown and Nuttall, 1984; Murugasu and Russell, 1996). This loss of amplification results in the suppression of depolarizing currents in IHCs, which in turn reduces the amplitude of sound-evoked compound action potentials in afferent fibers and elevates sound detection thresholds (Brown and Nuttall, 1984; Galambos, 1956). Thus, olivocochlear feedback in the cochlea dampens the detection of sound signals at specific frequencies by suppressing OHC activity, providing a mechanism for the control of hearing sensitivity and frequency selectivity. Olivocochlear activity enhances sound detection in background noise; auditory nerve responses to tones masked by background noise were increased by olivocochlear fiber stimulation, indicating that olivocochlear feedback suppresses low-level background noise (Kawase et al., 1993; Winslow and Sachs, 1987).

Protection against noise damage

Efferent inhibition also provides protection against noise overexposure that results in hair cell trauma and hearing loss. Stimulation of olivocochlear efferents attenuates the temporary increases in auditory nerve response thresholds that occur in response to high-intensity noise (Rajan, 1990; Reiter and Liberman, 1995) whereas sectioning the olivocochlear bundle results in increased susceptibility to both temporary and permanent threshold shifts and hair cell loss (Kujawa and Liberman, 1997; Zheng et al., 1997a; Zheng et al., 1997b). These effects are dependent on cholinergic transmission in OHCs, as demonstrated by the effects of α9-nAChR manipulation on susceptibility to noise-induced hearing damage. Mice that overexpress α9-nAChRs, or express a sensitized α9 mutant that enhances efferent inhibition of auditory sensitivity, exhibit significantly reduced temporary and permanent auditory threshold shifts after noise overexposure (Maison et al., 2002; Taranda et al., 2009b). Individual variability in α9-nAChR expression levels has also been associated with susceptibility to noise damage, such that guinea pigs with higher endogenous expression of α9 display greater effects of efferent stimulation and are less susceptible to noise overexposure (Luebke and Foster, 2002). Overexpression of SK2 channels, by contrast, increases the fast suppressive effects of olivocochlear activation on cochlear responses but provides no protection against permanent hearing threshold shifts following noise damage. These results indicate that the protective effects of cholinergic transmission are likely unrelated to SK2-mediated fast hair cell inhibition and may instead by achieved through alternate downstream effects

of nAChR Ca^{2+} currents (Maison et al., 2007). As discussed below, Ca^{2+}-induced Ca^{2+} release from subsurface cisternae may be involved in the role of α9/10-nAChRs in protection against noise-induced injury.

The role of Ca^{2+}-induced Ca^{2+} release in efferent inhibition

In addition to the rapid, direct activation of co-localized SK2 channels, Ca^{2+} influx through α9/10-nAChRs also induces Ca^{2+}-induced Ca^{2+} release (CICR) from a specialized subsynaptic cistern closely apposed to the postsynaptic membrane in mammalian and chicken hair cells (Martin and Fuchs, 1992; Saito, 1980). Fluorescent Ca^{2+} imaging experiments have demonstrated that cholinergic agonists elicit rapid Ca^{2+} transients originating at the synaptic pole of outer hair cells that occur simultaneously with hyperpolarizing potassium currents (Evans et al., 2000). Ryanodine receptors are associated with the postsynaptic cistern in outer hair cells (Grant et al., 2006; Lioudyno et al., 2004), and application of ryanodine or other CICR agonists enhances ACh-evoked potassium currents and efferent-induced suppression of afferent activity (Evans et al., 2000; Sridhar et al., 1997). However, the specific contribution or possible requirement for CICR in shaping IPSCs and efferent inhibition is difficult to assess due to multiple, concentration-dependent effects of ryanodine. Ryanodine acts as a CICR agonist and amplifies acetylcholine-evoked IPSCs at low concentrations (Lioudyno et al., 2004; Sridhar et al., 1997); at high concentrations, however, ryanodine blocks CICR but potentiates α9/10-nAChR-mediated Ca^{2+} currents by enhancing the receptor's sensitivity to acetylcholine

(Lioudyno et al., 2004; Zorrilla de San Martin et al., 2007). In one study, high concentrations of ryanodine that likely block RyRs and inhibit CICR reduced IPSC amplitude by approximately 30%. Interestingly, although IPSC amplitude was decreased, IPSC time course was unaffected, suggesting that α9/10-nAChRs and SK2 channels are tightly coupled to RyR-mediated Ca^{2+} signals (Lioudyno et al., 2004). In a separate study, however, the same concentration of ryanodine increased the affinity of α9/10-nAChRs for acetylcholine and thereby amplified acetylcholine induced Ca^{2+} entry and prolonged acetylcholine-evoked IPSCs (Zorrilla de San Martin et al., 2007). Thus, these conflicting studies indicate that the enhancement of nAChR activation versus inhibition of CICR by high concentrations of ryanodine may depend on specific experimental conditions. Overall, however, studies of CICR in hair cells indicate that Ca^{2+} influx through α9/10-nAChRs may activate SK2 channels directly, through tightly localized Ca^{2+} diffusion, and indirectly, through CICR from subsynaptic Ca^{2+} stores. The relative contributions of direct nAChR-SK2 coupling and CICR to fast, SK2-mediated hair cell inhibition are not yet clear.

The fast inhibition of sound-induced afferent nerve activity by efferent cholinergic transmission in hair cells is thought to occur through SK2 channel activation, but can be enhanced by CICR (Sridhar et al., 1997). In addition to this fast effect, α9/10-nAChR activation and subsequent CICR elicit a slow suppression of sound-induced afferent activity that occurs mainly with high frequency acoustic stimuli (Sridhar et al., 1997; Sridhar et al., 1995). In contrast to fast inhibition, which occurs within 50-100 milliseconds of efferent fiber

stimulation and decays quickly, the “slow effect” appears as a gradual reduction in afferent activity that occurs over tens of seconds following onset of efferent stimulation and lasts for minutes after olivocochlear stimulation ceases (Sridhar et al., 1995). Sridhar et al. (1997) propose that CICR enables slow suppressive effects by producing a gradual increase in hair cell Ca^{2+} levels through Ca^{2+} release from subsurface cisternae that line the basolateral membranes. The accumulation of Ca^{2+} between the cell membrane and subsurface cisternae may then trigger slow hyperpolarizating effects by activating large-conductance BK-type potassium channels localized outside of the postsynaptic region. The slow suppressive effect declines within 1-2 minutes of continued efferent stimulation; this decline may be caused by depletion of Ca^{2+} stores or by Ca^{2+} reuptake by SERCA Ca^{2+}-ATPases, as inhibition of SERCA activity amplified and prolonged the slow component of cochlear suppression (Sridhar et al., 1997; Sridhar et al., 1995).

In contrast to the slow effect, fast suppression of afferent transmission can be maintained over longer periods of efferent stimulation (Sridhar et al., 1995). The fast effect is thought to be attributable to the direct activation of SK2 by Ca^{2+} diffusion from closely co-localized α9/10-nAChRs; thus, it can be enhanced by Ca^{2+} release from internal stores but is maintained even as CICR-evoked Ca^{2+} waves are buffered or if internal Ca^{2+} stores are depleted (Evans et al., 2000; Sridhar et al., 1997).

Some evidence exists to support the notion that slow efferent inhibition and CICR are important for protection against noise-induced hearing loss. Stimulation

of efferent fibers was shown to reduce the shift in auditory nerve thresholds following noise overexposure; this protective effect occurred specifically with overexposure to high-frequency acoustic stimuli for short time periods, conditions which are known to induce slow hair cell suppression (Reiter and Liberman, 1995). Thus, these circumstantial data imply that noise protection provided by efferent cholinergic innervation is related to slow, CICR-mediated hair cell inhibition. The observation that SK2 channel overexpression enhances the fast suppression of cochlear responses by efferent fiber stimulation but does not provide protection against noise-induced afferent threshold shifts further suggests that noise protection is associated with slow suppressive effects that are independent of SK2 channel activation (Maison et al., 2007). The precise mechanisms that underlie these protective effects are unclear. However, prolonged Ca^{2+} transients resulting from α9/10-nAChR activation and CICR have been suggested to provide protection against noise overexposure by activating Ca^{2+}-dependent signaling pathways that may regulate the stiffness of the hair cell membrane (Cooper and Guinan, 2003), the structure of the underlying cytoskeleton (Zhang et al., 2003), and phosphorylation of the prestin motor protein and other hair cell proteins (Sziklai et al., 2001), changes which may in turn limit hair cell electromotile responses and protect the organ of Corti against noise-induced damage (Maison et al., 2007). Thus, CICR may provide an important mechanism for the protective effects of olivocochlear cholinergic input and α9/10-nAChR activation against noise overexposure.

The avian basilar papilla

Structure

The basilar papilla is the functional unit of hearing in avians and the equivalent of the mammalian organ of Corti. The basilar papilla is a long, flat epithelium that extends along the length of the tube-shaped, fluid-filled cochlear duct and narrows from the apical to the basal end (Figure 1.2). The basilar papilla, like the organ of Corti, shows tonotopic organization, with high frequencies detected at the base and low frequencies detected at the apex (Manley, 1989). Similar to the organ of Corti, the avian basilar papilla also contains two types of hair cells that receive afferent as well as efferent innervation, though the segregation of hair cell type, function, and innervation pattern is less distinct. Unlike the organ of Corti, which features distinct populations of inner and outer hair cells with largely distinct functions and innervation patterns, hair cells in the avian cochlea transition gradually between two extremes: tall hair cells located at the neural side of the sensory epithelium, closest to the afferent spiral ganglion; and short hair cells located at the abneural side (Hirokawa, 1978b; Takasaka and Smith, 1971). The relative abundance of tall and short hair cells varies along the length of the basilar papilla, with a greater proportion of tall hair cells at the apical, low-frequency end transitioning to a greater prevalence of short hair cells at the basal, high-frequency end (Figure 1.2a) (Fischer, 1992; Manley, 1989). Similar to mammalian IHCs, tall hair

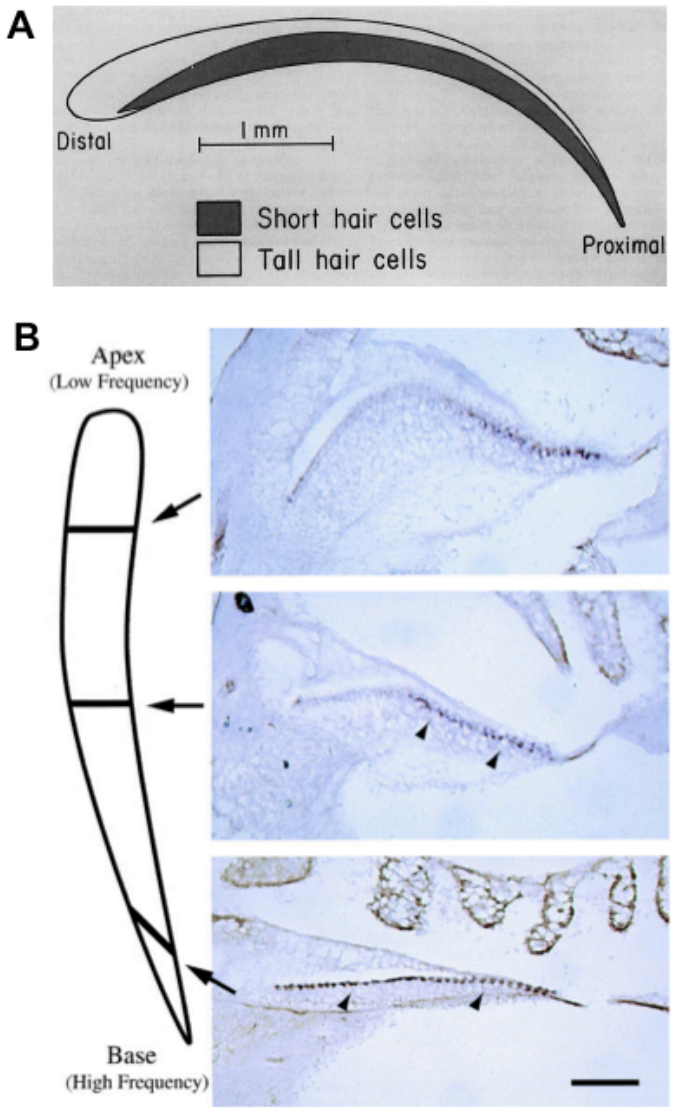

Figure 1.2: The avian basilar papilla.
(A) Schematic overview of the basilar papilla, with tall (inner-like) hair cells predominating at the distal (apical) region and short (outer-like) hair cells at the proximal (basal) region. Source: (Tanaka and Smith, 1978). (B) Cross-sections of the basilar papilla at basal, medial, and apical locations showing localization of α9-nAChRs in short hair cells by *in situ* hybridization (arrowheads) (Hiel et al., 2000).

cells are contacted mainly by afferent cochlear ganglion neurites, indicating that IHCs are primarily responsible for sound transmission, whereas short hair cells, similar to OHCs, receive significantly less afferent innervation and are thought to provide a mechanical sound amplification mechanism similar to that of mammalian OHCs (Fettiplace and Fuchs, 1999; Manley, 1989; Rebillard and Pujol, 1983; Takasaka and Smith, 1971). The greater prevalence of short hair cells at the basal end of the basilar papilla is consistent with the notion that sound amplification by short hair cells may allow heightened detection of high-frequency sounds (Fettiplace and Fuchs, 1999).

The avian cochlear amplifier

Spontaneous and sound-evoked otoacoustic emissions can be recorded from the avian ear and are abolished by treatment with ototoxic drugs that specifically destroy hair cells, suggesting that hair cells generate active forces similar to those generated in the mammalian cochlea (Chen et al., 2001; Kettembeil et al., 1995). Unlike mammalian OHCs, however, avian hair cells do not show somatic electromotility (He et al., 2003). Early observations of basilar papilla structure suggested that electromotility in avian hair cells is restricted by the supporting cells that completely encase them, in contrast to mammalian OHCs that are contacted by supporting cells only at the base and whose motility is therefore unrestricted (Brownell et al., 1985; Fettiplace and Fuchs, 1999; Zidanic, 2002). However, more recent studies indicate that the lack of hair cell somatic motility is caused by inter-species differences in the voltage-dependent motor capability of

the prestin protein. Mammalian prestins confer somatic motility when exogenously expressed in HEK cells, whereas zebrafish and chicken prestins do not (Tan et al., 2011). Schaechinger and Oliver (2007) propose that electromotility of mammalian prestins may have evolved concurrently with a loss of anion transport function; whereas prestin orthologs in non-mammalian vertebrates function as chloride/divalent anion exchangers, mammalian prestins bind chloride anions but may have lost the ability to bind to extracellular divalent anions, resulting in a truncated transport cycle that confers the conformational changes that permit hair cell somatic motility (Schaechinger and Oliver, 2007; Tan et al., 2011). Because avian hair cells do not demonstrate somatic electromotility, active hair bundle motility is thought to be the primary mechanism by which avian and other non-mammalian vertebrate hair cells generate electromechanical amplification forces (Brix and Manley, 1994; Chen et al., 2001; Sul and Iwasa, 2009).

Olivocochlear innervation

Similar to the mammalian olivocochlear system, the avian basilar papilla is innervated by two distinct populations of efferent olivocochlear neurons. Thick “inferior” olivocochlear efferents form cup-shaped calyx-like synapses on the bases of short hair cells, whereas thinner “superior” fibers form small bouton-shaped synapses onto tall hair cells (Zidanic, 2002). The degree of efferent versus afferent innervation varies both along the width and length of the basilar papilla; short hair cells that are the most prevalent at the base of the epithelium

are innervated nearly exclusively by calyx-type efferent terminals, whereas tall hair cells at the apex display few efferent boutons and are instead innervated mainly by afferent contacts (Fischer, 1992). At intermediate positions along the length of the basilar papilla, tall hair cells contacted by bouton-shaped efferent terminals transition gradually across the width of the epithelium to short hair cells with cup-shaped efferent terminals (Fischer, 1992; Hirokawa, 1978b; Zidanic, 2002). Efferent transmission in short hair cells has been well characterized; like the mammalian olivocochlear system, avian olivocochlear efferents are cholinergic and elicit hyperpolarization of short hair cells through functional coupling between α9/10-nAChRs (Figure 1.2b) and Ca^{2+}-activated SK2 channels (Fuchs and Murrow, 1992a, b; Matthews et al., 2005; Ofsie et al., 1997; Yuhas and Fuchs, 1999). During embryonic development of the avian cochlea, afferent synaptic contacts from the cochlear ganglion appear by embryonic day (E)9 and mature between E11 and E15 (Whitehead and Morest, 1985). Efferent axons innervate the basilar papilla several days later, appearing first at approximately E14 in the tall hair cell region and forming mature synapses on tall and short hair cells between E14 and E18-21 (Hirokawa, 1978a; Rebillard and Pujol, 1983). In summary, although the avian and mammalian cochleae differ in hair cell morphology and organization and their innervation patterns, the distinct functions of tall/inner and short/outer hair cells and the regulation of sound detection by the olivocochlear pathway are largely conserved from avians to mammals.

α9/10-nicotinic acetylcholine receptors

Structure and function

Olivocochlear synapse transmission in hair cells is mediated by α9/10-nAChR heteropentamers composed of two α9 and three α10 subunits (Elgoyhen et al., 2001; Plazas et al., 2005). α9-nAChR subunits are capable of forming functional homopentamers and were originally believed to be the sole cholinergic receptor in hair cells (Elgoyhen et al., 1994). However, more recent evidence indicates that, while α10-nAChRs do not form functional homopentameric receptors alone, their co-assembly with α9 is essential to cholinergic sensitivity in hair cells. The Ca^{2+} sensitivity, desensitization, and current-voltage relationship of ACh-evoked α9/10-nAChR heteropentamer responses more closely resemble native cholinergic responses in hair cells than α9 homopentamers (Elgoyhen et al., 2001). ACh-evoked currents are also significantly greater in *Xenopus laevis* oocytes expressing α9/10- than α9-nAChRs (Elgoyhen et al., 2001), and knockdown of α10 expression in mice results in a nearly complete loss of cholinergic responses in hair cells (Vetter et al., 2007). Hence, the α10-nAChR is a “structural subunit” that shapes the biophysical response of α9/10-nAChRs and may also contribute to its assembly and/or functional membrane localization (Elgoyhen et al., 2001; Vetter et al., 2007).

The α9/10-nAChR pentamer is a unique nicotinic receptor with distinct characteristics compared to other nicotinic acetylcholine receptors. The amino acid sequences of rat α9 and α10-nAChRs share comparatively little sequence homology with other nAChR subunits (Elgoyhen et al., 1994; Elgoyhen et al.,

2001). Pharmacological and structural characteristics of α9/10-nAChRs are also unusual; these receptors share common features with α7-nAChRs in that they are highly Ca^{2+}-permeable, can form pentamers lacking β-subunits, and are blocked by α-bungarotoxin (Elgoyhen et al., 2001; Weisstaub et al., 2002; Lustig, 2006). However, in contrast to other nicotinic receptors, α9-nAChRs and α9/10-nAChRs are blocked rather than activated by nicotine and are blocked by both nicotinic and muscarinic antagonists, suggesting a mixed nicotinic-muscarinic profile (Elgoyhen et al., 2001; Verbitsky et al., 2000). α9/10-nAChR-mediated currents can also be blocked by a variety of other compounds, including other neurotransmitter receptor antagonists such as strychnine, bicuculline, memantine, and the serotonergic antagonist ICS-205,930, as well as endogenous opioid peptides (Elgoyhen et al., 2001; Lioudyno et al., 2002; Oliver et al., 2001b).

Muscle-type nAChRs in the inner ear

In addition to the well-characterized role of α9/10-nAChRs in cholinergic transmission in the cochlea, a recent study has demonstrated that muscle-type nAChRs are transiently expressed in embryonic and early postnatal mouse hair cells (Scheffer et al., 2007). In this study, muscle nAChR α1, β1, δ, and γ subunits were expressed in the cochlea at E17.5-18.5, and the α1 and γ subunits were found in hair cells through P7 and P4, respectively. Co-expression of nicotine-sensitive α1 with α9 and/or α10-nAChRs in oocytes did not alter the biophysical properties of either α9- or α9/10-nAChRs or confer sensitivity to

nicotine, indicating that α1 does not co-assemble with α9/10. However, α1 and γ subunits have previously been demonstrated to form functional channels in *Xenopus* oocytes in the absence of β1 and δ subunits (Liu and Brehm, 1993), raising the possibility that a muscle-type receptor, possibly an α1γ pentamer, may be transiently expressed in hair cells before the onset of hearing. Nicotine sensitivity was not observed in early postnatal mouse hair cells as would be expected if functional muscle-type nAChRs were expressed, though this was only tested at an age by which the γ subunit was no longer expressed. Hence, the presence of functional muscle-type nAChRs and their potential role in the development of afferent or efferent innervation has yet to be demonstrated.

SK2 channels

Structure and Ca^{2+}-gating

Coupling of the Ca^{2+}-permeable α9/10-nAChRs to small conductance Ca^{2+}-activated potassium (SK2) channels is a critical step in efferent inhibition of hair cells. SK2 is one of three members of the SK potassium channel family. SK channels are tetramers; each subunit containing six transmembrane domains, which are highly conserved among the three channel subtypes, and long intracellular N- and C-terminal domains (Kohler et al., 1996; Stocker, 2004). SK channels are not voltage-dependent; instead, they are activated by submicromolar concentrations of Ca^{2+} (Kohler et al., 1996); Ca^{2+}-sensitivity and gating are mediated by binding of calmodulin (CaM) to the intracellular C-terminal (Xia et al., 1998). The SK channel CaM-binding domain, which is also highly

conserved, consists of two antiparallel α-helices, α1 and α2 (Schumacher et al., 2001). CaM has N- and C-terminal lobes, each containing two Ca^{2+}-binding EF hands. The C-lobe of CaM interacts constitutively with the SK channel α1 helix, independently of Ca^{2+} (Xia et al., 1998). Constitutive interaction with CaM allows channel gating to occur very rapidly in the presence of Ca^{2+} and is also essential for SK2 surface expression in heterologous cells (Lee et al., 2003; Xia et al., 1998). Ca^{2+} binding to the EF hands of the CaM N-lobe induces binding of the Ca^{2+}-bound N-lobe to the α2 helix of an adjacent SK subunit, forming an array of two antiparallel CaM molecules linking two antiparallel CaM-binding domains (Schumacher et al., 2001). This arrangement induces conformational changes that open the channel (Keen et al., 1999; Schumacher et al., 2001; Xia et al., 1998). SK channel currents activate quickly upon application of Ca^{2+}, with current onset within 1 millisecond and an activation time constant of approximately 6 milliseconds for SK1 and SK2, and deactivate with a time constant of approximately 30 milliseconds upon withdrawal of Ca^{2+} (Xia et al., 1998). SK channels can be reversibly blocked by the bee venom toxin apamin with different sensitivities; SK2 is the most highly sensitive, followed by SK3 and SK1 (Faber, 2009)

The response of SK2 channels to Ca^{2+} is further modulated by constitutive association of the assembled channels with the protein kinase CK2 and the protein phosphatase PP2A, which fine-tune the Ca^{2+} sensitivity of SK2 channels by regulating the phosphorylation status of CaM (Allen et al., 2007; Bildl et al., 2004). Phosphorylation of CaM by CK2, which occurs only when the channels

are closed, decreases the Ca^{2+} sensitivity of channel gating and accelerates deactivation (Bildl et al., 2004). CK2 activity requires contact with a lysine residue in the intracellular N-terminal of SK2; this contact may be restricted in the open channel conformation, thus providing a possible explanation for the inability of CK2 to phosphorylate CaM when the channels are open. In the open state, CaM dephosphorylation by PP2A restores sub-micromolar Ca^{2+} sensitivity, thus rendering SK2 channels increasingly sensitive to Ca^{2+} (Allen et al., 2007). Thus, the protein complex of SK2, CaM, CK2, and PP2A can dynamically regulate SK2 channel gating in response to changing local concentrations of Ca^{2+} (Allen et al., 2007; Bildl et al., 2004; Fakler and Adelman, 2008).

Ca^{2+}-activation and functions of SK2 channels

In inner hair cells

Numerous studies of SK2 channels in the cochlea, brain, and cardiac muscle show that SK2 can be activated by tight spatial coupling to a wide variety of Ca^{2+} sources. In the developing cochlea, SK2 channels are transiently expressed in inner hair cells, coincidentally with the brief innervation of IHCs by efferent olivocochlear fibers before the onset of hearing (Katz et al., 2004; Marcotti et al., 2004). In these immature IHCs, SK2-mediated hyperpolarizing currents, activated by several different Ca^{2+}-permeable receptors and channels, are necessary to maintain trains of spontaneous action potentials that shape the development of mature synaptic transmission (Johnson et al., 2007; Marcotti et al., 2004). Inner hair cells of SK2-null mice fail to develop mature patterns of

Ca^{2+}-activated vesicle exocytosis that are crucial for sound signal transmission in the adult animal (Johnson et al., 2007).

SK2 currents in immature IHCs can be activated by multiple Ca^{2+} sources, including tightly co-localized α9/10-nAChRs, which are also transiently expressed concurrently with SK2 channels and are activated by acetylcholine released from efferent terminals (Glowatzki and Fuchs, 2000; Johnson et al., 2011; Marcotti et al., 2004). SK2 can also be activated by close coupling to transiently expressed purinergic P2X receptors, which are transiently expressed in pre-hearing IHCs and are activated by ATP derived from supporting cells in the nearby Kölliker's organ (Housley et al., 2006; Johnson et al., 2011; Tritsch and Bergles, 2010). Voltage-gated $Ca_v1.3$ Ca^{2+} channels constitute a third source of Ca^{2+} that activates SK2 channels in IHCs. Activation or blockade of α9/10-nAChRs, P2X receptors, or $Ca_v1.3$ channels alter the shape and frequency of spontaneous action potentials in immature IHCs by altering the level of SK2-mediated hyperpolarization (Johnson et al., 2011; Marcotti et al., 2004). The specific combination of different Ca^{2+} sources produces different spontaneous firing patterns along the length of the cochlea, suggesting that Ca^{2+} activation of SK2 channels may be important for the tonotopic maturation of afferent sound transmission (Johnson et al., 2011).

In neurons

SK channels are widely localized in the brain, with different subtypes displaying different neuronal or subcellular localization patterns (Sailer et al.,

2002; Sailer et al., 2004). SK channels in multiple neuronal populations mediate the medium afterhyperpolarization (mAHP) current that follows action potentials, contributing to control neural excitability and firing patterns (for review, see (Faber, 2009). In CA1 neurons, the apamin-sensitive component of the mAHP is primarily mediated by SK2 channels, which are activated by voltage-gated Ca^{2+} channels and repolarize the membrane following action potential (Bond et al., 2004; Stocker et al., 1999). Hippocampal SK2 channels also regulate synaptic plasticity through their coupling to NMDA receptors in microdomains within dendritic spines. SK2 channels are rapidly activated by NMDAR-carried Ca^{2+} currents and shape NMDAR EPSPs by repolarizing the synaptic membrane and favoring NMDAR Mg^{2+} block (Ngo-Anh et al., 2005). Blocking SK2 channels with apamin facilitates synaptic plasticity by lowering the frequency threshold for LTP induction, and systemic apamin administration in mice results in improved memory encoding in behavioral tasks (Stackman et al., 2002). Conversely, overexpression of SK2 impairs LTP induction and memory encoding (Hammond et al., 2006). In response to LTP induction, SK2 channels are internalized from the synaptic membrane and are reinserted several hours later (Lin et al., 2008; Lin et al., 2010). SK2 endocytosis requires the insertion of AMPA receptors (Lin et al., 2010) as well as PKA phosphorylation of one or more of three consecutive serine residues within the C terminal (Lin et al., 2008; Ren et al., 2006). The specific mechanisms and interacting proteins that mediate the coupling of SK2 to NMDARs and their LTP-dependent internalization and re-insertion have not yet been defined.

The role of SK2 channels in hippocampal synaptic plasticity is regulated by the transcription of a second SK2 isoform from a different promoter within the *Kcnn2* (SK2) gene, whose intracellular N-terminal is extended by approximately 200 amino acids. This “SK2-long” (SK2-L) isoform co-precipitated with the originally identified shorter isoform from the mouse brain, indicating that the two isoforms form heterotetramers *in vivo* (Strassmaier et al., 2005). SK2-L displays increased clustering capability compared to “SK2-short” (SK2-S) when expressed in heterologous cells (Strassmaier et al., 2005) and is essential for the normal targeting of SK2 channels and their modulation of synaptic activity (Allen et al., 2011). SK2 channels in mice engineered to express only the SK2-S isoform are excluded from the postsynaptic density, and accordingly, fail to elicit the previously characterized effects on NMDAR-mediated EPSPs, LTP induction, or memory encoding. These results indicate that the extended N-terminal is essential for directing the synaptic localization of SK2 channels and possibly their coupling to NMDARs. A homologous SK2-L isoform has been identified in human hippocampus, but SK2-L transcripts have not yet been identified in other tissues or organisms (Allen et al., 2011).

In cardiac muscle

SK2 channels also contribute to membrane repolarization following action potentials in cardiac muscle (Xu et al., 2003). In cardiac myocytes, SK2 channels are activated by $Ca_v1.2$ and $Ca_v1.3$ voltage-sensitive Ca^{2+} channels, which are directly linked to SK2 by interaction with the actin-binding protein α-actinin-2 (Lu

et al., 2007). α-actinin-2 also promotes the functional membrane expression of SK2 channels in heterologous cells and in native cardiac myocytes, as shown by increased SK2 currents, membrane-associated immunolabeling, and surface-biotinylation levels in the presence compared to the absence or knockdown of α-actinin-2 (Lu et al., 2009; Lu et al., 2007). The association of SK2 with early endosomes, but not with Golgi markers, in the absence of α-actinin-2 suggests that α-actinin-2 may be particularly important for the membrane retention of SK2 and/or its reinsertion during endocytic recycling (Lu et al., 2009).

Coupling of α9/10-nAChRs to SK2 channels in hair cells

In mature outer hair cells in the cochlea, release of acetylcholine from efferent olivocochlear synaptic terminals elicits inhibitory responses through rapid functional coupling between α9/10-nAChRs and SK2 channels. Ca^{2+} influx through α9/10-nAChRs and the subsequent activation of SK2 channels is extremely fast; in response to release of acetylcholine from efferent terminals, Ca^{2+} currents recorded from OHCs peak within one millisecond of channel opening, resulting in estimated local Ca^{2+} concentrations of 10μM or greater and SK2-mediated potassium currents that occur with a 20-80% rise time of approximately 6 milliseconds (Oliver et al., 2000). These responses in OHCs are identical to those elicited by fast application of saturating Ca^{2+} concentrations to heterologously expressed SK2 channels in inside-out patches of *Xenopus* oocytes, indicating that the kinetics of acetylcholine-evoked hyperpolarization in OHCs are shaped solely by the kinetics of the SK2 channel and are not limited

by the rate of Ca^{2+} diffusion from α9/10-nAChRs (Oliver et al., 2000; Xia et al., 1998). This observation suggests that α9/10-nAChRs and SK2 channels are tightly co-localized. In support of this theory, efferent-induced SK2 currents can be attenuated by BAPTA, a fast, high-affinity Ca^{2+} chelator, but not by the slower chelator EGTA, further suggesting that nAChR-mediated Ca^{2+} increases activate SK2 channels within tightly localized microdomains (Oliver et al., 2000). Functional coupling in response to acetylcholine can be recapitulated by expressing α9/10-nAChRs and SK2 channels in *Xenopus* oocytes, though outward potassium currents occur more slowly than in hair cells. Thus, hair-cell specific mechanisms or protein interactions may be necessary for the co-localization that allows fast, efficient functional coupling (Nie et al., 2004; Oliver et al., 2001b). These mechanisms have previously been undefined. However, studies of α9/10-nAChR and SK2 channel expression patterns in developing hair cells, as well as nAChR subunit and SK2 knockout animals, provide clues to the relative contributions of nAChR-related and SK2-related mechanisms to the development of mature functional coupling.

Expression studies in developing hair cells

During early postnatal development, IHCs are briefly innervated by efferent olivocochlear fibers and demonstrate α9/10-nAChRs and SK2 channel expression and functional coupling before the onset of hearing (Bruce et al., 2000; Katz et al., 2004; Simmons et al., 1996). α9-nAChR mRNA expression in IHCs can be detected by embryonic day 18 (E18) (Simmons and Morley, 1998),

though IHCs show no detectable response to acetylcholine until P0 (Roux et al., 2011). mRNA expression of α10 is first detected at E21 (Morley and Simmons, 2002), just before the onset of acetylcholine responses, which implies that expression of α10 is necessary for the membrane localization or function of assembled α9/10-nAChR heteropentamers (Roux et al., 2011). These nAChR currents at P0 are not coupled to SK2 channels, indicating that α9/10-nAChRs are able to reach the IHC membrane in the absence of SK2. SK2 channel clusters and functional coupling between nAChRs and SK2 are first detected at P1 and increase significantly over the next several days. Notably, α-bungarotoxin-labeled membrane clusters of α9/10-nAChRs and responsiveness of IHCs to synaptically released acetylcholine also appear at P1 and closely mirror the development of SK2 clusters and coupled nAChR-SK2 electrophysiological responses. Similarly, in OHCs that receive efferent innervation and respond to acetylcholine several days later at P6, several studies have detected nAChR-only responses to acetycholine before functional coupling to SK2 channels is achieved (Dulon and Lenoir, 1996; Roux et al., 2011), though another study found only biphasic currents at P6, indicative of functional coupling, and did not observe isolated nAChR-mediated currents (He and Dallos, 1999). Although OHCs demonstrated nicotinic currents lacking an SK2 component at P6, responses to evoked efferent synaptic signals were not found until P8, when coupled nAChR-SK2 currents were first detected. Together these results suggest that, while initial, low-level membrane targeting of α9/10-nAChRs is possible independently of SK2 channels, SK2 may direct increased nAChR

membrane localization and clustering and is required for the cells to respond to synaptic signals (Roux et al., 2011).

By P15, expression of α10-nAChRs and SK2 channels are undetectable in IHCs; their downregulation is coincident with the loss of IHC responses to synaptically derived or exogenously applied acetylcholine (Katz et al., 2004; Morley and Simmons, 2002). α9-nAChRs continue to be expressed in IHCs through adulthood (Simmons and Morley, 1998). Significantly, transgenic expression of the α10 subunit in IHCs through adult stages does not result in continued responsiveness of IHCs to acetylcholine, indicating that other factors, potentially SK2 channels, are necessary for the function of α9/10-nAChRs (Taranda et al., 2009a).

Studies of knockout animals

A comparison of the phenotypes of α9, α10, and SK2 knockout mice further supports a crucial role of SK2 channels in directing the assembly and function of the nAChR-SK2 signaling complex in hair cells. Mice lacking either the α9- or α10-nAChR subunits display similar phenotypes, including the failure of olivocochlear fiber stimulation to suppress OHC activity and increase afferent detection thresholds, as well as fewer, hypertrophied efferent synaptic boutons on OHCs (Vetter et al., 2007; Vetter et al., 1999). OHCs of α10-nAChR knockout mice show significantly reduced currents in response to application of 1mM acetylcholine and do not respond to stimulated acetylcholine release from presynaptic terminals, indicating that remaining α9-nAChR homopentamers are

not sufficient to maintain normal innervation or efferent transmission (Vetter et al., 2007). These results support previous studies indicating that the α10 subunit modifies nAChR functional properties and increases nicotinic current amplitudes compared to α9-nAChRs, supporting an important role for the α10 subunit in directing the functional localization of α9/10-nAChRs (Elgoyhen et al., 2001).

In comparison to nAChR knockout animals, SK2 knockout mice display a more severe phenotype that underscores the critical role of SK2 channels in synapse assembly. Like α9 and α10-knockout mice, SK2-knockout animals lack olivocochlear-driven inhibition of hair cell responses. However, while nAChR knockouts retain OHC innervation by efferent boutons, though abnormal in number and morphology, SK2 knockout animals initially develop normal efferent innervation of OHCs but show a complete degeneration of this innervation by adulthood. Deletion of both α10-nAChRs and SK2 channels results in an identical phenotype to SK2-knockout mice, indicating an upstream requirement for SK2 in the maintenance of efferent innervation (Murthy et al., 2009a).

Importantly, hair cells of SK2 knockout mice show no detectable responses to acetylcholine, despite normal levels of α9 and α10-nAChR mRNA expression, demonstrating that SK2 expression is necessary for the normal assembly or membrane localization of α9/10-nAChRs (Kong et al., 2008; Murthy et al., 2009a). By comparison, α9-knockout mice show an initial upregulation and mislocalization of SK2 channels in early postnatal OHCs but demonstrate normal SK2 synaptic localization by adulthood, suggesting that nAChRs are not essential to the proper localization of SK2 channels (Murthy et al., 2009a). Taken

together, these studies lead to the hypothesis that SK2 channels and α9/10-nAChRs form a multimolecular complex that requires SK2-specific interacting proteins for its assembly, membrane expression, and/or clustering (Kong et al., 2008; Murthy et al., 2009a).

Overall, studies to date strongly suggest that α9/10-nAChRs and SK2 channels are tightly co-localized within membrane microdomains to allow rapid SK2-mediated hair cell hyperpolarization in response to nAChR activation and Ca^{2+} influx. The presence of low-level cholinergic responses in IHCs and OHCs prior to the appearance of SK2 clusters and currents suggests the presence of mechanisms specific to α9/10-nAChRs that promote their functional membrane expression. However, the correlation between the acquisition of responses to efferent synaptic signals and the onset of SK2 channel function in developing hair cells, combined with a complete loss of cholinergic function in the absence of SK2, suggests that co-clustering of nAChRs and SK2 channels within membrane microdomains may depend particularly on SK2-intrinsic mechanisms.

Proposed model of the postsynaptic complex in hair cells

We propose a molecular model of the olivocochlear postsynaptic site in hair cells based on prior work in our lab on neuronal nicotinic synapses. Adenomatous polyposis coli (APC), originally identified as a tumor suppressor protein (Su et al., 1992) has recently been identified as a key nicotinic synapse organizer in neurons and at the neuromuscular junction. In mouse myotubes, interaction of APC with muscle β-type nAChRs is required for agrin-induced

nAChR clustering (Wang et al., 2003). APC also interacts with α7-nAChRs at presynaptic terminals in hippocampal neurons to promote their localization and clustering in response to *Wnt* pathway activation (Farias et al., 2007).

Studies in our lab of nicotinic synapses in chicken ciliary ganglion neurons have demonstrated that APC organizes a multiprotein postsynaptic complex of scaffolding proteins, cytoskeletal regulators, and retrograde signaling proteins that are required for targeting α3-containing nAChRs to the synapse and coordinating pre- and postsynaptic differentiation (Figure 1.3) (Rosenberg et al., 2008; Rosenberg et al., 2010; Temburni et al., 2004). APC associates with microtubules, both directly and through interaction with microtubule plus-end binding protein (EB1) (Nathke, 2006; Su et al., 1992; Wen et al., 2004). APC and EB1 interact with the cytoskeletal regulators IQGAP1 and microtubule-actin crosslinking factor (MACF), which cross-link and stabilize microtubules and F-actin and tether postsynaptic components to the cytoskeleton (Slep et al., 2005; Watanabe et al., 2004). The trans-synaptic adhesion molecule N-cadherin flanks the APC postsynaptic complex and links pre- and postsynaptic sites. β-catenin and APC also interact with the scaffolding proteins synaptic scaffolding molecule (S-SCAM) and postsynaptic density protein (PSD)-93, which link the APC complex to synaptic adhesion and signaling molecules such as neuroligin (Hirao et al., 1998; Ide et al., 1999; Iida et al., 2004; Nishimura et al., 2002; Rosenberg et al., 2010; Stan et al., 2010). α3-containing nAChRs are tethered to APC through the small linker molecule 14-3-3, which may be necessary for nAChR retention at the synapse (Rosenberg et al., 2008).

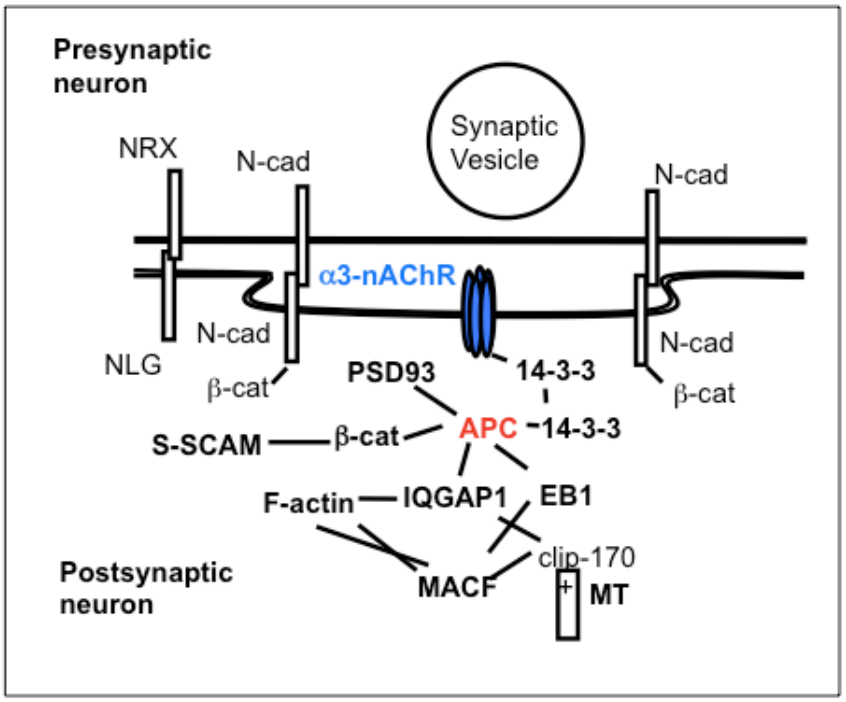

Figure 1.3: Model of neuronal α3-nAChR postsynaptic sites

Blocking interactions between APC and EB1 or between β-catenin and S-SCAM using dominant-negative peptides reduces the functional levels and cell surface stability of α3-nAChRs in chicken ciliary ganglion neurons (Rosenberg et al., 2010; Temburni et al., 2004). Postsynaptic levels of EB1, IQGAP1, MACF, S-SCAM, neuroligin, F-actin, and 14-3-3, as well as presynaptic neurexin and other active zone proteins, are also downregulated when APC::EB1 binding is disrupted, demonstrating that this interaction is essential for postsynaptic protein accumulation and assembly of the postsynaptic scaffold (Rosenberg et al., 2008; Rosenberg et al., 2010). These studies suggest a model in which synaptically-targeted APC captures microtubule plus-ends via interaction with EB1, directing microtubule-based delivery of nAChRs to the synaptic region, where they are

anchored to the postsynaptic complex by the 14-3-3 adapter protein (Rosenberg et al., 2008; Temburni et al., 2004).

Adapter proteins

We suggest that the APC-organized protein complex identified at α3-nAChR synapses in neurons could also function to organize postsynaptic sites in cochlear hair cells. We hypothesize that the core complex of APC and cytoskeletal and scaffolding proteins are conserved between neurons and the specialized epithelial hair cells, with specific adapter proteins binding to α9/10-nAChRs and SK2 channels to anchor them to the synaptic complex.

Only two proteins, rapsyn and prosaposin, have been identified as direct binding partners for α9 and α10-nAChRs, respectively, in hair cells (Akil et al., 2006; Osman et al., 2008). However, their roles in α9/10-nAChR localization *in vivo* are unclear. Prosaposin is a precursor of the sphingolipid activator saposin that localizes to hair cells and support cells in the mammalian organ of Corti. Prosaposin-knockout animals display hearing deficits, hair cell and supporting cell morphological abnormalities, and degeneration of OHCs from the apical turn of the cochlea; however, the mechanisms underlying the role of prosaposin and its interaction with α10-nAChRs in the cochlea has not been identified (Akil et al., 2006) Rapsyn, which plays an essential role in the clustering of muscle-type nAChRs, is expressed in hair cells, and rapsyn interactions increase α9-nAChR surface clusters in heterologous cell lines, suggesting that common mechanisms may contribute to nAChR clustering at the neuromuscular junction and in hair

cells (Osman et al., 2008). However, the failure of α9-nAChR pentamers to maintain normal hair cell cholinergic responses in α10-nAChR knockout mice suggests that the α10 subunit may provide critical protein interactions or mechanisms to promote α9/10-nAChR surface localization, anchoring, or function (Vetter et al., 2007). We propose candidate adapter proteins that may specifically link α9/10-nAChRs and SK2 channels to the core synaptic complex, including α-actinin, an actin-binding protein that regulates SK2 channel localization in cardiac muscle (Lu et al., 2009; Lu et al., 2007); the linker protein 14-3-3, which we predict as a link between SK2 channels and APC based on canonical sequence motifs in SK2 C-terminal; and cortactin, an actin-binding protein that we predict as a binding partner for α10-nAChRs based on canonical binding motifs within the α10 cytoplasmic domain.

α-actinins

α-actinins are actin crosslinking proteins with multiple isoforms that are expressed specifically in smooth or skeletal muscle, brain, or other non-muscle tissues (Beggs et al., 1992; Millake et al., 1989; Waites et al., 1992). α-actinins bind to actin filaments via binding domains in the N-terminal and form antiparallel dimers mediated by the central rod domains to promote their actin crosslinking activity (Sjoblom et al., 2008). α-actinins also contain C-terminal EF hands, and one major difference among different α-actinin isoforms is the Ca^{2+}-binding capability of these EF hands. EF hands of non-muscle α-actinins bind Ca^{2+}, which negatively regulates actin crosslinking. By contrast, critical Ca^{2+}-binding

residues are missing from the EF hands of muscle α-actinin isoforms, and the actin-crosslinking function of these isoforms is not sensitive to Ca^{2+} (Beggs et al., 1992; Waites et al., 1992).

In mouse cardiac muscle, SK2 channels interact with α-actinin-2 (Lu et al., 2006). This interaction links SK2 channels to nearby $Ca_v1.3$ channels and regulates SK2 membrane localization (Lu et al., 2009; Lu et al., 2007). In neurons, α-actinin-1 binds to the NR1 subunit of NMDARs and regulates NMDAR inactivation by competing for NR1 binding with CaM, which participates in the Ca^{2+}-induced inactivation of the channels (Krupp et al., 1999; Merrill et al., 2007; Wang et al., 2008). Interactions of SK2 with α-actinin-2 require the EF hands of α-actinin-2 and two consecutive amino acids within the α1 helix of the SK2 CaM-binding domain (Lu et al., 2009). Additionally, 5 amino acids within the SK2 α2 helix show significant sequence conservation with the C0 domain of NR1 that is necessary for binding to α-actinin-1 (Figure 1.4a) (Krupp et al., 1999; Merrill et al., 2007). Based on these studies, we propose that α-actinin interacts with SK2 in hair cells and may anchor SK2 channels to the actin cytoskeleton. Because regions of SK2 predicted to interact with α-actinin are located within the CaM binding domain, we also predict that α-actinin may compete with CaM for binding to SK2.

14-3-3

14-3-3 proteins are a family of seven small linker proteins that interact with canonical consensus motifs and form dimers to connect their binding partners

Figure 1.4: Predicted adapter protein binding regions in SK2 and α10-nAChRs. (A) Predicted binding motifs for α-actinin-1 in chicken SK2 channels. Blue shaded region: α1 helix (Ca^{2+}-independent CaM binding domain). Green shaded region: α2 helix (Ca^{2+}-dependent binding region). Consensus with α-actinin-1 binding region of NR1 highlighted in red (Merrill et al., 2007). (B) 14-3-3 consensus motifs in the SK2 intracellular C-terminal (Yaffe, 2002). (C) Cortactin-SH3 consensus motifs in the a10-nAChR cytosolic loop. Consensus with cortactin binding motifs in cortactin binding protein 90 (CBP90), drosophila zonula occludens 1 protein (DZO1), and large conductance Ca^{2+}-activated (BK) channels highlighted in red (Daly, 2004). Asterisks in A indicate residues necessary for interaction with a-actinin-2 (Lu et al., 2009); asterisks in B, C indicate critical binding residues. Numbers indicate amino acids.

(Aitken et al., 2002; Yaffe, 2002). In neurons, 14-3-3 proteins promote the surface localization of multiple neurotransmitter receptors and ion channels by masking endoplasmic reticulum retention motifs and promoting multimer assembly (Couve et al., 2001; Exley et al., 2006; Heusser et al., 2006; Jeanclos et al., 2001; O'Kelly et al., 2002). 14-3-3 also serves as a direct link between α3-nAChRs and APC at neuronal synapses in chicken peripheral neurons (Rosenberg et al., 2008). The intracellular C-terminal tail of the SK2 channel contains six canonical 14-3-3 binding motif of the type RX_{2-3}(pS/T)X(X/P), where phosphorylation of the central serine or threonine residue is often essential for 14-3-3 interaction (Figure 1.4b, scansite.mit.edu) (Yaffe, 2002). Significantly, phosphorylation of SK2 at three consecutive serine residues, each of which is the central serine in a 14-3-3 binding motif, has been demonstrated to regulate the surface expression of SK2 channels; however, the specific mechanisms are undefined (Ren et al., 2006). We therefore suggest that 14-3-3 may provide a mechanism for phosphorylation-dependent regulation of SK2 membrane localization.

Cortactin

Cortactin is an F-actin binding protein that plays important roles in the regulation of the actin cytoskeleton. Cortactin interacts with the Arp2/3 actin remodeling complex to stimulate actin polymerization, branching, and stabilization (Weaver et al., 2001). Accumulating evidence suggests that cortactin plays a role in synapse assembly. Cortactin co-localizes with muscle-type

nAChRs and regulates actin dynamics at the neuromuscular junction in response to agrin-MuSK signaling that are critical for formation of nAChR clusters (Dai et al., 2000; Madhavan et al., 2009; Peng et al., 1997). In hippocampal neurons, cortactin binds to δ-catenin, which in turn binds to S-SCAM (Ide et al., 1999; Martinez et al., 2003). Interactions of δ-catenin with postsynaptic density proteins in dendritic spines are essential for normal spine morphology and clustering of AMPA receptors (Abu-Elneel et al., 2008; Silverman et al., 2007). Cortactin binds directly to Kv1.2 potassium channels in neurons and regulates their functional surface expression (Hattan et al., 2002). Cortactin also interacts with large conductance Ca^{2+}-activated (BK) potassium channels in neurons, providing a link to the cytoskeleton that modulates BK channel activity in response to changes in the local cytoskeletal network (Tian et al., 2006; Tian et al., 2008).

Sequence analysis of the long cytoplasmic loop of the α10-nAChR reveals two canonical proline-rich binding motifs for the SH3 domain of cortactin (Figure 1.4c; scansite.mit.edu). These motifs contain the minimal cortactin-SH3 binding sequence PXXP and show significant sequence conservation with other known cortactin binding proteins. Thus, we propose that cortactin interacts directly with α10-nAChRs to regulate α9/10-nAChR cell surface localization and anchorage to the actin cytoskeleton and to the APC postsynaptic complex via its interaction with δ-catenin and S-SCAM.

Preface to experiments

Cholinergic innervation of cochlear hair cells by efferent olivocochlear fibers plays important roles in the sensitivity of sound detection, frequency selectivity, and protection against hair cell trauma and hearing loss resulting from noise over-exposure (Brown and Nuttall, 1984; Galambos, 1956; Rajan, 1990). The nicotinic synapse in hair cells is unique in the nervous system with respect to the unconventional α9/10-nAChRs that mediate cholinergic sensitivity and the inhibitory nature of the synapse due to functional coupling of nAChRs to Ca^{2+}-sensitive SK2 potassium channels (Elgoyhen et al., 1994; Elgoyhen et al., 2001; Fuchs and Murrow, 1992a). The mechanisms that govern the assembly of nicotinic postsynaptic sites and the synaptic localization of α9/10-nAChRs and SK2 channels in hair cells are poorly understood compared to the more well-characterized nicotinic synapses in muscle and in neurons. Therefore, we set out to identify proteins and mechanisms that are important for synapse assembly and function in hair cells.

We based our initial work on previous studies of proteins that regulate the assembly of neuronal and neuromuscular nicotinic synapses. By immunolabeling of hair cells in the chicken basilar papilla, we show that postsynaptic sites in hair cells share multiple protein components with nicotinic synapses in neurons and muscle, indicating that common mechanisms may underlie the development and function of diverse synapses. We next sought to identify specific mechanisms that control the synaptic localization and functional coupling of α9/10-nAChRs and SK2 channels, which are believed to co-localize to within approximately 10

nanometers of one another in order to allow acetylcholine-induced inhibition of hair cells on a millisecond time scale (Fuchs and Murrow, 1992a; Oliver et al., 2000). Because studies of α9/10-nAChR interactions and localization in hair cells are impeded by the lack of specific antibodies against either subunit, we co-expressed epitope-tagged α9/10-nAChRs with SK2 channels in *Xenopus* oocytes to study their interactions and membrane expression. Using this expression system, we show that α9/10-nAChRs and SK2 channels physically associate with one another, implying that this interaction underlies their close functional coupling in hair cells. We also use surface biotinylation and endocytosis assays to demonstrate that, consistent with previous reports, the surface expression of α9/10-nAChRs depends strongly on the expression and surface targeting of SK2 channels (Kong et al., 2008; Murthy et al., 2009a; Roux et al., 2011). Together, these results support a model in which the synaptic localization of α9/10-nAChRs and SK2 channels occurs through the interaction of nAChRs and SK2 channels in a protein complex whose targeting requires SK2-specific protein interactions or trafficking mechanisms.

Using the oocyte expression system and studies of direct protein interactions in recombinant peptide binding assays, we show that alternative splicing of SK2 channels and synaptic Ca^{2+} signaling represent potential mechanisms to modulate the surface expression and interaction of α9/10-nAChRs and SK2 channels in hair cells. The SK2-ARK splice variant, previously identified in chicken hair cells (Matthews et al., 2005), shows distinct differences from SK2 in its interaction with α9/10-nAChRs and surface expression levels, indicating that

its expression could alter the synaptic localization or function of coupled nAChRs and SK2 channels. We also demonstrate that interactions of SK2 and nAChRs are affected by Ca^{2+}, suggesting a mechanism by which efferent synaptic activity could dynamically regulate the postsynaptic nAChR-SK2 complex.

Lastly, we present preliminary data on novel interacting proteins of SK2 channels and α10-nAChR subunits. Our results show that 14-3-3 and cortactin interact with SK2 channels and α10-nAChRs, respectively. We suggest that these interactions may participate in synapse assembly in hair cells by regulating the synaptic targeting or retention of α9/10-nAChRs and SK2 channels and providing links between the membrane-bound channels and the newly identified components of the postsynaptic protein complex. Taken together, our studies contribute to a better understanding of the composition, assembly, and regulation of olivocochlear nicotinic synapses in hair cells and suggest promising new lines of study in this field.

Chapter 2

Immunolocalization of postsynaptic proteins in chicken cochlear hair cells

Elizabeth K. Storer, R. Keith Duncan, and Michele H. Jacob

This chapter will be submitted for publication in the Journal of the Association for Research in Otolaryngology.

Abstract

Hearing sensitivity is modulated by efferent olivocochlear fibers that directly contact mechanosensory hair cells in the cochlea. At postsynaptic sites in hair cells, α9/10 nicotinic acetylcholine receptors (nAChRs) are functionally coupled to Ca^{2+}-activated small conductance K^{+} (SK2) channels to produce inhibitory responses. Little is known of the protein composition of efferent synapses or mechanisms that localize α9/10-nAChRs and SK2 channels. Here, we show that protein components of neuronal nicotinic synapses are conserved at the nicotinic synapse in cochlear hair cells. Our results provide new insights into the mechanisms that direct efferent postsynaptic development in hair cells and suggest that diverse nicotinic synapses share similar protein composition and assembly mechanisms.

Introduction

Mechanosensory hair cells in the mammalian and avian cochlea are innervated by efferent olivocochlear fibers that originate in the superior olivary complex of the brainstem (Campbell and Henson, 1988). This efferent input is primarily cholinergic, though other neurotransmitters have been demonstrated at efferent terminals (Eybalin, 1993). In contrast to typically excitatory cholinergic synapses elsewhere in the nervous system, acetylcholine evokes inhibitory responses in hair cells. Cholinergic receptivity in hair cells is mediated by Ca^{2+}-permeable α9/10 nicotinic acetylcholine receptors (nAChRs), which are functionally coupled to small-conductance Ca^{2+}-activated K^+ (SK2) channels, such that ACh-induced Ca^{2+} influx through α9/10-nAChRs evokes K^+ efflux through the nearby SK2 channels (Oliver et al., 2000; Yuhas and Fuchs, 1999). The resulting hyperpolarization of the hair cell suppresses the voltage-dependent mechanical processes that amplify sound signals within the cochlea, resulting in frequency-specific increases in sound detection thresholds (Brownell et al., 1985; Galambos, 1956; Murugasu and Russell, 1996). Thus, olivocochlear synaptic input regulates sound sensitivity and frequency selectivity. Efferent activity may also provide protection against hearing loss resulting from acoustic overexposure (Maison et al., 2002; Reiter and Liberman, 1995; Taranda et al., 2009b).

Little is known of how α9/10-nAChRs and SK2 channels are localized at postsynaptic sites in hair cells. The millisecond time scale of postsynaptic Ca^{2+} influx and subsequent SK2 channel activation suggest that α9/10-nAChRs and SK2 channels are closely co-localized (Oliver et al., 2000), but how their co-

localization and functional coupling are accomplished is unknown. Studies of nAChRs that mediate excitatory transmission in neurons and in muscle show that adenomatous polyposis coli protein (APC), originally identified as a tumor suppressor protein (Su et al., 1992), plays a key role in nAChR localization. Our lab has demonstrated an essential role for APC in the clustering of α3-nAChRs at postsynaptic sites in chicken peripheral neurons. At these sites, APC organizes a complex of proteins that stabilize the local cytoskeletal network, anchor α3-nAChRs at the synaptic membrane, and localize adhesion proteins that align the postsynaptic site with presynaptic terminals (Rosenberg et al., 2008; Rosenberg et al., 2010; Temburni et al., 2004). Included in the APC protein complex are microtubule end-binding protein EB1, whose interaction with APC is essential for α3-nAChR surface clustering in neurons (Temburni et al., 2004); synaptic scaffolding molecule (S-SCAM), a PDZ domain-containing structural protein that localizes to neuronal synapses and promotes pre- and postsynaptic differentiation via interactions with neuroligin and β-catenin (Iida et al., 2004; Rosenberg et al., 2010; Stan et al., 2010); and microtubule-actin crosslinking factor (MACF), which binds to both microtubules and actin as well as to EB1 (Leung et al., 1999; Slep et al., 2005).

The importance of APC at nicotinic postsynaptic sites in both neurons and in muscle raises the possibility that APC and its interacting partners constitute a core protein complex that directs the assembly of nicotinic synapses throughout the nervous system. Thus, we wondered whether APC and associated proteins may also function at efferent olivocochlear postsynaptic sites. In agreement with

this model, we find that APC, S-SCAM, EB1, and MACF are specifically localized to postsynaptic termini in chicken hair cells. These results provide new insights into mechanisms that may direct efferent olivocochlear synapse assembly and proper localization of α9/10-nAChRs and their partner SK2 channels.

Methods

Antibodies

Primary antibodies used were: polyclonal anti-MAGI-2/S-SCAM (Sigma); polyclonal anti-SK2 potassium channel (Sigma); monoclonal anti-SV2 (Developmental Studies Hybridoma Bank); polyclonal anti-myosin-VIIa (Proteus Biosciences); monoclonal anti-APC (clone ALi 12-28, Abcam); polyclonal anti-synapsin (clone G-304, gift of Dr. Paul Greengard, Rockefeller University); monoclonal anti-EB1 (BD Transduction Laboratories); polyclonal anti-kakapo, which detects MACF (gift of Dr. Talila Volk, Weizmann Institute of Science). Secondary antibodies used were: Cy3- and FITC-conjugated donkey anti-rabbit, anti-mouse, and anti-guinea pig (Jackson ImmunoResearch); Alexa-Fluor-488- and 594-conjugated goat anti-mouse and donkey anti-mouse and anti-rabbit (Molecular Probes).

Chicken embryos

Embryonated White Leghorn chicken eggs were obtained from the University of Connecticut Poultry Farm (Storrs, CT) or Charles River Spafas. Embryos were

kept at 37°C in forced air-draft humidified incubators until embryonic day (E)19-20.

Tissue fixation and immunolabeling

Cochlear ducts were dissected from chicken embryos at E19-20. Cochleae were fixed at room temperature or at 4°C for 30 minutes to 1 hour in 2-4% paraformaldehyde, or in 4% paraformaldehyde with 15% picric acid. Tissue was cryoprotected by immersion in increasing concentrations of sucrose and embedded in TissueTek OCT compound (Electron Microscopy Sciences) or in 7.5% gelatin with 15% sucrose. 10μm cryosections were blocked with 5-10% normal donkey serum (Jackson ImmunoResearch) or 0.25% teleost gelatin in phosphate buffered saline (PBS) (Sigma Aldrich, St. Louis, MO, USA) and incubated at room temperature with primary antibodies diluted in 5% normal donkey serum or 0.125% teleost gelatin for 1 hour and secondary antibodies for 45 minutes.

Single hair cell immunolabeling

Hair cell isolation was performed according to previously described methods (Li et al., 2009) with minor modifications. Cochlear ducts were dissected from E19-E20 chicken embryos, and basilar papillae were dissociated in extracellular fluid (ECF) (in mM: 154 NaCl, 6 KCl, 5 $CaCl_2$, 2 $MgCl_2$, 10 glucose, 5 HEPES pH 7.4) or in low-divalent ECF ($CaCl_2$ reduced to 100mM, $MgCl_2$ omitted). In some experiments, cochlear ducts were incubated for 1 minute in 0.01% Type XXIV

protease (Sigma) in ECF before dissection of the basilar papillae. Cells were allowed to adhere to SuperFrost Plus slides (Fisher Scientific) and fixed in 2% paraformaldehyde for 30 minutes. The cells were then permeabilized with 0.1% Triton X-100 and blocked in 5% normal donkey serum with 0.1% Triton X-100 and incubated with primary antibodies for 1 hour and secondary antibodies for 45 minutes. All steps were performed at room temperature.

Image analysis

Epifluorescence images were captured using a Zeiss Axioskop epifluorescence microscope (Thornwood, NJ, USA) and QImaging Retiga 200R CCD camera (Surrey, BC, Canada) with Nikon Instruments NIS Elements software. Confocal images were captured using a Leica TCS SP2 confocal microscope with HeNe (633nm), Kr (568 nm), and Ar (488nm) lasers and a 63x 1.32 numerical aperture lens. Optical sections were taken in 0.5μM steps. For each cell, 3 consecutive sections through a representative region were compressed for analysis. For labeled cochlea sections, epifluorescence images or confocal stacks from representative cells were used to assess co-localization of double-labeled proteins. Pixel intensities were measured along ~3μM lines drawn across a representative region of the efferent synapse. Postsynaptic localization was concluded if peak intensity coincided with that of a known postsynaptic protein or was distinct from that of a known presynaptic protein.

Results

Our aim in this study was to determine whether the efferent nicotinic synapse in cochlear hair cells shares common protein components with nicotinic synapses in neurons or in muscle. In the process, we hoped to gain a better understanding of the mechanisms that direct α9/10-nAChRs and SK2 channel membrane expression and functional coupling. We examined the localization of candidate postsynaptic proteins by immunofluorescent labeling of sectioned cochlear ducts from chicken embryos at E19-20, by which time calyx-shaped efferent terminals have formed on short hair cells (Rebillard and Pujol, 1983). To determine whether we could specifically distinguish postsynaptic protein localization, we examined the localization of SK2, the postsynaptic localization of which has been previously established (Matthews et al., 2005; Oliver et al., 2000), relative to that of presynaptic synaptic vesicle protein (SV2). We measured pixel intensities of SK2 and SV2 immunofluorescence along a line drawn across the efferent synaptic terminal and basal membrane of the hair cell. As shown in Figure 2.1a, although SK2 and SV2 pixel intensities partially overlapped, peak SK2 intensity was distinct from peak SV2 intensity. To corroborate this method, we also examined SK2 immunofluorescence in acutely dissociated hair cells. As expected, SK2 was clearly localized to the basal pole of short hair cells and was distinct from SV2-labeled fragments of efferent terminals that remained after dissociation (Figure 2.1a, bottom).

Using these methods, we identified synaptic scaffolding molecule (S-SCAM), a scaffolding protein at neuronal nicotinic synapses (Rosenberg et al., 2008), as

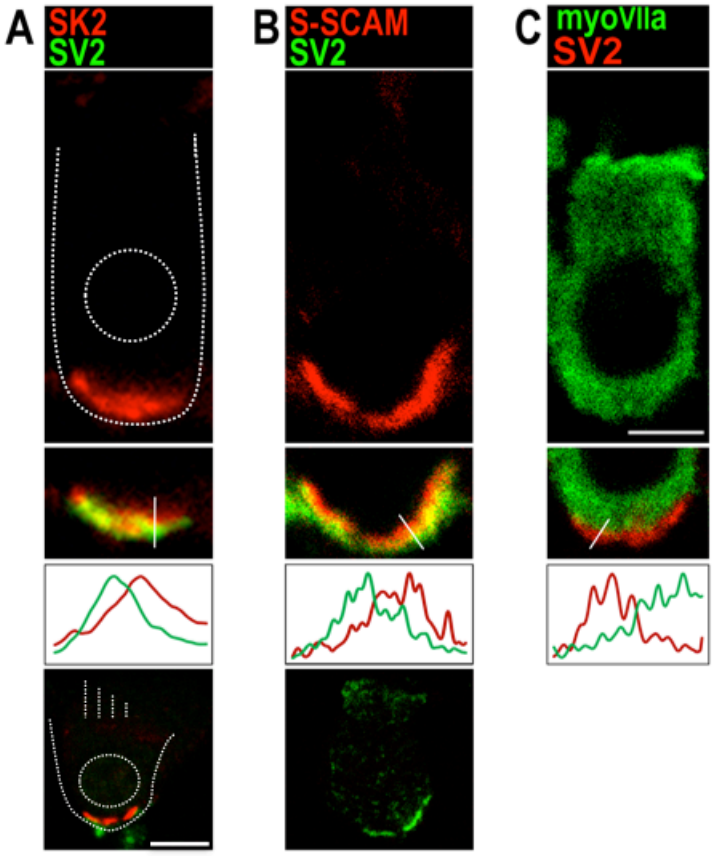

Figure 2.1: Localization of SK2 and S-SCAM in E19-20 chick hair cells.
(A) Epifluorescence image of SK2 and presynaptic SV2 immunofluorescence in chick hair cells. (B) Confocal image of S-SCAM and SV2 immunofluorescence in chick hair cells. (C) Confocal image of myosin VIIa and SV2 immunofluorescence. Top panels: hair cells in cryosections of chick cochlear duct. Middle panels: Fluorescence intensity profiles of lines indicated in image showing juxtaposition of pre and postsynaptic labeling. Bottom panels in A,B: confocal images of SK2 (red), SV2, and S-SCAM (green) immunofluorescence in acutely dissociated E20 chick hair cells. Scale bars: 5μM.

a postsynaptic marker at efferent hair cell synapses. Similar to SK2, S-SCAM immunofluorescence was concentrated at the basal pole of hair cells and was juxtaposed to presynaptic SV2, as shown by separation of peak pixel intensities across the synaptic region (Figure 2.1b). S-SCAM immunofluorescence was also concentrated at the basal pole of dissociated hair cells in the absence of SV2-labeled presynaptic terminals, confirming postsynaptic localization of S-SCAM. As a control, we measured the localization of myosin VIIa, a motor protein that is found in the inner ear exclusively in hair cells (Hasson et al., 1995). Consistent with previous reports, myosin VIIa expression in hair cells was localized to the cytoplasm and heavily associated with the hair bundle but showed no concentration near the efferent synaptic contact (Figure 2.1c). Similarly to SK2 and S-SCAM, peak pixel intensity of myosin VIIa was distinct from that of SV2, underscoring its hair cell-specific localization and validating our measurement method.

Using S-SCAM as a postsynaptic marker, we next examined the localization of three candidate postsynaptic proteins that participate in the localization of nAChRs at neuronal synapses. We found that APC shows strong concentration in the synaptic region. APC immunofluorescence was juxtaposed to that of presynaptic synapsin and co-localized with postsynaptic S-SCAM, indicating that APC is present at hair cell postsynaptic sites (Figure 2.2a). EB1, a binding partner of APC, was also concentrated at the synapse and co-localized with S-SCAM (Figure 2.2b). Finally, MACF showed postsynaptic localization as demonstrated by juxtaposition to SV2 and co-localization with S-SCAM (Figure

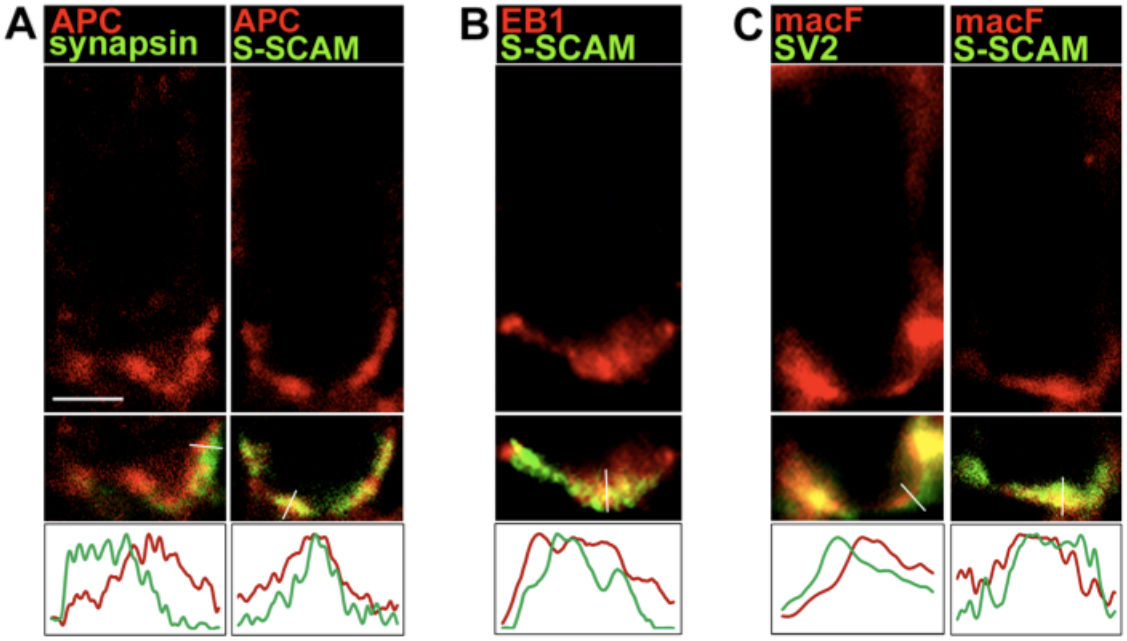

Figure 2.2: Postsynaptic proteins in chick hair cells.
Immunolabeled cryosections of E19-20 chick cochleae with pixel intensity profiles (lines in middle panels). (A) Confocal images showing juxtaposition of APC immunofluorescence to presynaptic synapsin and co-localization with postsynaptic S-SCAM in chick hair cells. (B) Epifluorescence image of EB1 labeling showing co-localization with postsynaptic S-SCAM. (C) Epifluorescence image of MACF labeling showing juxtaposition to SV2 and confocal image showing co-localization with S-SCAM. Scale bars: 5μM.

2.2c). Thus, these results indicate that three protein components of nicotinic postsynaptic sites in neurons are also expressed in hair cells and are concentrated at olivocochlear postsynaptic terminals.

Discussion

We have identified four novel protein components of efferent postsynaptic sites in cochlear hair cells. We show that S-SCAM is a postsynaptic marker in hair cells, based on its similar distribution to SK2 channels, apposition to the efferent presynaptic calyx, and concentration at the basal end of dissociated cells in the absence of presynaptic terminals. We also found that APC, EB1, and MACF, are concentrated at hair cell efferent synapses and co-localized with S-SCAM. Roles for these proteins in nicotinic synapse assembly have been previously characterized in neurons and at the developing neuromuscular junction (Rosenberg et al., 2008; Rosenberg et al., 2010; Temburni et al., 2004). Our demonstration that these proteins are also present at α9/10-nAChR synapses in hair cells further supports the hypothesis that a core set of proteins participates in nicotinic synapse development across diverse cell types and nAChR subtypes (Rosenberg et al., 2008). APC is also present at glutamatergic synapses, where it forms a protein complex with N-methyl-D-aspartate (NMDA) receptors (Yanai et al., 2000) and is essential for proper clustering of alpha-amino-3-hydroxy-5-methyl-isoxazole-4-proprionate (AMPA) receptors (Shimomura et al., 2007). S-SCAM is localized to glutamatergic as well as inhibitory synapses, where it forms scaffolds that organize receptors, signaling

complexes, and synaptic adhesion proteins (Hirao et al., 1998; Stan et al., 2010; Sumita et al., 2007). Hence, APC, S-SCAM, and other proteins that participate in the assembly of nicotinic synapses may have a more widespread function at diverse synapses throughout the nervous system.

Though APC is crucial for neurotransmitter receptor clustering at multiple synapses, the specific mechanisms and interactions that mediate its role appear to be unique to each synapse and receptor. In chicken peripheral neurons, APC is thought to cluster α3-nAChRs by capturing EB1-tagged microtubules and thereby directing microtubule-based vesicle trafficking to synaptic sites (Temburni et al., 2004). The interaction between APC and EB1 is essential specifically for the surface clustering of α3-nAChRs; disrupting APC-EB1 binding significantly reduces α3-nAChR clusters, but extrasynaptic α7-nAChRs localized outside of the postsynaptic density (Jacob and Berg, 1983) are unaffected, as are glycine receptors localized at the same postsynaptic site (Temburni et al., 2004; Tsen et al., 2000). Neither APC nor EB1 interact with α3-nAChRs directly; α3-nAChRs are linked to APC by the small adapter protein 14-3-3, which may promote the retention of receptors in the synaptic membrane (Rosenberg et al., 2008; Temburni et al., 2004). In contrast, the agrin-induced clustering of β-nAChRs in myotubes is achieved through direct interaction of APC with the β-nAChR intracellular loop (Wang et al., 2003). Similarly, APC and its interaction with the postsynaptic PDZ-domain protein PSD-95 are essential for clustering AMPA-Rs in hippocampal neurons, perhaps by directing microtubule-based receptor trafficking and/or by anchoring synaptic receptors to the cytoskeleton

(Shimomura et al., 2007). However, though APC interacts with NMDA-Rs via PSD-95 in the brain, clustering of NMDA-Rs does not require APC (Shimomura et al., 2007; Yanai et al., 2000). Together these studies indicate that the role of APC in synapse assembly may involve receptor-specific adapter proteins.

Based on the above studies of APC's role in receptor trafficking, we propose that interaction of APC with microtubules via EB1 targets α9/10-nAChR and SK2 channel delivery to synaptic sites, where interactions with specific adapter proteins, yet to be identified, anchor them to the APC postsynaptic complex. The unique dependence of hair cell nicotinic signaling on the functional coupling between two different channels raises the possibility that either α9/10-nAChRs, SK2 channels, or both may require specific adapter proteins to anchor them close together in the postsynaptic membrane. An essential role of the SK2 channel in this process is suggested by the phenotype of SK2-knockout mice, which demonstrate an absence of acetylcholine-evoked α9/10-nAChR currents from hair cells. These studies indicate that SK2 may be necessary for the normal membrane expression or function of α9/10-nAChRs, possibly through the formation of a postsynaptic protein complex whose proper membrane insertion and/or retention is dependent upon proteins interacting with SK2 (Kong et al., 2008; Murthy et al., 2009a). Thus, it is possible that SK2-specific adapter proteins anchor an SK2-nAChR complex to APC or to other proteins in the postsynaptic scaffold. The loss of presynaptic terminals from SK2-knockout hair cells further suggests that SK2 may be necessary for the maintenance of transsynaptic adhesion, though the mechanisms involved are unclear (Murthy et

al., 2009a). α9/10-nAChRs are also necessary for coordinated pre- and postsynaptic development, as α9- and α10-knockout mice demonstrate abnormal efferent fiber targeting and bouton structure, and abnormal expression of synaptic adhesion and active zone proteins (Murthy et al., 2009b; Vetter et al., 2007; Vetter et al., 1999). Thus, interactions of both α9/10-nAChRs and SK2 channels with postsynaptic components are likely required for the maturation and maintenance of hair cell efferent innervation. Further studies will be required to determine whether and how α9/10-nAChRs and SK2 channels interact with the APC protein complex and to identify the specific roles of these interactions. It will also be interesting to examine the potential involvement of other APC-associated synaptic proteins in olivocochlear synapse assembly, including PSD-93, PSD-95, and/or neurexin and neuroligin (Rosenberg et al., 2010; Temburni et al., 2004; Yanai et al., 2000). In summary, our identification of conserved nicotinic synapse components at the unique inhibitory nicotinic synapse in hair cells indicates that common mechanisms may direct the assembly of diverse synapses and suggests new possibilities for future studies of olivocochlear synapse assembly.

Chapter 3

Regulation of SK2 channel and α9/10-nAChR interactions and localization by alternative splicing and calcium

Elizabeth K. Storer, Antonella Pirone, Daniel H. Cox, and Michele H. Jacob

This chapter will be submitted as a manuscript for publication in the Journal of Neuroscience.

Abstract

Hearing sensitivity in the cochlea is modulated by efferent olivocochlear innervation of outer hair cells. At olivocochlear postsynaptic sites in hair cells, α9/10 nicotinic acetylcholine receptors (nAChRs) activate small conductance Ca^{2+}-sensitive SK2 potassium channels, resulting in hair cell hyperpolarization and frequency-selective suppression of afferent sound transmission. These inhibitory responses are critical for normal regulation of sound sensitivity and frequency selectivity. However, the mechanisms underlying the functional coupling of α9/10-nAChRs and SK2 channels are undefined. Here we show that SK2 channels form a multiprotein complex with α9/10-nAChRs and the actin-binding protein α-actinin-1. The composition and localization of this complex are regulated by alternative splicing, as shown by the expression during chick cochlear development of a previously identified SK2 splice variant, SK2-ARK, that differs from SK2 in its protein interactions, and surface expression. We also show that changes in Ca^{2+} concentration and calmodulin interactions that occur during synaptic activity differentially alter the protein interactions of SK2 and SK2-ARK. Thus, our studies implicate multiple interacting mechanisms in the assembly and function of olivocochlear postsynaptic sites.

Introduction

Mechanosensory hair cells in the cochlea are innervated by efferent olivocochlear (OC) fibers originating in the brainstem (Campbell and Henson, 1988). Inhibitory signals from OC efferents suppress the active mechanical processes by which outer hair cells (OHCs) amplify afferent auditory signals detected by inner hair cells (IHCs) (Brown and Nuttall, 1984; Galambos, 1956; Murugasu and Russell, 1996). Efferent inhibition is critical to normal hearing sensitivity and frequency selectivity (Walsh et al., 1998; Wersinger and Fuchs, 2010) and may protect the cochlea from noise-induced damage (Maison et al., 2002; Taranda et al., 2009b; Zheng et al., 1997a; Zheng et al., 1997b).

Efferent inhibition in mammals and avians is mediated by α9/10 nicotinic acetylcholine receptors (nAChRs), which are functionally coupled to small conductance Ca^{2+}-activated potassium (SK2) channels: Ca^{2+} influx through α9/10-nAChRs and subsequent activation of SK2 channels results in potassium efflux and hair cell hyperpolarization (Fuchs and Murrow, 1992a; Oliver et al., 2000; Yuhas and Fuchs, 1999). SK2 channels are activated by increases in intracellular Ca^{2+} in the sub-micromolar range. Gating is controlled by calmodulin (CaM), which binds to two antiparallel α-helices in the SK2 C-terminal. The C-lobe of CaM interacts constitutively with the SK channel α1 and a2 helices, independently of Ca^{2+} (Xia et al., 1998). In the presence of Ca^{2+}, the CaM N-lobe binds to the α2 helix of an adjacent SK subunit, inducing conformational changes in the SK2-CaM complex and opening of the channel (Xia et al., 1998; Keen et al., 1999; Schumacher et al., 2001). SK2 activity is also regulated by opposing

effects of CK2 kinase and protein phosphatase 2A (PP2A), which associate with the channels and regulate Ca^{2+} sensitivity through phosphorylation of CaM (Allen et al., 2007; Bildl et al., 2004).

The fast kinetics of synaptic Ca^{2+} influx and subsequent SK2-mediated potassium currents suggest that SK2 channels and α9/10-nAChRs are co-localized to microdomains in the hair cell membrane, possibly within 10nm (Oliver et al., 2000). The ability of fast- but not slow-binding Ca^{2+} buffers to reduce or eliminate the potassium component of the hair cell synaptic currents also supports the fast activation of SK2 channels by localized nAChR-mediated Ca^{2+} entry (Fuchs and Murrow, 1992a; Oliver et al., 2000). The mechanisms that direct the assembly of efferent postsynaptic sites and the localization of α9/10-nAChRs and SK2 channels are not well understood. Though electrophysiological studies strongly suggest that nAChRs and SK2 co-localize, lack of antibodies against α9- or α10-nAChRs has precluded immunohistochemical or biochemical studies to identify the underlying mechanisms. However, studies of SK2 deletion and developmental expression patterns suggest that, in addition to their central role in hair cell hyperpolarization, SK2 channels may also play a crucial role the development and/or maintenance of efferent synapses. The appearance of SK2 clusters in inner hair cells during neonatal development tightly coincides with the appearance of α-bungarotoxin-labeled α9/10-nAChR clusters and with synaptic responses to efferent stimulation (Roux et al., 2011). Significantly, acetylcholine-evoked currents are completely absent from OHCs of SK2-knockout mice, despite normal α9- and α10-nAChR mRNA levels (Kong et al., 2008).

Furthermore, SK2-knockout mice show complete degeneration of efferent presynaptic terminals between postnatal stages and adulthood (Murthy et al., 2009a). By contrast, α9- and α10-knockout mice retain efferent innervation, though bouton morphology is abnormal and cholinergic sensitivity is lost (Vetter et al., 2007; Vetter et al., 1999). α9-knockout mice also show normal postsynaptic SK2 localization (Murthy et al., 2009a). Together, these studies indicate that SK2 is specifically required for the maintenance of efferent synapses and functional surface expression of α9/10-nAChRs. How SK2 may direct α9/10 localization is unclear, though it has been suggested that SK2 channels and α9/10-nAChRs are indirectly linked in a pre-assembled complex whose membrane expression and localization are controlled via SK2 (Kong et al., 2008; Murthy et al., 2009a).

Several protein binding partners that modulate SK2 surface expression have already been identified. Constitutive, Ca^{2+}-independent association of CaM is required for SK2 surface expression, as demonstrated by a lack of functional surface expression of an SK2 mutant with weakened CaM binding (Lee et al., 2003). SK2 channels have also been shown to interact with α-actinin-2 (Lu et al., 2007). α-actinins are a family of actin cross-linking proteins which contain an N-terminal actin binding domain, a central rod domain with four spectrin repeats, and four C-terminal EF hands. Multiple α-actinin isoforms have been characterized in skeletal and smooth muscle, as well as in the brain and other tissues. These isoforms differ in the Ca^{2+}-binding capability of the EF hands. EF hands of non-muscle α-actinin-1 and -4 isoforms bind Ca^{2+}, which negatively

regulates binding to actin. Muscle-specific α-actinin-2 and -3 isoforms lack critical Ca^{2+}-binding residues in the EF hands and consequently are not sensitive to Ca^{2+} (Sjoblom et al., 2008). In cardiac myocytes, α-actinin-2 links SK2 channels to $Ca_v1.3$ channels, thereby positioning the Ca^{2+}-sensitive SK2 channels close to a Ca^{2+} source (Lu et al., 2007). Interaction with α-actinin-2 is also required for functional SK2 membrane localization in native cardiac myocytes and in heterologous cells, suggesting that α–actinin-2 may promote SK2 membrane insertion and/or retention via linkage to the actin cytoskeleton (Lu et al., 2009; Lu et al., 2007).

In our studies, we sought to identify protein interactions and other mechanisms involved in the assembly and trafficking of a putative SK2-α9/10-nAChR protein complex. We begin by identifying new interactions of SK2 channels. We show that SK2 interacts with α9/10-nAChRs when expressed in *Xenopus laevis* oocytes. We also identify α-actinin-1 as a novel binding partner of SK2 channels in chick hair cells. We then show that an SK2 alternative splice variant (Matthews et al., 2005) is expressed during chicken cochlear development and demonstrates altered Ca^{2+} sensitivity, protein interactions, and localization of SK2 channels and co-expressed α9/10-nAChRs. Finally, we investigate the potential effects of synaptic activity on the SK2 complex and show that Ca^{2+} and CaM modulate interactions of SK2 with its binding partners. Overall, our results suggest a model in which synaptic activity regulates olivocochlear synapse assembly and function in chick hair cells by changing the composition of the postsynaptic SK2-nAChR protein complex. These effects may

be further modulated by expression of the SK2-ARK splice variant, which differs from SK2 in its protein interactions, surface localization, and response to activity.

Methods

Antibodies

Primary antibodies used were: monoclonal anti-α-actinin (clone BM-75.2, Sigma); monoclonal anti-α-actinin-1 (United States Biological); polyclonal anti-MAGI-2/S-SCAM (Sigma); polyclonal anti-SK2 potassium channel (Sigma); monoclonal anti-SV2 (Developmental Studies Hybridoma Bank); polyclonal anti-MBP (maltose binding protein; New England Biolabs); monoclonal anti-GST (glutathione S-transferase; B-14, Santa Cruz Biotechnology); monoclonal anti-calmodulin (clone 6D4, Sigma); monoclonal anti-HA (clone 3F10, Roche Diagnostics); monoclonal anti-cortactin (clone 4F11, Millipore); monoclonal anti-sodium/potassium ATPase (Thermo Scientific). Secondary antibodies used were: Cy3 donkey anti-mouse IgM (Jackson ImmunoResearch); Alexa-Fluor-488 and -594 donkey anti-rabbit and goat anti-mouse IgG (Molecular Probes); horseradish peroxidase-conjugated goat anti-mouse and anti-rabbit (Bio-Rad); horseradish peroxidase-conjugated goat anti-rat (GE Healthcare).

Chicken embryos

Embryonated White Leghorn chicken eggs were obtained from the University of Connecticut Poultry Farm (Storrs, CT) or Charles River Spafas. Embryos were

kept at 37°C in forced air-draft humidified incubators until embryonic day (E)12-20.

Immunolabeling

Cochlear ducts were dissected from chicken embryos at E19-20. For SK2 immunolabeling, cochleae were fixed for 1 hour in 2% paraformaldehyde at 4°C, cryoprotected by immersion in increasing concentrations of sucrose, and embedded in 7.5% gelatin with 15% sucrose. For S-SCAM and α-actinin immunolabeling, cochleae were fixed in 4% paraformaldehyde with 15% picric acid, cryoprotected, and embedded in TissueTek OCT compound (Electron Microscopy Sciences). 10μM cryosections were blocked with 5% normal donkey serum (Jackson Immunoresearch) or 0.25% teleost gelatin (Sigma Aldrich, St. Louis, MO, USA) and incubated at room temperature with primary antibodies for 1 hour and secondary antibodies for 45 minutes.

Single hair cell immunolabeling

Hair cell isolation was performed according to previously described methods (Li et al., 2009) with minor modifications. Cochlear ducts were dissected from E19-E20 chicken embryos, and basilar papillae were dissociated in extracellular fluid (ECF) (in mM: 154 NaCl, 6 KCl, 5 $CaCl_2$, 2 $MgCl_2$, 10 glucose, 5 HEPES pH 7.4) or in low-divalent ECF ($CaCl_2$ reduced to 100mM, $MgCl_2$ omitted). In some experiments, cochlear ducts were incubated for 1 minute in 0.01% Type XXIV protease (Sigma) in ECF before dissection of the basilar papillae. Cells were

allowed to adhere to SuperFrost Plus slides (Fisher Scientific) and fixed in 2% paraformaldehyde for 30 minutes. The cells were then permeabilized and blocked in 5% normal donkey serum with 0.1% Triton X-100 and incubated with primary antibodies for 1 hour and secondary antibodies for 45 minutes. All steps were performed at room temperature.

Image analysis

Epifluorescence images were captured using a Zeiss Axioskop epifluorescence microscope (Thornwood, NJ, USA) and QImaging Retiga 200R CCD camera (Surrey, BC, Canada) with Nikon Instruments NIS Elements software. Confocal images were captured using a Leica TCS SP2 confocal microscope with HeNe (633nm), Kr (568nm), and Ar (488nm) lasers and a 63x 1.32 numerical aperture lens. Optical sections were taken in 0.5μM steps. For each cell, 3 consecutive sections through a representative region were compressed for analysis. For labeled cochlea sections, epifluorescence images or confocal stacks from representative cells were used to assess co-localization of double-labeled proteins. Pixel intensities were measured along ~3μM lines drawn across a representative region of the efferent synapse. Postsynaptic localization was concluded if peak intensity coincided with that of a known postsynaptic protein or was distinct from that of a known presynaptic protein.

RT-PCR and α-actinin sequencing

Total RNA was isolated from cochlear ducts dissected from E19 chicken embryos using TRIzol Reagent (Invitrogen). Reverse transcription was performed using oligo (dT) primers and SuperScript II reverse transcriptase (Invitrogen). PCR amplification was performed with Taq DNA Polymerase (Invitrogen) and primers common to chicken skeletal muscle, smooth muscle, and non-muscle α-actinin isoforms: 5'- GACAACAAGCACACCAACTACACCATGGAGCA-3' (forward), 5'- ATCTGCTGTTTCCCGGGACATGAAGTCAATGAAGG-3' (reverse). PCR product of the expected size was extracted from agarose gel and sequenced.

SK2-ARK splice variant quantification

Total RNA isolated from chicken cochlear ducts at E12-14, E17, and E20 was used for reverse transcription PCR as described above, using SK2-specific primers flanking the ARK splice insertion site: 5'-ACTTACGGATCCAATTTCATGATGGACACCCA-3' (forward), 5'-CATGTATGACATGATCTCTGCTCGAGTCAGTA-3' (reverse). PCR products were subcloned into pcDNA3.1 (Invitrogen) and grown on LB-ampicillin plates. SK2 clones were amplified by PCR from individual colonies, and PCR products were digested with the restriction enzyme Hpy188I (New England Biolabs), whose recognition site is uniquely present in the ARK splice insertion. The presence or absence of digestion products were assessed by agarose gel

electrophoresis. Results were verified by sequencing of randomly selected clones.

Protein expression in Xenopus laevis oocytes

Full length chicken SK2 or SK2-ARK (GenBank accession no. NM_204798), a9-nAChRs (no. NM_204760), C-terminal HA-tagged α10-nAChRs (no. XM_428183), and human α-actinin-1 (no. NM_001130004) were cloned into the pOx oocyte expression vector. *In vitro* cRNA synthesis was performed using the mMessage mMachine T3 transcription kit (Applied Biosystems). Oocytes were obtained from adult *Xenopus laevis* frogs and defolliculated in OR2 (in mM: 82.5 NaCl, 2 KCl, 0.5 $MgCl_2$, 5 HEPES pH 7.6) containing 2mg/ml collagenase (Sigma) and 1mg/ml dispase II (Roche Applied Science). Stage V oocytes were injected with 14-15ng each of α9-nAChR and α10-nAChR-HA cRNA, 10-14ng of α-actinin-1 cRNA, and/or 3-8ng of SK2 or SK2-ARK cRNA. Oocytes were maintained at 19°C for 2-3 days in ND96 (in mM: 96 NaCl, 2 KCl, 1 $MgCl_2$, 1.8 $CaCl_2$, 5 HEPES pH 7.6) supplemented with 2.5mM sodium pyruvate, 50mg/ml tetracycline, 50mg/ml gentamicin, 100mg/ml amikacin, and 100mg/ml ciprofloxacin (all from Sigma).

Electrophysiology

cRNAs encoding the chicken SK2 subunits were injected into Stage V Xenopus oocytes at 3 ng/oocyte. SK2 currents were recorded under voltage clamp from these oocytes between 2 and 5 days after injection. Recordings were

made in the inside-out patch-clamp configuration using an Axon 200B patch-clamp amplifier, and a Macintosh-based computer system running PatchMaster Software (HEKA Inc.). Patch pipettes were made of borosilicate glass and had resistances of between 1 and 1.5 Mohms in our standard internal and external solutions.

The internal (bath) solution contained in mM: 140 $KMeS0_3$, 20 HEPES, 2 KCl, 1 EGTA and $CaCl_2$ as needed (see below). The external (pipette) solution contained in mM: 140 $KMeS0_3$, 20 HEPES, 2 KCl, and 2 $MgCl_2$. After patch excision, solutions containing differing concentrations of free Ca^{2+} were superfused onto the cytoplasmic face of each patch using a DAD12 (ALA Scientific) sewer-pipette style superfusion system. Solutions were exchanged in less than 1 sec.

During each experiment a voltage step from 0 to +50 mV was applied for 20 milliseconds five times consecutively. The resulting five current responses were later averaged before analysis. Current responses where recorded from each patch at the following Ca^{2+} concentrations in μM: 0.01, 0.1, 0.2, 0.5, 0.7, 1, 3, and 10. Ca^{2+} solutions were prepared by adding to our standard internal solution, which contained 1 mM EGTA, the correct amount of $CaCl_2$ (100 mM Orion Standard), as calculated with MaxChelator Software (http://maxchelator.stanford.edu/) to achieve the desire free [Ca^2]. We assumed our standard internal solution contains 10μM total Ca^{2+}, when no Ca^{2+} was intentionally added — as we have measured previously.

The amplitude of the SK2 current was measured as the difference between the current observed at 0 mV and that observed at +50 mV at the center of the voltage step. These current amplitudes ΔI were then used to plot Ca^{2+} dose-response curves for each patch. Each curve was then fitted with the Hill equation (Hill, 1910) below and normalized to the maximum of the fit:

$$\Delta I = \Delta I_{Min} + \frac{\Delta I_{Max}[Ca]^H}{[Ca]^H + KD^H}$$

Here ΔI_{Min} and ΔI_{Max} are the minimum and maximum of the curve respectively. *KD* is the [Ca^{2+}] at half-maximal response, and *H* is the Hill coefficient. Normalized dose-response curves from patches expressing the same channel type were then averaged to produce the mean dose-response curves shown in Figure 3.4.

Recombinant peptide binding assays

Maltose binding protein (MBP) fusions of chicken SK2 and SK2-ARK were created by cloning of C-termini PCR products (aa 368-553) into the pMalC2 vector (New England Biolabs). A glutathione S-transferase (GST) fusion of α-actinin-1 (97% homology to chicken non-muscle α-actinin) was created by cloning full-length α-actinin-1 (kind gift of Dr. David Critchley, University of Leicester) into the pGex4T3 vector (GE Healthcare). Fusion peptides were expressed in Rosetta-gami 2(DE3) cells (EMD Chemicals) and grown in LB media containing 0.5M NaCl and 2.5 mM betaine. Peptides were purified using GST-sepharose or amylose resin.

For binding assays, SK2- or SK2-ARK-MBP peptides and amylose resin were incubated with α-actinin-1-GST in Tris-Tx buffer (in mM: 10 Tris pH 7.6, 50 NaCl, 5 EDTA, 30 $Na_4P_2O_7$, 50 NaF, 0.4 Na_3VO_4, 1% Triton X-100) supplemented with protease inhibitor cocktail (Thermo Scientific) and phosphatase inhibitor cocktail (Roche Applied Science). Beads were washed 3 times with Tris-Tx buffer. Complexes were eluted, separated on SDS-PAGE gels, and transferred to nitrocellulose membranes (Bio-Rad). Pulldown of α-actinin-1-GST was detected using anti-GST antibody, ECL Plus detection system (GE Healthcare) and LAS-4000 imaging system (Fujifilm Life Sciences). Band densities were quantified using Nikon Instruments NIS Elements software and normalized to SK2 or SK2-ARK levels in the same lane detected with anti-MBP antibody. SK2- or SK2-ARK-MBP peptides were also used to pull down purified bovine brain calmodulin (EMD Chemicals). Bound proteins were separated by SDS-PAGE and transferred to PVDF membranes (Bio-Rad). Membranes were fixed in 0.2% glutaraldehyde for 1 hour before immunoblotting with anti-calmodulin antibody. Specificity controls included pulldown of GST with SK2- or SK2-ARK-MBP, and pulldown of α-actinin-1-GST or calmodulin by MBP.

For α-actinin-1/calmodulin competition assays, SK2- or SK2-ARK-MBP were incubated with amylose resin and α-actinin-1-GST in Tris-Tx buffer containing either 5mM BAPTA (EMD Chemicals) or 1mM $CaCl_2$. Bound complexes were washed, and calmodulin was added at 0, 0.5, 1, or 10mM. Alternatively, SK2 or SK2-ARK peptides and amylose resin were incubated first with 10mM calmodulin

in BAPTA or $CaCl_2$ buffer, washed, then incubated with α-actinin-1-GST. Proteins were eluted and α-actinin-1-GST pulldown was assayed as above.

Co-immunoprecipitation from cochlear membrane fractions

Membrane fractions were prepared from cochlear ducts dissected from E19-20 chick embryos. Tissue was homogenized on ice in sucrose buffer (in mM: 320 sucrose, 10 HEPES, 1 EGTA) with protease inhibitor cocktail and centrifuged at approximately 2,000 x g for 10 minutes. The supernatant was centrifuged at 100,000 x g for 1 hour, and the resulting membrane pellet was resuspended in membrane buffer (in mM: 190 NaCl, 10 KCl, 1 EGTA, 10 HEPES pH 7.4) with protease inhibitors. The suspension was sonicated and centrifuged again at 100,000 x g for 30 minutes to remove insoluble material. The supernatant was pre-cleared for 1 hour with protein G agarose beads (Roche Applied Science) and incubated overnight at 4°C with 8mg of anti-SK2 antibody. Immunocomplexes were precipitated with protein G agarose beads and washed 6 times with membrane buffer supplemented with 0.1% Triton X-100. Proteins were eluted, separated on SDS-PAGE gels, and immunoblotted using anti-α-actinin-1 antibody, ECL Plus detection, and exposure to X-ray film (GE Healthcare). As a specificity control, equivalent membrane fractions were immunoprecipitated with 8mg anti-HA antibody. In some experiments, 5mM BAPTA was added to all buffers.

Co-immunoprecipitation from oocytes

Xenopus laevis oocytes were injected with cRNA encoding chicken SK2 or SK2-ARK, HA-tagged chicken α10-nAChR, chicken α9-nAChR, and human α-actinin-1 as above. Oocytes for control experiments were injected with only α9, α10-HA, and α-actinin-1 cRNA. Total oocyte membrane fractions were used for SK2 immunoprecipitation. 3 days after injection, 45-75 oocytes were homogenized in 4-6mL/oocyte ice cold buffer H (in mM: 83 NaCl, 1 $MgCl_2$, 5 EDTA, 5 EGTA, 10 HEPES pH 7.8) and centrifuged for 10 minutes at 750 x g. Pellets were resuspended in a second volume of buffer H and centrifuged again. Combined supernatants were layered onto 7mL 15% sucrose in buffer H and centrifuged for 90 minutes at 160,000 x g. Membrane pellets were resuspended in 2-4mL/oocyte Tris-Tx buffer with protease and phosphatase inhibitors and incubated for 1 hour at 4°C with gentle agitation to solubilize membrane proteins. Insoluble material was removed by centrifugation at 100,000 x g for 1 hour. Soluble proteins were pre-cleared with protein G agarose and incubated overnight with 6-9mg anti-SK2 antibody. Immunocomplexes were precipitated with protein G agarose beads and washed 3 times with Tris-Tx buffer. Bound proteins were separated on SDS-PAGE gels and transferred to nitrocellulose membranes. Co-precipitation of α9/10-nAChRs and α-actinin-1 was assessed by immunoblotting with anti-HA or anti-α-actinin-1 antibodies. Band intensities were normalized to precipitated SK2 in the same lane and to total expression in membrane inputs.

For BAPTA-AM experiments, oocytes were incubated for 2 hours at 19°C with 50mM BAPTA-AM in ND96 or control ND96 before membrane fractionation and immunoprecipitation. 10mM BAPTA was added to all buffers used for BAPTA-AM-treated samples; for untreated controls, BAPTA and/or EGTA were omitted.

Surface biotinylation and endocytosis assay

Surface expression and endocytosis of proteins expressed in oocytes were measured by cell surface biotinylation assays (Harris et al., 2008; Rosenberg et al., 2008). 3 days after injection, oocytes were incubated for 30 minutes at 4°C in 1mg/ml EZ-Link Sulfo-NHS-LC-Biotin (Thermo Scientific) to biotinylate surface proteins. Excess reagent was quenched by 3 washes in cold quench buffer (192mM glycine, 25mM Tris-HCl in ND96). Biotinylated oocytes were collected immediately to measure baseline surface expression or returned to 19°C to allow endocytosis of biotinylated proteins. 34-40 oocytes per collection time were used to prepare membrane fractions essentially as described above, using 400mL volumes of buffer H. Membrane pellets were resuspended in ASB-14 buffer (in mM: 120 NaCl, 5 EDTA, 30 $Na_4P_2O_7$, 50 NaF, 50 Tris-HCl pH 7.6, 0.1% ASB-14) with protease inhibitors and incubated overnight at 4°C with gentle agitation. Insoluble material was removed by centrifugation at 16,000 x g for 30 minutes. Streptavidin-agarose beads (Thermo Scientific) were added to precipitate biotinylated proteins and washed 4 times in Tris-Tx buffer. Bound proteins were eluted and separated on SDS-PAGE gels. Levels of biotinylated SK2 and α9/10-nAChRs were assessed by immunoblotting and normalized to input membrane

expression. Background precipitation from unbiotinylated samples was subtracted from each measurement. As a negative control, membranes were probed with antibodies against intracellular proteins to confirm specific biotinylation of surface proteins.

Results

α-actinin-1 is expressed in hair cells and interacts with SK2 channels

To explore mechanisms of SK2 channel localization and functional modulation in cochlear hair cells, we sought to identify proteins that interact with SK2. In cardiac muscle, SK2 channels interact with α-actinin-2, which is necessary for functional membrane expression (Lu et al., 2009; Lu et al., 2007). To determine whether α-actinins also interact with SK2 channels at postsynaptic sites in cochlear hair cells, we looked for postsynaptic localization of immunolabeled α-actinin in sections of chick basilar papilla (Figure 3.1). We have previously identified synaptic scaffolding molecule (S-SCAM), a scaffolding protein at neuronal nicotinic synapses (Rosenberg et al., 2008), as a postsynaptic marker at efferent hair cell synapses (see Chapter 2). We found that α-actinin was concentrated at efferent postsynaptic sites in chicken hair cells based on co-localization with postsynaptic S-SCAM (Figure 3.1a). To better understand the function of α-actinin in hair cells, we isolated and sequenced a reverse-transcription PCR product of α-actinin amplified from E19 chick cochlea RNA. Our results indicated that the α-actinin isoform expressed in hair cells is not

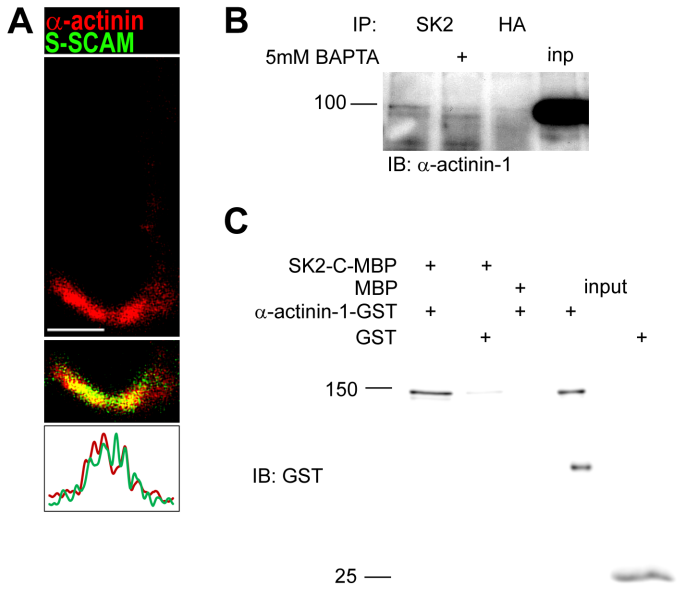

Figure 3.1: α-actinin-1 localizes to postsynaptic sites in hair cells and interacts with SK2 channels.

(A) Confocal image and pixel intensity profile showing co-localization of α-actinin and S-SCAM immunofluorescence in an E19 chick hair cell. Scale bar = 5μM. (B) Immunoprecipitation of SK2 channels from E20 chicken cochlea lysates shows co-precipitation of α-actinin-1 in the presence or absence of 5mM BAPTA. Negative control shows no α-actinin-1 co-precipitated with anti-HA antibody. (C) Direct interaction of GST-tagged α-actinin-1 with the MBP-tagged C-terminal of SK2. Negative controls show no nonspecific interactions with MBP or GST alone (lanes 2,3).

the α-actinin-2 isoform that interacts with SK2 in heart muscle, but a Ca^{2+}-sensitive non-muscle α-actinin isoform whose amino acid sequence is 97% homologous to human α-actinin-1 (Millake et al., 1989; Waites et al., 1992). Accordingly, we used an α-actinin-1-specific antibody for Western blotting and co-immunoprecipitation assays to determine whether the α-actinin-1 isoform that is expressed in the cochlea interacts with SK2. We found that α-actinin-1 is expressed in chick cochlea membrane fractions and co-immunoprecipitated with SK2 channels (Figure 3.1b). Because sequences in the C terminal of SK2 channels have been previously shown to bind to α-actinin-2 (Lu et al., 2009; Lu et al., 2007), we tested for binding of α-actinin-1 to the SK2 C terminal in recombinant peptide binding assays. We found that an MBP-tagged SK2 C-terminal construct pulled down GST-tagged α-actinin-1 (Figure 3.1c). GST alone did not co-precipitate with SK2-C-MBP, and MBP alone could not co-precipitate α-actinin-1-GST. Taken together, our results show that α-actinin-1 is concentrated at postsynaptic sites in chick hair cells and interacts directly with SK2 channels.

SK2 interacts with α9/10-nAChRs

Because studies of α9/10-nAChRs endogenously expressed in the cochlea are limited by unavailability of antibodies, we expressed them in *Xenopus laevis* oocytes in order to determine whether they interact and co-traffick with SK2 channels. We tagged the chicken α10-nAChR subunit with a hemagglutinin (HA) epitope tag and injected oocytes with cRNA encoding α9- and HA-α10-nAChRs,

SK2, and α-actinin-1. Three days after injection, we prepared membrane fractions from oocytes and immunoprecipitated SK2 channels. Significantly, we also found that HA-tagged α9/10-nAChRs co-immunoprecipitated with SK2 channels from oocyte membranes; this interaction was specific, as sodium potassium ATPase did not co-precipitate with SK2 (Figure 3.2a). As a negative control, SK2 antibody did not co-precipitate α9/10-nAChRs from oocytes not expressing SK2 (data not shown). To our knowledge, this is the first demonstration of a physical association between SK2 and α9/10-nAChRs. In accord with interaction of α-actinin-1 with SK2 in the cochlea (Figure 3.1), we also found that exogenously expressed α-actinin-1 co-precipitated with SK2 from oocyte membranes (Figure 3.2b).

Expression of the SK2-ARK splice variant during chick embryonic development

The SK2-ARK splice variant, containing a 3-residue "ARK" insertion in the C terminal, was previously identified in postnatal chicken short hair cells (Matthews et al., 2005). This insertion is constitutively present in trout SK2 channels, and a similar AQK sequence is found in the same region in mammalian SK1 channels; however, the ARK splice insertion has not been reported in mammalian SK2 channels (Figure 3.3a; Matthews et al., 2005). We wondered whether expression of SK2-ARK during development might play a role in the assembly and function of the efferent olivocochlear synapse. To determine whether SK2-ARK is present at embryonic stages in chickens, we isolated and subcloned SK2 RT-PCR

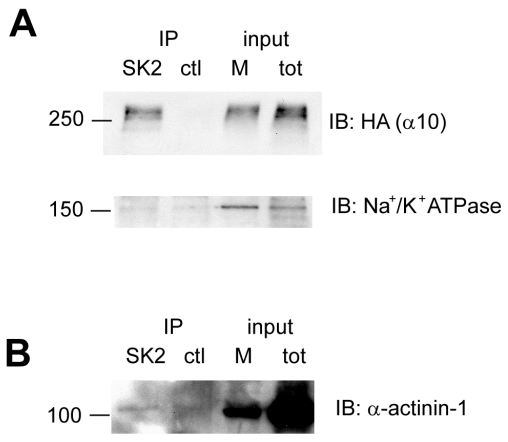

Figure 3.2: α9/10-nAChRs and α-actinin-1 interact with SK2 channels in *Xenopus* oocytes.
Immunoprecipitation of SK2 channels exogenously expressed in *Xenopus laevis* oocytes shows co-precipitation of co-expressed HA-tagged α9/10-nAChRs (A) and α-actinin-1 (B). Negative controls show no protein co-precipitation with an unrelated anti-mGluR5 antibody (ctl lane) and no co-precipitation of Na^+/K^{2+} ATPase with SK2.

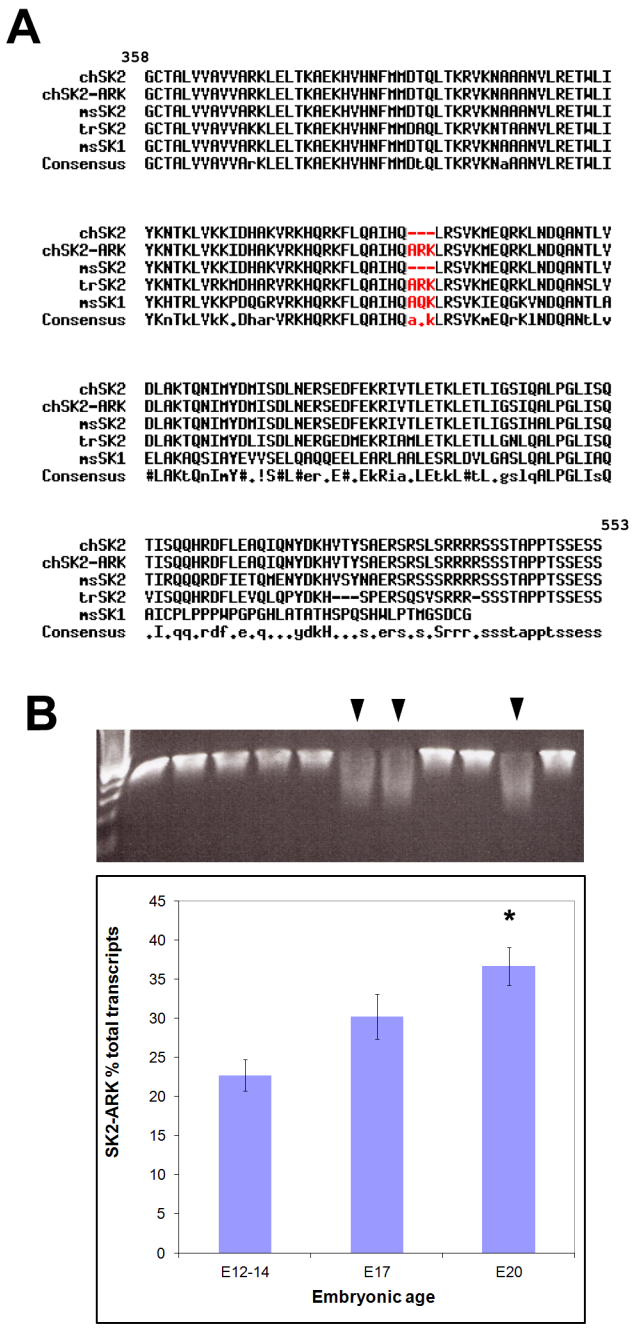

Figure 3.3: Expression of the SK2-ARK splice variant.
(A) C-terminal sequence alignments of chicken SK2 and SK2-ARK variants with mouse (GenBank accession no. P58390) and trout (no. NP_001117783) SK2 and mouse SK1 (no. Q9EQR3) channels showing the position of the ARK splice insertion. Numbers indicate amino acids of chicken SK2 channels. (B) RT-PCR products from E12-20 chicken cochleae were subcloned into pcDNA3.1 and grown in JM109 chemically competent cells. SK2 PCR products from individual clones were digested with Hpy188I and separated on 1% agarose gels (top). Arrowheads indicate digested SK2-ARK clones. Bottom: quantification of SK2-ARK transcripts. N = 3, 50-60 clones per age. * $p < 0.01$ compared to E12-14.

transcripts from E12-E20 chicken cochleae. Using an Hpy188I restriction digest site within the ARK splice insertion sequence (Figure 3.3b), we quantified the relative abundance of SK2 and SK2-ARK transcripts at different developmental stages. Our results demonstrate that the abundance of the SK2-ARK variant increases from approximately 23% of transcripts at E12-E14 to approximately 37% at E20 (Figure 3.3b; N=3, 50-60 clones analyzed per age per experiment.)

Functional characterization of the SK2-ARK variant

Because the ARK splice insertion is located within the Ca^{2+}-dependent CaM binding domain in the SK2 C-terminal, we wondered whether it might affect the CaM-mediated Ca^{2+} gating of SK2-ARK channels. We therefore tested for differences in Ca^{2+} sensitivity between the two variants. Two to three days after injection of cRNA encoding SK2 or SK2-ARK into *Xenopus laevis* oocytes, we recorded Ca^{2+} responses from inside-out patches to generate Ca^{2+} dose-response curves. Ca^{2+}-activated potassium currents recorded from SK2-expressing patches had an EC_{50} of 0.48 ± 0.0067 μM and a Hill coefficient of 4.90 ± 0.40. SK2-ARK channels demonstrated a steeper, right-shifted Ca^{2+} response curve caused by a significantly reduced normalized response to 0.5 mM Ca^{2+}, with an increased EC_{50} of 0.61 ± 0.019 μM and a Hill coefficient of 10.14 ± 1.84 (Figure 3.4a). These results demonstrate that the ARK insertion alters the response of the assembled channels to Ca^{2+}, which could suggest altered interactions with CaM. To test this possibility, we tested for changes in

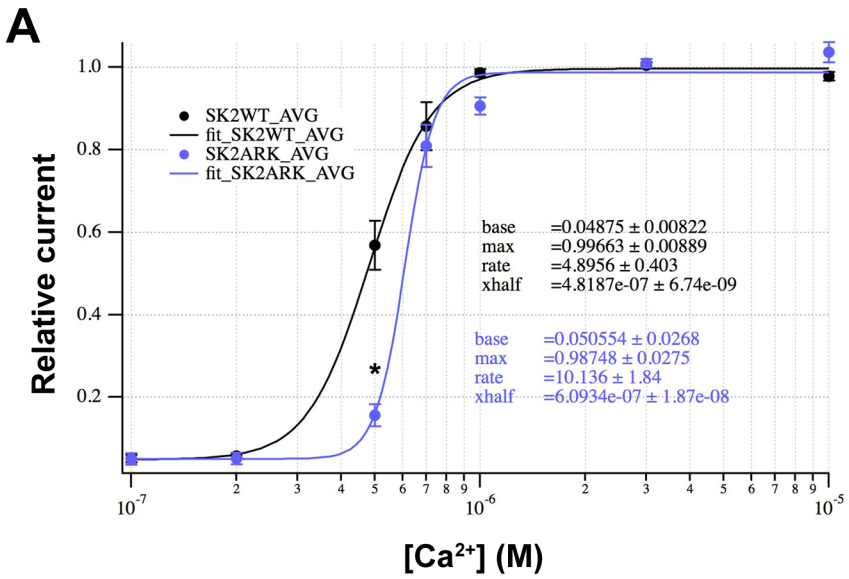
A
Relative current
1.0
0.8
0.6
0.4
0.2
SK2WT_AVG
fit_SK2WT_AVG
SK2ARK_AVG
fit_SK2ARK_AVG
base =0.04875 ± 0.00822
max =0.99663 ± 0.00889
rate =4.8956 ± 0.403
xhalf =4.8187e-07 ± 6.74e-09
base =0.050554 ± 0.0268
max =0.98748 ± 0.0275
rate =10.136 ± 1.84
xhalf =6.0934e-07 ± 1.87e-08
*
10-7
10-6
10-5
[Ca2+] (M)

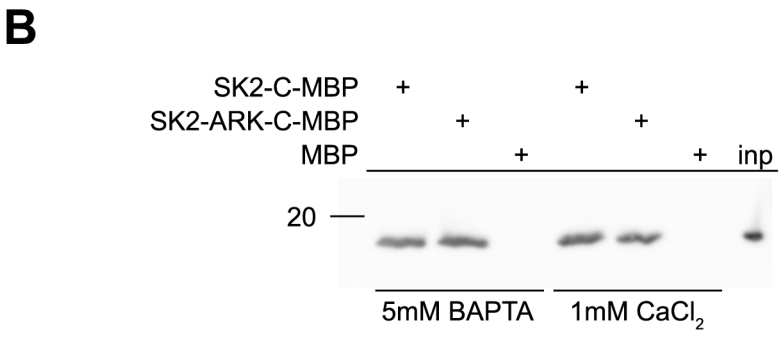
B
SK2-C-MBP + +
SK2-ARK-C-MBP + +
MBP + +
inp
20
5mM BAPTA
1mM CaCl2

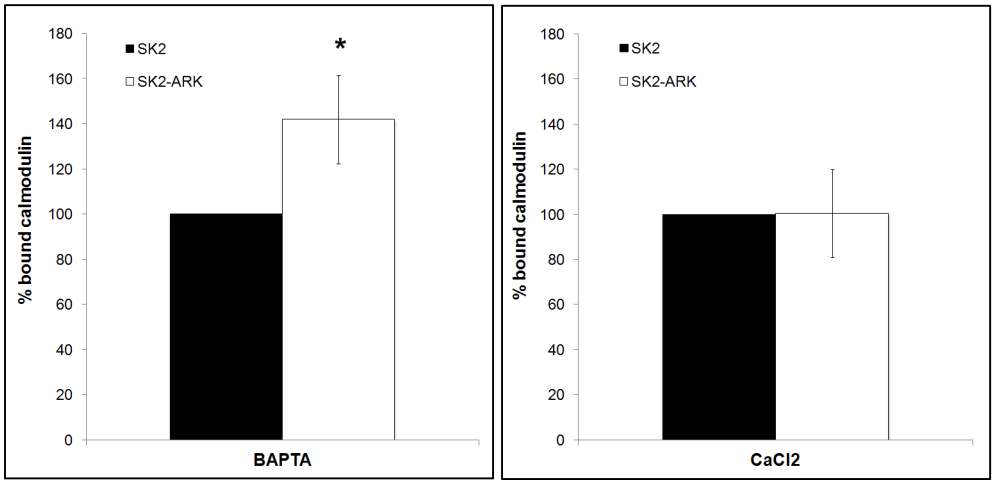
SK2
SK2-ARK
% bound calmodulin
180
160
140
120
100
80
60
40
20
0
*
BAPTA
CaCl2

binding of CaM to the MBP-tagged C-terminal of SK2 or SK2-ARK in recombinant peptide binding assays. We found no difference in binding of Ca^{2+}-bound CaM to the SK2-ARK C-terminal; however, we observed a small but significant increase in binding of SK2-ARK to CaM when Ca^{2+} was chelated with 5mM BAPTA (141.84 ± 19.44% compared to SK2; $p<0.05$, Figure 3.4b). Thus, our results demonstrate that the ARK splice insertion alters SK2 interactions with CaM and sensitivity to Ca^{2+}.

ARK splicing alters SK2-α9/10-nAChR interactions and surface expression

We have demonstrated interactions between SK2 channels and α-actinin-1 and α9/10-nAChRs. We wanted to determine whether the ARK splice insertion affects these interactions. We used co-immunoprecipitation and recombinant peptide binding assays to test for differences between SK2 and SK2-ARK in interactions with α9/10-nAChRs and α-actinin-1. We co-expressed SK2 or SK2-ARK with HA-tagged α9/10-nAChRs and α-actinin-1 in *Xenopus* oocytes and immunoprecipitated SK2 channels from membrane fractions. Intriguingly, we found a 73% increase in α9/10-nAChR co-precipitation with SK2-ARK compared

Figure 3.4: Ca^{2+} gating of SK2 and SK2-ARK channels.
(A) Mean normalized Ca^{2+} response curves for SK2 (black) and SK2-ARK (blue) currents recorded in inside-out patches of *Xenopu*s oocytes. SK2 and SK2-ARK currents during 50mV voltage steps were recorded in different Ca^{2+} concentrations. Curves were fitted with the Hill equation, and the resulting Hill coefficient (rate), EC_{50} (xhalf), and normalized base and maximum currents are indicated. (B) Interaction of purified recombinant calmodulin with MBP-tagged SK2 and SK2-ARK C-termini in direct peptide binding assays with 5mM BAPTA or 1mM $CaCl_2$. Graphs show normalized band densities of co-precipitated CaM. * in B: confidence interval at $p < 0.05$.


A
SK2
SK2-ARK
no SK2
IP
input
SK2 ctl M tot
250
IB: HA (α10)
IB: SK2
% nAChR co-precipitation
SK2
SK2-ARK
*

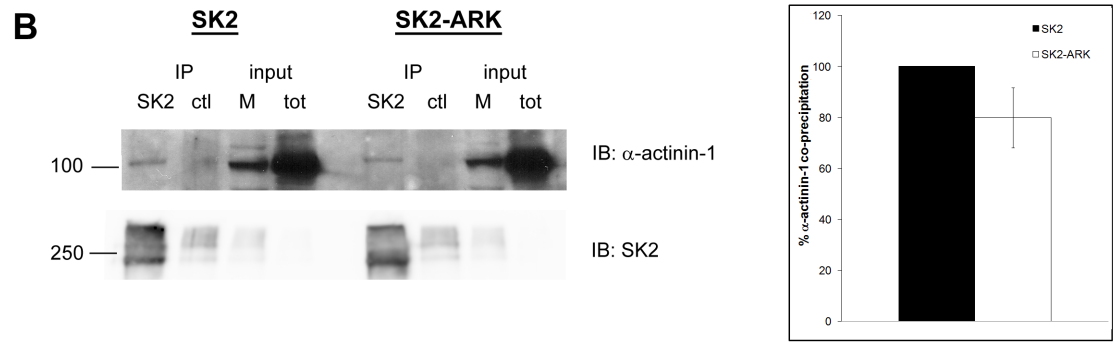
B
SK2
SK2-ARK
IP
input
SK2 ctl M tot
100
250
IB: α-actinin-1
IB: SK2
% α-actinin-1 co-precipitation
SK2
SK2-ARK

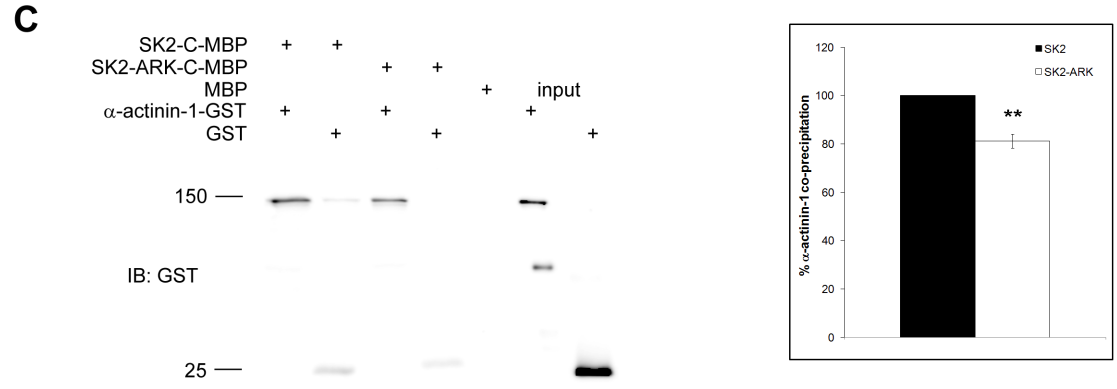
C
SK2-C-MBP
SK2-ARK-C-MBP
MBP
α-actinin-1-GST
GST
input
150
IB: GST
25
% α-actinin-1 co-precipitation
SK2
SK2-ARK
**

to SK2 (Figure 3.5a, $p<0.05$). In contrast, we found a non-significant 20% decrease in co-precipitation of α-actinin-1 with SK2-ARK compared to SK2 (Figure 3.5b, $p<0.09$). In recombinant peptide binding assays, we saw a similar decrease in binding of α-actinin-1-GST to SK2-ARK-MBP compared to SK2-MBP (Figure 3.5c, $p<10^{-10}$). Overall, these results demonstrate that the ARK splice insertion changes the interaction capabilities of SK2 channels. The absence of nAChR function in SK2-knockout hair cells suggests that SK2 may be critical for functional surface expression of α9/10-nAChRs (Kong et al., 2008; Murthy et al., 2009a). Furthermore, our observed increase in interaction of SK2-ARK with α9/10-nAChRs raises the possibility that the two variants of SK2 may exert different effects on α9/10 trafficking. To test this hypothesis, we looked for changes in surface expression of SK2 channels and α9/10-nAChRs expressed in *Xenopus* oocytes using cell surface biotinylation assays. We expressed HA-tagged α9/10-nAChRs and α-actinin-1 in oocytes alone or with SK2 or SK2-ARK. Surface proteins were biotinylated using a membrane-impermeant biotinylation reagent and precipitated with streptavidin-agarose beads (Figure 3.6a). We found that levels of surface biotinylated SK2-ARK were reduced to ~30%

Figure 3.5: ARK alternative splicing alters interactions of SK2 with α9/10-nAChRs and α-actinin-1.
Co-immunoprecipitation of HA-tagged α9/10-nAChRs (A) and α-actinin-1 (B) with SK2 and SK2-ARK channels exogenously expressed in *Xenopus laevis* oocytes. Negative controls show no α9/10-nAChR or α-actinin-1 co-precipitation with an unrelated antibody (ctl lanes) or with SK2 antibody from oocytes with no SK2 expression. (C) Direct interactions of GST-tagged α-actinin-1 with MBP-tagged SK2 or SK2-ARK C-termini. Negative controls show little or no nonspecific interactions with MBP or GST alone (lanes 2,4,5). Graphs show normalized band densities of co-precipitated proteins. Asterisks indicate confidence intervals at * $p < 0.05$ and ** $p < 10^{-10}$; n = 3.

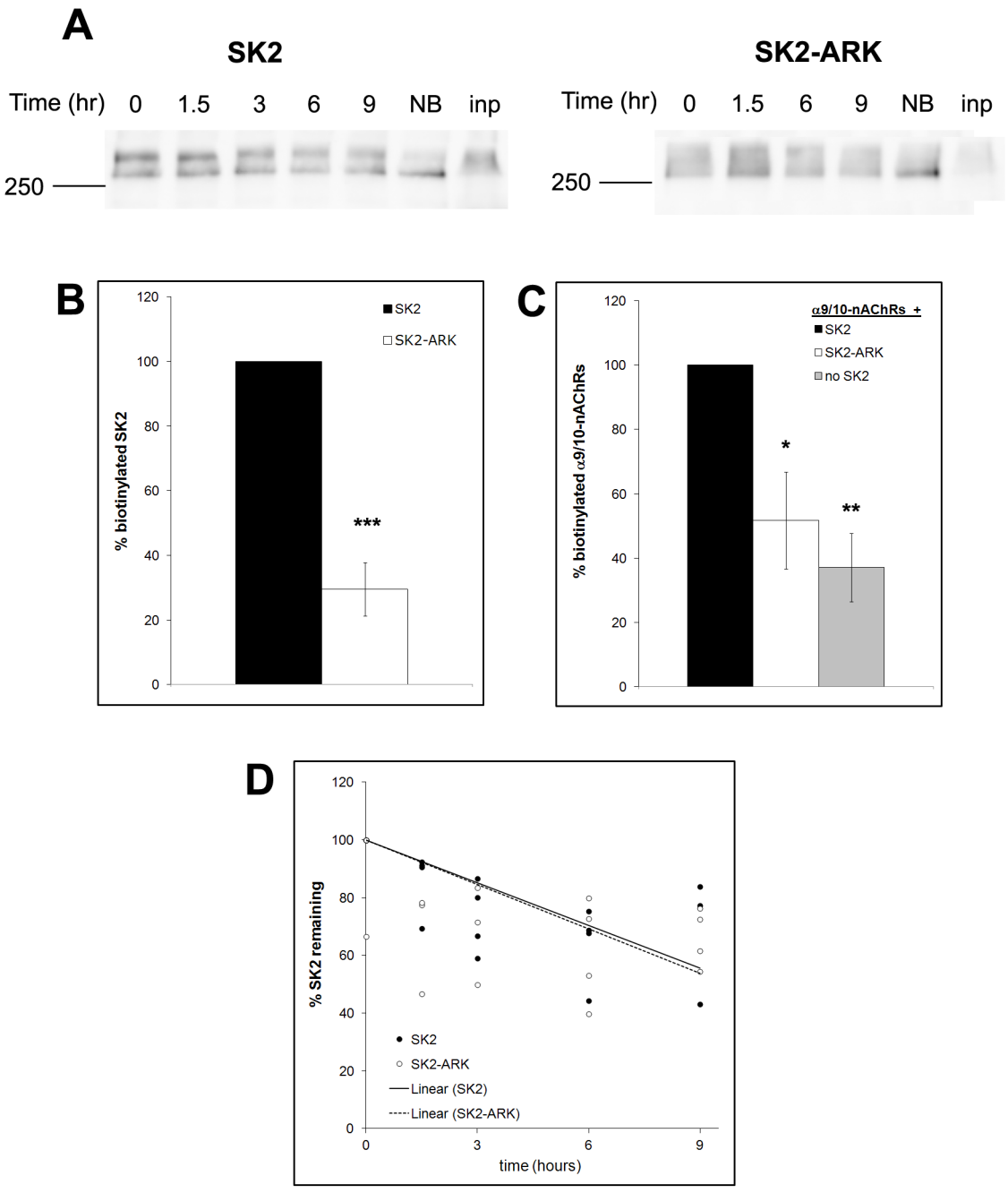
A
SK2
Time (hr) 0 1.5 3 6 9 NB inp
250
SK2-ARK
Time (hr) 0 1.5 6 9 NB inp
250
B
SK2
SK2-ARK
% biotinylated SK2
***
C
α9/10-nAChRs +
SK2
SK2-ARK
no SK2
% biotinylated α9/10-nAChRs
*
**
D
% SK2 remaining
SK2
SK2-ARK
Linear (SK2)
Linear (SK2-ARK)
time (hours)

compared to SK2 (Figure 3.6b, $p<10^{-16}$). Importantly, surface levels of HA-tagged α9/10-nAChRs were also significantly lower when they were expressed alone compared to co-expression with SK2 (37% compared to levels with SK2; Figure 3.6c, $p<10^{-8}$). Similarly, surface levels of α9/10-nAChRs co-expressed with SK2-ARK were reduced to ~50% compared to co-expression with SK2 (Figure 3.6c, $p<0.002$). Interestingly, there was no significant difference in surface levels of α9/10 when co-expressed with SK2-ARK versus alone.

In the same experiments, oocytes were incubated following biotinylation to allow endocytosis of labeled surface proteins. Percentages of initial surface biotinylated SK2 and SK2-ARK remaining at several time points after labeling were similar, suggesting that although membrane insertion of SK2-ARK is reduced compared to SK2, the two variants have similar surface stability over time (Figure 3.6a,d). Taken together, these data suggest that the SK2-ARK variant shows marked differences from SK2 in its linkage to α9/10-nAChRs, surface expression, and ability to facilitate α9/10 surface membrane expression.

Figure 3.6: Membrane expression of SK2, SK2-ARK, and α9/10-nAChRs. Surface biotinylation and endocytosis assays were performed on oocytes expressing HA-tagged α9/10-nAChRs and α-actinin-1 alone or with SK2 or SK2-ARK. Biotinylated proteins from oocytes collected at the indicated time points were precipitated with streptavidin-agarose. (A) Representative immunoblot of biotinylated SK2 and SK2-ARK. NB: background SK2 precipitation from non-biotinylated samples was subtracted from biotinylated band densities. Inp: input, oocyte membrane fractions showing total SK2 expression were collected prior to biotinylated protein precipitation. (B) Normalized band densities of biotinylated SK2 and SK2-ARK at time 0 (immediately following biotinylation). (C) Normalized time 0 band densities of α9/10-nAChRs expressed alone with α-actinin-1 or with SK2 or SK2-ARK as indicated. (D) Remaining levels of biotinylated SK2 or SK2-ARK at the indicated time points, relative to levels at time 0. Asterisks indicate confidence intervals at *$p < 0.005$, **$p < 10^{-9}$, and ***$< 10^{-15}$; n = 3-5.

SK2 interactions are modulated by Ca^{2+} and calmodulin

Activation of the efferent olivocochlear synapse and the resulting rise in local Ca^{2+} concentration triggers Ca^{2+}-dependent binding of calmodulin (CaM) to SK2 and conformational changes that mediate channel gating (Keen et al., 1999; Schumacher et al., 2001; Xia et al., 1998). Interaction of SK2 with α-actinin-2 is mediated by residues within the CaM-binding domain (CaMBD) (Lu et al., 2009; Lu et al., 2007). Furthermore, interactions of α-actinin-1 with other membrane proteins such as NR1 receptors have been shown to be inhibited by Ca^{2+}-bound CaM (Merrill et al., 2007). Therefore, we asked whether efferent synapse activity and the resulting conformational changes in Ca^{2+}-CaM interactions with SK2 might affect interactions of α-actinin-1 with SK2 or the SK2-ARK variant. We performed recombinant peptide binding assays to test for changes in binding of α-actinin-1-GST to SK2- or SK2-ARK-MBP in the presence of Ca^{2+} and after addition of CaM (Figure 3.7a). We found that Ca^{2+} alone strongly promoted binding of α-actinin-1-GST to both SK2 variants in the absence of CaM. SK2- and SK2-ARK-MBP showed, respectively, 3.2 ($p<10^{-15}$) and 6.8-fold ($p<0.0001$) increases in binding to α-actinin-1-GST in the presence of 1mM $CaCl_2$ compared to 5mM BAPTA. Similarly, we found reduced co-immunoprecipitation of α-actinin-1 with SK2 from *Xenopus* oocytes that were loaded with BAPTA-AM before membrane fractionation in 5mM BAPTA (Figure 3.7b; 79% compared to untreated, $p<0.05$). SK2-ARK showed a similar trend (80% compared to untreated; $p<0.09$). These data suggest that increased Ca^{2+} concentration upon

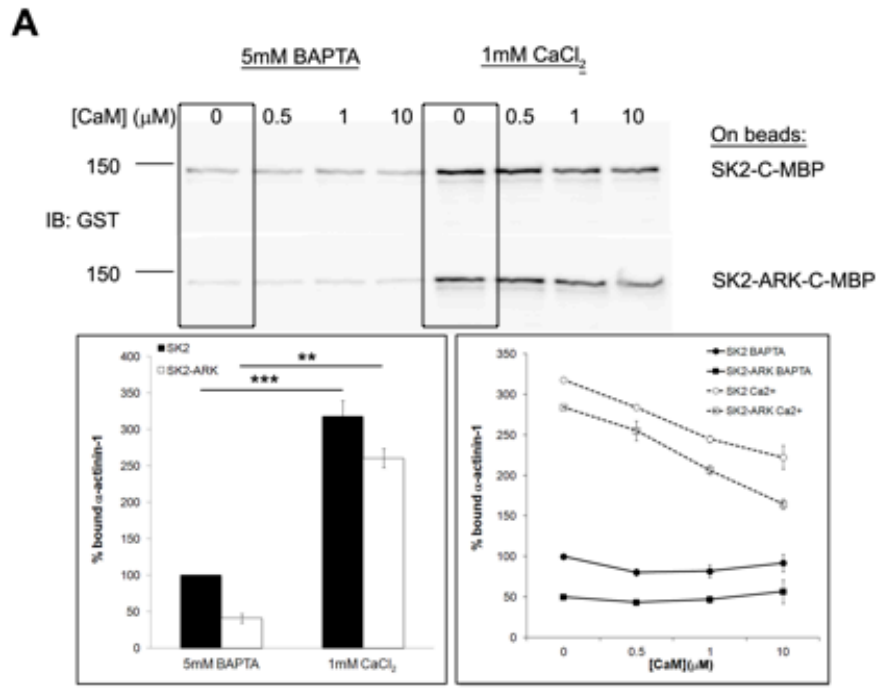
A
5mM BAPTA
1mM CaCl2
[CaM] (μM)
0
0.5
1
10
0
0.5
1
10
On beads:
150
SK2-C-MBP
IB: GST
150
SK2-ARK-C-MBP
SK2
SK2-ARK
**
***
% bound α-actinin-1
5mM BAPTA
1mM CaCl2
SK2 BAPTA
SK2-ARK BAPTA
SK2 Ca2+
SK2-ARK Ca2+
% bound α-actinin-1
[CaM](μM)

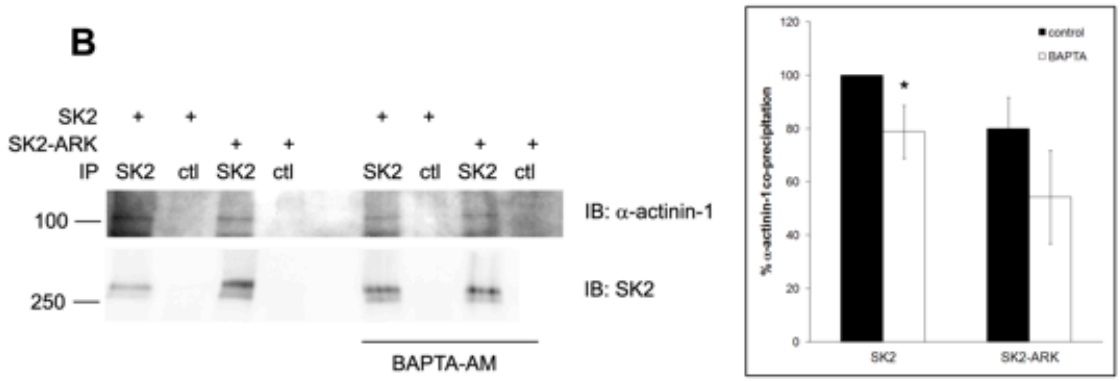
B
SK2
SK2-ARK
IP
SK2
ctl
SK2
ctl
SK2
ctl
SK2
ctl
100
IB: α-actinin-1
250
IB: SK2
BAPTA-AM
control
BAPTA
*
% α-actinin-1 co-precipitation
SK2
SK2-ARK

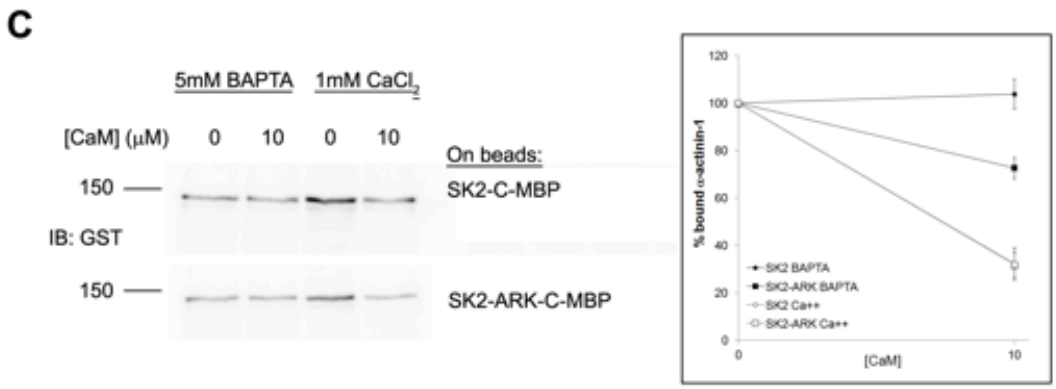
C
5mM BAPTA
1mM CaCl2
[CaM] (μM)
0
10
0
10
On beads:
150
SK2-C-MBP
IB: GST
150
SK2-ARK-C-MBP
% bound α-actinin-1
SK2 BAPTA
SK2-ARK BAPTA
SK2 Ca++
SK2-ARK Ca++
[CaM]

synaptic activation may strengthen interaction of both SK2 and SK2-ARK channel subunits with α-actinin-1.

We also tested for competition between α-actinin-1 and CaM for binding to SK2. We found that, in the presence of 1mM $CaCl_2$, addition of CaM reduced the binding of α-actinin-1-GST to both SK2- and SK2-ARK-MBP in a concentration-dependent manner; however, CaM had little effect when available Ca^{2+} was chelated by addition of 5mM BAPTA (Figure 3.7a). Similarly, Ca^{2+}-CaM, when added to SK2 first, partially blocked binding of α-actinin-1-GST to SK2- and SK2-ARK-MBP (Figure 3.7c, $p<10^{-15}$). Interestingly, CaM alone (in 5mM BAPTA) partially blocked binding of α-actinin-1-GST to SK2-ARK-MBP, but not to SK2-MBP (Figure 3.7c, $p<10^{-9}$). Taken together, our data suggest that α-actinin-1 and CaM may bind simultaneously to SK2 channels, though CaM partially competes

---

Figure 3.7: Ca^{2+} and CaM modulate interactions of SK2 channels with α-actinin-1.
(A) Effects of CaM and Ca^{2+} on binding of α-actinin-1 to SK2 and SK2-ARK C-terminal constructs. GST-tagged α-actinin-1 was incubated with MBP-tagged SK2 or SK2-ARK C-terminal constructs and amylose beads in buffer containing 5mM BAPTA or 1mM $CaCl_2$ prior to addition of purified recombinant CaM at the indicated concentrations. Blots show remaining bound GST-tagged α-actinin-1. Bottom left graph shows normalized levels of co-precipitated α-actinin-1 in BAPTA or $CaCl_2$ buffer with no added CaM (boxed lanes). Bottom right graph shows normalized levels of co-precipitated α-actinin-1 following incubation with the indicated CaM concentrations. (B) Co-immunoprecipitation of α-actinin-1 with SK2 and SK2-ARK channels exogenously expressed in *Xenopus laevis* oocytes. Oocytes were incubated with BAPTA-AM as indicated to chelate intracellular Ca^{2+} immediately prior to lysis in 10mM BAPTA and SK2 immunoprecipitation. Graph shows normalized α-actinin-1 co-precipitation. (C) CaM blocks α-actinin-1 binding to SK2. CaM was incubated with SK2 or SK2-ARK constructs and amylose beads in the indicated buffers prior to addition of α-actinin-1. Blots show bound GST-tagged α-actinin-1, graph shows normalized band densities. * confidence interval at $p < 0.05$; ** $p < 0.0005$ in student t-test; *** confidence interval at $p < 10^{-15}$.

with α-actinin-1 for binding to SK2-ARK. Furthermore, Ca^{2+} and Ca^{2+}-CaM have opposing effects on interaction of SK2 channels with α-actinin-1; Ca^{2+} appears to increase the affinity of α-actinin-1 for SK2, while Ca^{2+}-CaM competes with α-actinin-1 for binding to SK2.

Finally, we tested for effects of Ca^{2+} on interaction of α9/10-nAChRs with SK2 channels in *Xenopus* oocytes by pre-incubating oocytes expressing α9/10-HA, α-actinin-1, and SK2 or SK2-ARK with BAPTA-AM before immunoprecipitating SK2. Significantly, we found that SK2 and SK2-ARK show different effects of Ca^{2+} chelation on interaction with α9/10-nAChRs. BAPTA-AM treatment significantly increased co-precipitation of α9/10-HA with SK2 by two-fold compared to controls (Figure 3.8, $p<10^{-4}$), suggesting that Ca^{2+} influx in hair cells may reduce linkage of SK2 to α9/10. In contrast, the same treatment produced a small but non-significant decrease in co-precipitation with SK2-ARK, suggesting that Ca^{2+} does not inhibit or may even weakly promote the association of α9/10-nAChRs with SK2-ARK. Overall, our studies suggest that Ca^{2+} influx and changes in CaM binding that result from synaptic activity may modulate protein interactions within the SK2 postsynaptic complex, and that these effects differ between SK2 and the SK2-ARK splice variant.

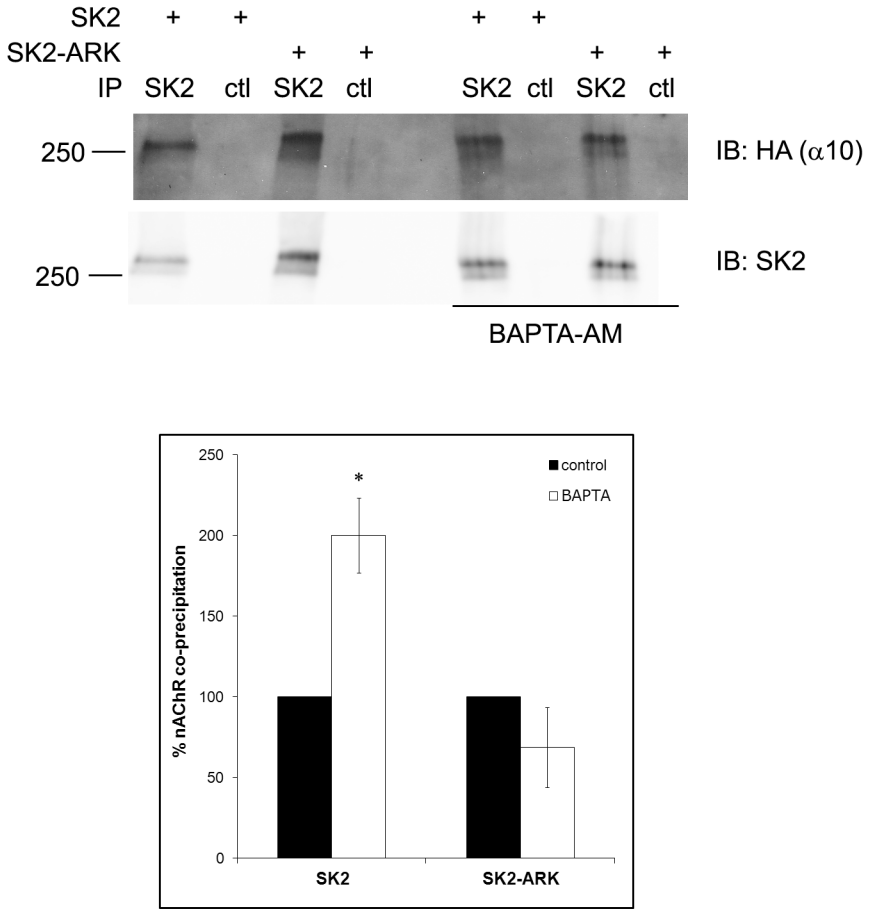

Figure 3.8: Ca^{2+} differentially modulates interactions of SK2 and SK2-ARK with α9/10-nAChRs.

Co-immunoprecipitation of HA-tagged α9/10-nAChRs with SK2 and SK2-ARK channels exogenously expressed in *Xenopus laevis* oocytes. Oocytes were incubated with BAPTA-AM as indicated to chelate intracellular Ca^{2+} immediately prior to lysis in 10mM BAPTA and SK2 immunoprecipitation. Graph shows normalized α9/10-nAChR co-precipitation. * confidence interval at $p < 10^{-4}$.

Discussion

Functional coupling between Ca^{2+}-permeable α9/10-nAChRs and Ca^{2+}-activated SK2 channels is a crucial step in the efferent inhibition of cochlear hair cells and modulation of hearing sensitivity. The work that we present here identifies novel and interrelated mechanisms that mediate the localization of SK2 channels and α9/10-nAChRs at olivocochlear synapses in hair cells. We have demonstrated that α9/10-nAChRs interact with SK2 channels, as does the actin-binding protein α-actinin-1. The composition and localization of the SK2-nAChR complex can be modulated by alternative splicing of SK2, as demonstrated by differences in protein interactions and membrane expression of the SK2-ARK variant. We also show that changes in Ca^{2+} concentration and calmodulin that accompany synaptic activation alter protein interactions within the SK2 complex. These Ca^{2+} and CaM-induced changes differ between SK2 and SK2-ARK, suggesting that the two variants may respond differently to synaptic activity. Together, these studies suggest a model in which multiple mechanisms during development and synaptic activity regulate the functional coupling and localization of SK2 channels and α9/10-nAChRs.

Previous studies of efferent olivocochlear synapses suggest a “two-channel” model of hair cell inhibition, in which SK2 channels are directly activated by closely co-localized α9/10-nAChRs within membrane microdomains (Fuchs and Murrow, 1992a; Nie et al., 2004; Oliver et al., 2000). The necessity of SK2 channels for α9/10-nAChR membrane clustering and cholinergic function further suggests that SK2 may interact with nAChRs in a protein complex whose

localization is directed by SK2-specific mechanisms or binding partners (Kong et al., 2008; Murthy et al., 2009a; Roux et al., 2011). In agreement with this hypothesis, we have demonstrated that SK2 channels interact with α9/10-nAChRs. We found that epitope-tagged α9/10-nAChRs specifically co-immunoprecipitated with SK2 when exogenously expressed in *Xenopus* oocytes. Furthermore, surface membrane expression of α9/10-nAChRs was correlated with that of SK2 channels; levels of surface biotinylated α9/10-nAChRs in oocytes were dramatically reduced in the absence compared to the presence of SK2. To our knowledge, this work represents the first demonstration of a physical association between SK2 channels and α9/10-nAChRs. Whether they interact directly or through intermediate proteins has yet to be determined. In other studies, electrophysiological recordings of SK2 channels and α9/10-nAChRs co-expressed in *Xenopus* oocytes recapitulate biphasic responses to acetylcholine that are observed in OHCs; however, these responses are significantly slower, suggesting that interacting proteins specific to hair cells may be required to link SK2 with nAChRs and allow fast functional coupling (Nie et al., 2004; Oliver et al., 2001b).

We show that SK2 channels also interact with the actin-binding protein α-actinin-1, both in chicken hair cells and when exogenously expressed in *Xenopus* oocytes. This interaction is direct and is mediated by the intracellular C-terminus of SK2. In cardiac muscle, binding of SK2 channels to α-actinin-2 anchors them to nearby $Ca_v1.3$ Ca^{2+} channels, thereby allowing fast functional coupling (Lu et al., 2007). These studies suggest the possibility that α-actinin-1 may play a

similar role in cochlear hair cells by mediating the interaction between SK2 channels and α9/10-nAChRs. However, our observation that the SK2-ARK variant (discussed below) shows slightly reduced binding to α-actinin-1 but does not demonstrate a similar decrease in binding to α9/10-nAChRs – in fact, SK2-ARK shows a significant *increase* in α9/10-nAChR interaction – may indicate that SK2 and α9/10 interact via another, as yet unidentified, protein and not through α-actinin-1. Future studies will be required to further define the nature of the interaction between SK2 channels and nAChRs, and the role of α-actinin-1 in this complex.

While our demonstration of a physical link between α9/10-nAChRs and SK2 channels strongly supports the two-channel model of hair cell efferent inhibition, numerous studies support a second model of efferent inhibition in which Ca^{2+} influx through α9/10-nAChRs activates SK2 channels indirectly through Ca^{2+}-induced Ca^{2+} release (CICR) from a subsynaptic cistern closely apposed to the postsynaptic membrane (Martin and Fuchs, 1992; Saito, 1983). CICR-mediated Ca^{2+} transients have been proposed to enhance the rapid, millisecond-level activation of SK2 channels and fast suppression of cochlear responses in response to efferent signals, while also promoting a slower suppression of outer hair cell mechanics that has been linked to protection against noise-induced damage and hearing threshold shifts (Reiter and Liberman, 1995; Sridhar et al., 1997; Sridhar et al., 1995). Hence, our data showing that α9/10-nAChRs and SK2 channels are physically associated are consistent with a model in which

both direct coupling between nAChRs and SK2 channels and CICR contribute to fast efferent inhibition.

We present SK2 alternative splicing as a mechanism that regulates the interactions and surface membrane expression of the SK2-nAChR synaptic complex, based on our characterization of the SK2-ARK splice variant. The significance of the 3-residue ARK insertion in the SK2 C terminal has been previously undefined (Matthews et al., 2005). We find that the ARK insertion changes SK2 channel interactions with known binding partners. As discussed above, SK2-ARK demonstrated a slight (approximately 20%) reduction in binding to α-actinin-1 compared to SK2. More significantly, we show a stronger interaction of SK2-ARK with α9/10-nAChRs compared to SK2, though the specific nature of the SK2-nAChR interaction and effects of the ARK insertion remain unclear. The existence of SK2 subunit variants with different α9/10-nAChR interaction capabilities raises the intriguing possibility that, by altering the relative expression levels of SK2 and SK2-ARK, hair cells could subtly modulate the level of interaction and functional coupling between α9/10 and SK2, and thereby fine-tune the strength and efficiency with which efferent signals are translated into the suppression of afferent auditory transmission.

In addition to changes in protein interactions, the surface expression of the SK2-ARK variant was significantly reduced, as demonstrated by surface biotinylation assays in *Xenopus* oocytes. Surface levels of tagged α9/10-nAChRs were also decreased when co-expressed with SK2-ARK compared to SK2, further supporting the dependence of α9/10-nAChR trafficking on that of SK2

channels. Although we saw a dramatic reduction in baseline surface levels of SK2-ARK compared to SK2, we found no difference in rates of internalization and degradation, suggesting that SK2 channel membrane targeting or insertion, but not membrane stability and endocytosis rate, are affected by the splice insertion. Alternatively, the ARK insertion may cause differences in fast endocytic recycling that were not detected in measurements of SK2 internalization on an hours-long time scale.

What are the mechanisms that mediate the trafficking of the SK2-nAChR protein complex, and how does the ARK splice insertion affect these mechanisms? Constitutive, Ca^{2+}-independent Interaction with CaM is required for SK2 surface localization in COS cells (Lee et al., 2003). However, we show that SK2-ARK does not display decreased CaM-binding capability compared to SK2, indicating that other mechanisms account for the dramatic difference between the two variants in their surface expression. Alternatively, interaction of SK2 with α-actinin-1 could regulate its surface expression. SK2 surface expression is known to be affected by interaction with α-actinins; when exogenously expressed in HEK cells, SK2 channel current density was found to be greatly enhanced by co-expression of α-actinin-2; disruption of actin networks using cytochalasin D inhibited this effect, suggesting that α-actinin-2 promotes SK2 surface expression via anchorage to the actin cytoskeleton (Lu et al., 2007). Immunofluorescent labeling of SK2 in HEK cells is localized to the cell membrane when co-expressed with α-actinin-2, whereas SK2 expressed alone is confined to the cytoplasm and associated with early endosomes, suggesting that α-actinin-2-

mediated anchorage may also regulate SK2 trafficking by preventing endocytosis or promoting its recycling back to the cell membrane (Lu et al., 2009). The reduced interaction of SK2-ARK with α-actinin-1 that we observe, combined with a decrease in biotinylated surface levels, raises the possibility that α-actinin-1 may play a role similar to that of α-actinin-2 in promoting SK2 membrane expression. However, the relatively small decrease (~20%) in SK2-ARK interaction with α-actinin-1 compared to its 70% decrease in biotinylated surface levels suggests that other mechanisms and/or interaction partners may contribute to the impact of the ARK insertion on SK2 surface localization.

Another mechanism that may regulate SK2 channel interactions or surface expression is PKA-phosphorylation of the C-terminal. Phosphorylation of three consecutive serine residues near the end of the C-terminal negatively regulates the surface expression of SK2 channels exogenously expressed in COS7 cells (Ren et al., 2006). In hippocampal neurons, where SK2 channels couple to NMDA receptors to modulate EPSP amplitude and LTP induction (Hammond et al., 2006; Ngo-Anh et al., 2005; Stackman et al., 2002), LTP triggers SK2 channels endocytosis in a manner dependent on PKA phosphorylation (Lin et al., 2008). Thus, PKA phosphorylation in different cell types appears to negatively regulate SK2 surface levels, though the precise mechanisms are undefined. Interestingly, sequence analysis of the SK2-ARK C-terminal using ScanSite (scansite.mit.edu) predicts that the ARK splice insertion introduces a PKA phosphorylation at S^{438} of chicken SK2 (Ser^{465} in rat SK2). Evidence of Ser^{465} phosphorylation by PKA has been demonstrated, though its phosphorylation

levels were found to be minor and the functional impact is unknown (Ren et al., 2006). It is tempting to speculate that, consistent with the negative regulation of SK2 surface levels by PKA phosphorylation in other cell types, increased phosphorylation at Ser^{438} of SK2-ARK could contribute to the reduction compared to SK2 that we observe in its surface expression. Alternatively, Ser^{438} phosphorylation of SK2-ARK could regulate interactions with binding partners, perhaps even providing a mechanism for its strengthened interaction with α9/10-nAChRs. It will be interesting in future studies to identify the role, if any, of PKA phosphorylation in the trafficking and/or coupling of SK2 channels and α9/10-nAChRs.

Our results indicate that both CaM and Ca^{2+} affect SK2 channel interactions, suggesting that Ca^{2+} influx and changes in SK2-CaM binding that occur during efferent synapse activity may change the composition of the SK2 postsynaptic complex. Thus, synaptic Ca^{2+} signaling represents a potential mechanism to dynamically regulate hair cell efferent responses. We show that interactions of SK2 with both α-actinin-1 and α9/10-nAChRs were affected by addition of CaM and/or by manipulating Ca^{2+} availability. We found that Ca^{2+} and Ca^{2+}-bound CaM exert opposing effects on the interaction of SK2 with α-actinin-1. In recombinant peptide assays, addition of CaM had little effect on the amount of α-actinin-1 bound to SK2 when available Ca^{2+} was chelated with BAPTA. In the presence of Ca^{2+}, however, CaM competed with α-actinin-1 for binding to SK2 in a dose-dependent manner, and pre-incubation of SK2 with Ca^{2+}-CaM partially blocked binding of α-actinin-1. Ca^{2+}-CaM binding to the distal region of the α2

helix that constitutes the Ca^{2+}-dependent CaM-binding domain may directly compete with α-actinin-1, which would suggest that this is a necessary region for α-actinin-1 interaction. Alternatively, conformational changes in the SK2-CaM complex that occur in response to Ca^{2+} may indirectly inhibit α-actinin-1 binding to a separate region via steric hindrance, though, as above, it is difficult to determine whether the three-dimensional structure of the SK2-CaM complex and effects of Ca^{2+} on the conformation of this complex are preserved in recombinant peptide assays using only the C-terminal of SK2. In contrast to inhibitory effects of Ca^{2+}-CaM, we show that Ca^{2+} alone strongly promotes the interaction of α-actinin-1 with SK2, as SK2 with no added CaM showed significantly greater α-actinin-1 co-precipitation in the presence of Ca^{2+} compared to 5mM BAPTA. Thus, the nature of SK2 interaction with α-actinin-1 is markedly different from its interaction with α-actinin-2, which is unaffected by Ca^{2+} but is inhibited by Ca^{2+}-free CaM (Lu et al., 2009). It is interesting to note that levels of remaining bound α-actinin-1 even at the highest added concentration of Ca^{2+}-bound CaM exceeded α-actinin-1 binding in the absence of Ca^{2+} (see Figure 3.7a), suggesting that the enhancement of SK2-α-actinin-1 interaction by Ca^{2+} outweighs the inhibitory effect of Ca^{2+}-CaM. It is also possible that the balance between Ca^{2+}-CaM-induced displacement versus Ca^{2+}-mediated enhancement of α-actinin-1 binding may shift depending on Ca^{2+} concentration to increase or decrease SK2-α-actinin-1 interaction in response to activity.

We also show that the interaction of SK2 with α9/10-nAChRs is influenced by Ca^{2+}. Co-precipitation of tagged α9/10-nAChRs with SK2 was significantly

enhanced by Ca^{2+} chelation with BAPTA-AM, indicating that Ca^{2+} inhibits this interaction and suggesting the possibility that increases in Ca^{2+} levels during efferent synapse activity could weaken the interaction between α9/10 and SK2. It is not yet clear whether the Ca^{2+}-induced decrease in interaction of SK2 with α9/10 is due to a direct effect of Ca^{2+} on α9/10, SK2, or a putative intermediate protein, or caused by CaM-mediated conformational changes. Taken together, our results suggest a model in which activity-induced Ca^{2+} influx inhibits the association of SK2 with α9/10-nAChRs. Meanwhile, although Ca^{2+} influx also causes displacement of α-actinin-1 from SK2 due to competition by Ca^{2+}-CaM, this effect is countered or even outweighed by the direct Ca^{2+}-induced enhancement of α-actinin-1 binding. Strengthened binding to α-actinin-1 could anchor membrane-bound SK2 more strongly to the actin cytoskeleton or promote further membrane insertion of SK2 channels. In this manner, synaptic activity could uncouple SK2 channels from nAChRs to dynamically regulate the time course of fast efferent inhibition, while maintaining SK2 channels in the membrane to allow their activation by CICR-derived Ca^{2+} transients or to facilitate re-association with nAChRs in preparation for detection of subsequent synaptic signals.

We show that these mechanisms are further modified by SK2 alternative splicing. In addition to its effects on SK2 channel interactions and membrane expression, as discussed above, the ARK insertion in the SK2 C terminal changes the manner in which SK2 and its binding partners are affected by Ca^{2+} and CaM. The ARK insertion is located within the α2 helix of the CaM-binding

domain, a region which is important both for Ca^{2+}-dependent and independent CaM interaction. Matthews et al. (2005) note that the similarity in Ca^{2+}-sensitivity between mammalian SK2 channels, which lack the ARK splice insertion, and SK1 channels, which contain a similar AQK sequence at the same position, suggests that the presence of the 3-amino acid insertion at this site does not strongly affect CaM binding or Ca^{2+} sensitivity. Accordingly, we demonstrate a small, though statistically significant, decrease in the Ca^{2+}-sensitivity of SK2-ARK potassium currents, with an EC_{50} of ~0.6 μM compared to SK2 currents with an EC_{50} of ~0.5 μM. The fast activation of α9/10-nAChRs in hair cells is thought to increase the Ca^{2+} concentration within nAChR-SK2 microdomains to 10 μM or higher on a sub-millisecond time scale (Oliver et al., 2000). Therefore, it is unlikely that the small decrease that we observe in the Ca^{2+} sensitivity of SK2-ARK channels would alter their Ca^{2+} gating on a physiologically relevant scale. However, we cannot rule out the possibility that the ARK insertion causes changes in potassium current amplitudes that were not addressed in this experiment.

We found a small increase in Ca^{2+}-independent CaM binding of the SK2-ARK C-terminal compared to SK2, which is perhaps inconsistent with the observed reduction in Ca^{2+} sensitivity. Previous studies of SK2-CaM interactions indicate that two residues immediately downstream of the ARK insertion, R464 and K467 of the rat SK2 channel, are required specifically for constitutive, Ca^{2+}-independent CaM binding (Keen et al., 1999). Thus, it is possible that conformational changes induced by the ARK insertion in this critical region could

favor CaM binding in the absence of Ca^{2+} but hinder the Ca^{2+}-dependent interactions and structural rearrangement necessary for channel gating. However, because we cannot determine whether the isolated, MBP-tagged C-terminal of SK2 recapitulates the three-dimensional structure of the SK2-CaM complex and the conformational changes induced by Ca^{2+} (Schumacher et al., 2001), it is unclear whether this experiment accurately reflects the CaM-binding capabilities of SK2 and SK2-ARK.

SK2-ARK also differs from SK2 in the effects of Ca^{2+}- and CaM on interactions with α-actinin-1 and α9/10-nAChRs. SK2-ARK was largely similar to SK2 in the effects of Ca^{2+} and/or CaM on α-actinin-1 binding; interaction with α-actinin-1 was inhibited or blocked to similar degrees by CaM in the presence of Ca^{2+}. However, whereas binding of α-actinin-1 to SK2 was minimally affected by CaM alone, binding to SK2-ARK was partially blocked by pre-incubation with CaM in 5mM BAPTA. This effect could be due to conformational changes introduced by the ARK insertion that favor interaction with CaM over α-actinin-1. We also find that interaction of SK2-ARK with α9/10-nAChRs is differently affected by Ca^{2+} compared to SK2. In contrast to SK2, which demonstrated increased interaction with α9/10-nAChRs in oocytes treated with BAPTA-AM, BAPTA-AM treatment of SK2-ARK-expressing oocytes produced a trend towards *decreased* interaction with α9/10-nAChRs. These results indicate that, whereas Ca^{2+} inhibits the interaction of α9/10-nAChRs with SK2, Ca^{2+} has little effect on or may even weakly promote their association with SK2-ARK.

Together, our data suggest several interacting mechanisms that regulate the localization and functional coupling of SK2 channels and α9/10-nAChRs at efferent postsynaptic sites in cochlear hair cells. We propose a model, similar to the model proposed by Kong et al. (2008) and Murthy et al., (2009), in which SK2 channels and α9/10-nAChRs physically interact within a protein complex that includes the actin-binding protein α-actinin-1 (Figure 3.9a). In response to synaptic activity, Ca^{2+} influx and Ca^{2+}-dependent CaM binding elicit changes in the protein interactions within the SK2-nAChR synaptic complex. In this model, the interaction of SK2 channels with α-actinin-1 is altered both by Ca^{2+} and by Ca^{2+}-CaM, the combined effects of which may alter the stability or insertion of SK2 channels in the synaptic membrane. Ca^{2+} influx also antagonizes the association between SK2 and α9/10-nAChRs. Uncoupling of SK2 channels from α9/10-nAChRs may provide mechanisms to regulate both fast inhibitory signaling that results from direct nAChR-SK2 coupling as well as CICR-mediated Ca^{2+} transients that may contribute to slow, prolonged efferent inhibition (Sridhar et al., 1997).

These effects may be further modulated by expression of the SK2-ARK splice variant, which differs from SK2 in its protein interactions, surface localization, and response to activity (Figure 3.9b). Given the dramatic reductions in the surface expression of SK2-ARK and of accompanying α9/10-nAChRs, expression of this splice variant may provide a mechanism to modulate the surface levels of the SK2-nAChR complex. Furthermore, because the physical coupling of α9/10-nAChRs to SK2-ARK appears to be stronger than to SK2 and less prone to

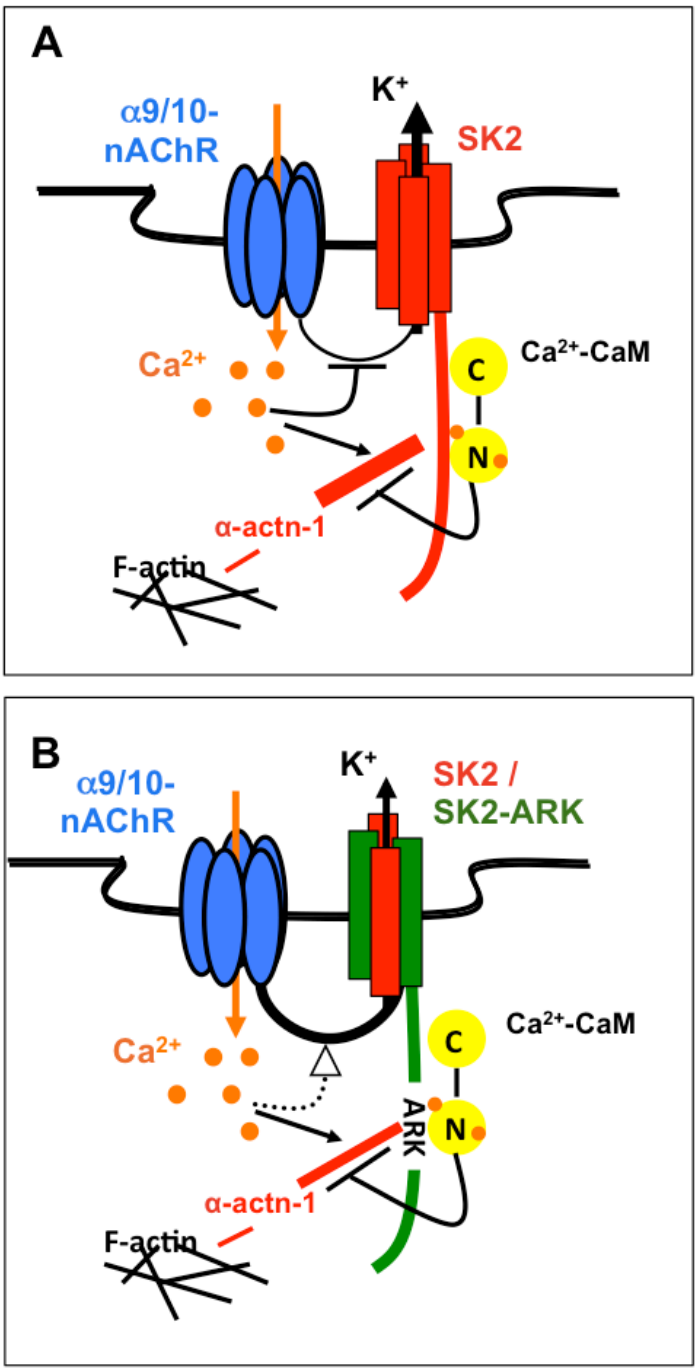

Figure 3.9: Schematic model of the effects of alternative splicing and Ca^{2+} signaling on the nAChR-SK2 channel postsynaptic complex.
SK2-only (A) versus SK2-ARK-containing channels (B) at postsynaptic sites. (A) SK2 channels interact directly with a-actinin-1; this interaction is enhanced by Ca^{2+} but inhibited by Ca^{2+}-bound CaM. SK2 also interacts with a9/10-nAChRs, and this interaction is inhibited by Ca^{2+}. (B) SK2-ARK exhibits a slightly reduced interaction with α-actinin-1; this interaction is also enhanced by Ca^{2+} and inhibited by Ca^{2+}-CaM. SK2-ARK interacts more strongly with a9/10-nAChRs; this interaction may be weakly enhanced by Ca^{2+} (dotted arrow; see Figure 3.8).

inhibition by Ca^{2+}, the level of SK2-ARK subunit incorporation into synaptic SK2 channels may also modulate the strength, efficiency, and/or time course of direct SK2-nAChR coupling.

The increases that we demonstrate in SK2-ARK expression levels during embryonic stages of hair cell development and innervation raise the compelling possibility that alternative splicing could play a role in the development of mature efferent innervation patterns and inhibition by modulating the ability of developing hair cells to respond to nascent synaptic signals. It will be of great interest in future studies to examine the subcellular localization of SK2-ARK compared to SK2, determine whether the two variants co-assemble in functional tetramers, and how splicing may be regulated during embryonic and early post-hatch development or during regeneration following acoustic or ototoxic trauma. SK2-ARK has previously been detected only in a subset of chicken SK2 channels and is constitutively present in the trout SK2 sequence (Matthews et al., 2005). However, preliminary results suggest the presence of SK2 channels in the mouse hippocampus that contain an ARK insertion at the same site (A. Pirone, unpublished data). Thus, the mechanisms that we show here may not be limited to avian hair cells but may be relevant in mammalian species as well. Future studies may therefore address the roles of SK2-ARK alternative splicing in both avian and mammalian cochleae.

Chapter 4

Identification of novel adapter proteins for α10-nAChRs and SK2 channels

Introduction

At olivocochlear synapses in hair cells, α9/10 nicotinic acetylcholine receptors (nAChRs) and Ca^{2+}-activated SK2 potassium channels function together to mediate efferent control of hearing sensitivity (for review, see Wersinger and Fuchs, 2010). In response to acetylcholine released from efferent presynaptic terminals, Ca^{2+} influx through α9/10-nAChRs activates potassium efflux through SK2 channels and results in hair cell hyperpolarization and inhibition of the hair cell-driven cochlear amplifier (Fuchs and Murrow, 1992a; Galambos, 1956; Oliver et al., 2000). Previous research has indicated that α9/10-nAChRs and SK2 channels may be co-localized within membrane microdomains at hair cell synapses (Oliver et al., 2000) However, the specific mechanisms that direct α9/10-SK2 co-localization and coupling are undefined.

The work presented in this thesis has identified novel protein components of the postsynaptic scaffold at hair cell synapses (Chapter 2) and presented the first evidence of a physical interaction between α9/10-nAChRs and SK2 channels (Chapter 3). We show that a multiprotein complex that organizes neuronal nicotinic synapses (Rosenberg et al., 2008) is conserved at the hair cell nicotinic synapse; this complex includes the cytoskeletal regulatory proteins adenomatous polyposis coli (APC), microtubule end-binding protein (EB1), and microtubule-actin crosslinking factor (MACF), as well as synaptic scaffolding molecule (S-SCAM). Based on our lab's previous studies of nAChR trafficking in neurons, we propose a model in which the APC protein complex organizes microtubule-based delivery of α9/10-nAChRs and SK2 channels to the synaptic membrane in hair

cells, where interactions with specific adapter proteins anchor them to the postsynaptic scaffold. The dependence of α9/10-nAChR functional membrane localization upon SK2 channel expression suggests that α9/10 and SK2 may be trafficked as a pre-assembled complex whose correct localization, membrane insertion, or stabilization requires SK2-specific protein interactions (Kong et al., 2008; Murthy et al., 2009a), though it is likely that adapter proteins that bind to α9/10 are also involved in their proper localization and anchoring at the postsynaptic membrane. Furthermore, though we have shown that α9/10-nAChRs do indeed form a complex with SK2 channels when expressed in *Xenopus* oocytes, it is not known whether they interact directly or through intermediate proteins. Thus, identification of proteins that bind to SK2 channels and/or to α9/10-nAChRs to link them to the postsynaptic scaffold and to one another will be essential to improving our understanding of the mechanisms required for proper functional coupling and efferent synaptic transmission.

Previous studies of nAChRs indicate that the intracellular loop between the third and fourth transmembrane domains is particularly important for their trafficking (Kracun et al., 2008; Williams et al., 1998). Sequence analysis of the cytoplasmic loop of the α10-nAChR subunit predicts binding sequences for cortactin, a Src homology 3 (SH3) domain-containing protein that interacts with canonical proline-rich motifs (scansite.mit.edu). The α10-nAChR cytosolic loop contains two motifs that include the minimal cortactin-SH3 binding sequence PXXP and show significant sequence conservation with other known cortactin-SH3 binding partners (see Figure1.4c). Cortactin is an F-actin binding protein

that regulates dynamic cortical actin networks and thereby participates in multiple cellular functions, including cell motility, cell adhesion, endocytosis, and neuronal growth cone motility (Daly, 2004). In hippocampal neurons, cortactin binds to the adherens junction protein δ-catenin, which in turn interacts with S-SCAM (Ide et al., 1999; Martinez et al., 2003). Cortactin and δ-catenin in neurons regulate dendritic growth and branching, activity-dependent dendritic spine remodeling, and anchorage of AMPA receptors (Hering and Sheng, 2003; Naisbitt et al., 1999; Silverman et al., 2007) In addition, a role for cortactin in nAChR clustering has previously been demonstrated at the neuromuscular junction (NMJ), where cortactin phosphorylation downstream of agrin-MuSK signaling is essential for F-actin remodeling that supports the clustering of muscle-type nAChRs (Dai et al., 2000; Madhavan et al., 2009).

Sequence analysis of the SK2 intracellular C-terminal predicts six binding motifs for the 14-3-3 family of small linker proteins (see Figure1.4b). Serine phosphorylation at three of the six predicted 14-3-3 binding motifs in the C terminal of the SK2 channel has been demonstrated to regulate its functional membrane expression; however, the mechanisms and required interacting proteins are unknown (Ren et al., 2006). 14-3-3 proteins are a family of seven isoforms that interact with a wide variety of proteins and form dimers to link their binding partners (Aitken et al., 2002; Yaffe, 2002). 14-3-3 proteins interact with canonical consensus motifs of the type RX_{2-3}(pS/T)X(X/P), where binding is often dependent on phosphorylation of the central serine or threonine (Yaffe, 2002). In neurons, 14-3-3 proteins regulate the cellular localization of multiple

neurotransmitter receptors and ion channels by masking endoplasmic reticulum (ER) retention motifs or by regulating subunit assembly (Couve et al., 2001; Exley et al., 2006; Heusser et al., 2006; Jeanclos et al., 2001; O'Kelly et al., 2002; Rajan et al., 2002). Our lab has recently found that 14-3-3ζ binds directly to α3-nAChRs and links them to APC, thereby providing a direct link between nAChRs and the postsynaptic complex in neurons (Rosenberg et al., 2008).

Based on these previous studies, we propose a model in which cortactin and 14-3-3 bind to the α10 nAChR subunit and to SK2, respectively, and function as adapter proteins that tether the nAChR-SK2 complex to the postsynaptic scaffold. In our model, 14-3-3 dimers link SK2 to APC, while cortactin provides a link between α9/10-nAChRs and the actin cytoskeleton and to the APC postsynaptic complex through δ-catenin and S-SCAM. Our preliminary studies support this model and suggest future studies to further clarify the roles of cortactin and 14-3-3 in efferent olivocochlear synapse assembly.

Methods

Antibodies

Primary antibodies used were: monoclonal anti-cortactin (Millipore); monoclonal anti-δ-catenin (BD Transduction Laboratories); polyclonal anti-MAGI-2/S-SCAM (Sigma); polyclonal anti-synapsin (clone G-304, gift of Dr. Paul Greengard, Rockefeller University); monoclonal anti-hemagglutinin (HA) tag (clone 3F10, Roche Applied Science); polyclonal anti-MBP (maltose binding protein; New England Biolabs); monoclonal anti-GST (glutathione S-transferase;

B-14, Santa Cruz Biotechnology). Secondary antibodies used were: Cy3- and FITC-conjugated donkey anti-rabbit and anti-mouse (Jackson ImmunoResearch); Alexa-Fluor-488-, 555-, and 594-conjugated goat anti-mouse and anti-rat and donkey anti-mouse and anti-rabbit (Molecular Probes).

Chicken embryos

Embryonated White Leghorn chicken eggs were obtained from the University of Connecticut Poultry Farm (Storrs, CT) or Charles River Spafas. Embryos were kept at 37°C in forced air-draft humidified incubators for 12-20 days.

Tissue fixation and immunolabeling

Cochlear ducts were dissected from chicken embryos at embryonic day (E)19-20. Cochleae were fixed at room temperature for 1 hour in 2-4% paraformaldehyde, or in 4% paraformaldehyde with 15% picric acid. Tissue was cryoprotected by immersion in increasing concentrations of sucrose and embedded in TissueTek OCT compound (Electron Microscopy Sciences) or in 7.5% gelatin with 15% sucrose. 10μM cryosections were blocked with 5-10% normal donkey serum (Jackson Immunoresearch) or 0.25% teleost gelatin (Sigma Aldrich) and incubated at room temperature with primary antibodies for 1 hour and secondary antibodies for 45 minutes.

Image analysis

Epifluorescence images were captured using a Zeiss Axioskop epifluorescence microscope and QImaging Retiga 200R CCD camera with Nikon Instruments NIS Elements software. Confocal images were captured using a Leica TCS SP2 confocal microscope with HeNe (633nm), Kr (568 nm), and Ar (488nm) lasers and a 63x 1.32 numerical aperture lens. Optical sections were taken in 0.5μM steps. For each cell, 3 consecutive sections through a representative region were compressed for analysis. Epifluorescence images or confocal stacks from representative cells were used to assess co-localization of double-labeled proteins. Pixel intensities were measured along ~3μM lines drawn across a representative region of the efferent synapse. Postsynaptic localization was concluded if peak intensity coincided with that of a known postsynaptic protein or was distinct from that of a known presynaptic protein.

HEK cell immunoprecipitation

An α10L-CD25-HA fusion construct (referred to as α10L-HA) was created by cloning a C-terminal-hemagglutinin (HA)-tagged PCR product of the cytosolic domain and fourth transmembrane domain of the chicken α10-nAChR (gift of Dr. Paul Fuchs, Johns Hopkins University) into the 4810 CMV CD25.TM.mCFP vector (gift of Dr. Steve Bunnell, Tufts University School of Medicine). The α10L-HA construct was transfected into HEK 293 cells using GenJet In Vitro DNA Transfection Reagent (SignaGen Laboratories). Transfected cells or mock-transfected control cells were maintained for two days at 37°C with 5% CO_2 in

DMEM supplemented with 10% fetal bovine serum, 100μg/ml streptomycin, and 100U/ml penicillin (Invitrogen). Cells were lysed in Tris-Tx buffer (in mM: 10 Tris pH 7.6, 50 NaCl, 5 EDTA, 30 $Na_4P_2O_7$, 50 NaF, 0.4 Na_3VO_4, 1% Triton X-100) supplemented with protease inhibitor cocktail (Thermo Scientific) and centrifuged at 16,000 x g for 20 minutes to remove cell debris. The supernatant was pre-cleared with protein G agarose (Roche Applied Science). 1mg of pre-cleared sample was incubated with 500ng of anti-HA antibody overnight at 4°C followed by incubation with protein G agarose beads to precipitate the α10L-HA construct. Beads were washed with Tris-Tx buffer and boiled in SDS-PAGE sample buffer (Boston BioProducts) to elute proteins. Eluates were separated on SDS-PAGE gels, transferred to nitrocellulose membranes (Bio-Rad), and blotted with anti-cortactin or anti-HA antibodies.

Immunocytochemistry

Transfected HEK 293 cells plated on glass coverslips were fixed two days post-transfection in 2% paraformaldehyde, washed in PBS, and permeabilized with 0.1% Triton X-100. Cells were blocked with 0.25% teleost gelatin and incubated with anti-HA antibody and Alexa-Fluor-555-conjugated goat anti-rat for 1 hour each.

Recombinant peptide binding assays

Maltose binding protein (MBP) fusions of chicken SK2 and SK2-ARK were created by cloning of C-termini PCR products (aa 368-553) into the pMalC2

vector (New England Biolabs). A glutathione S-transferase (GST) fusion of 14-3-3 in pGex2TK was a gift of Dr. Stephen Moss (Tufts University School of Medicine). Fusion peptides were expressed in Rosetta-gami 2(DE3) cells (EMD Chemicals) and grown in LB media containing 0.5M NaCl and 2.5 mM betaine. Peptides were purified using GST-sepharose or amylose resin.

For binding assays, SK2- or SK2-ARK-MBP peptides and amylose resin were incubated with 14-3-3-GST in Tris-Tx buffer (in mM: 10 Tris pH 7.6, 50 NaCl, 5 EDTA, 30 $Na_4P_2O_7$, 50 NaF, 0.4 Na_3VO_4, 1% Triton X-100) supplemented with protease inhibitor cocktail (Thermo Scientific) and phosphatase inhibitor cocktail (Roche Applied Science). Beads were washed 4 times with Tris-Tx buffer and boiled in 4x sample buffer to elute bound proteins. Eluates were separated on SDS-PAGE gels, transferred to nitrocellulose membranes, and blotted with anti-GST antibody to detect pulldown of 14-3-3-GST. Band densities were quantified using Nikon Instruments NIS Elements software and normalized to SK2 or SK2-ARK levels in the same lane detected with anti-MBP antibody.

Results

Cortactin and δ-catenin are localized to efferent hair cell synapses

In order to determine whether cortactin and its binding partner δ-catenin may play a role in olivocochlear synapse assembly, we first tested for expression of these two proteins at postsynaptic sites in hair cells. Consistent with our model, immunolabeling of cross-sections of the chicken basilar papilla shows strong concentration of cortactin at the basal pole of hair cells and co-localization with

S-SCAM, which we have previously identified as a postsynaptic marker at olivocochlear synapses (Figure 4.1a; see Chapter 2). δ-catenin also shows strong postsynaptic localization, as evidenced by juxtaposition to synapsin-labeled efferent terminals and co-localization with S-SCAM (Figure 4.1b), consistent with prior studies showing interaction between δ-catenin and S-SCAM (Ide et al., 1999).

Cortactin interacts with the α10-cytosolic loop

The cytoplasmic loop of the α10-nAChR subunit contains two predicted proline-rich cortactin-SH3 domain binding motifs. To test for an interaction of the α10 cytoplasmic loop with cortactin, we created a membrane-targeted fusion construct consisting of the CD25 membrane protein, whose diffuse membrane localization has been previously demonstrated (McKillop et al., 2009), and the α10 cytoplasmic loop and fourth transmembrane domain, with an extracellular C-terminal hemagglutinin (HA) epitope tag. We expressed this construct in HEK 293 cells and tested for interaction with endogenous cortactin. As shown in Figure 4.2a, cortactin co-immunoprecipitated with the α10L-HA construct from transfected HEK cell lysates, but was not pulled down from control mock-transfected cells. Cortactin was also not co-precipitated from transfected lysates by incubation with non-specific antibody (data not shown). These results were inconsistent, however, showing cortactin co-immunoprecipitation with the α10L-HA construct in 50% of experiments. These inconsistencies may be due to improper localization of the α10L-HA construct, as immunofluorescent labeling of

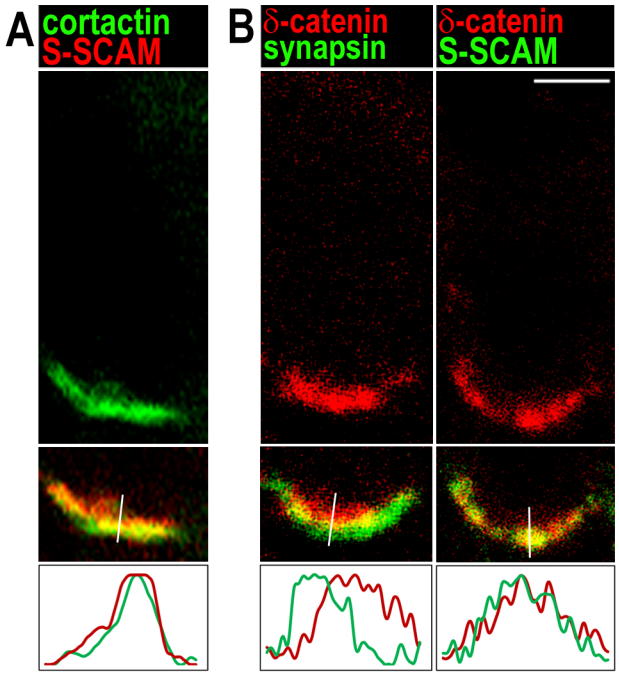

Figure 4.1: Postsynaptic localization of cortactin and δ-catenin in chick hair cells.
Confocal images of immunolabeled E19-20 chick cochlea sections with pixel intensity profiles (lines in middle panels) showing cortactin (A) immunofluorescence and co-localization with postsynaptic S-SCAM and δ-catenin (B) immunofluorescence with juxtaposition to presynaptic synapsin and co-localization with postsynaptic S-SCAM. Scale bar: 5μM.

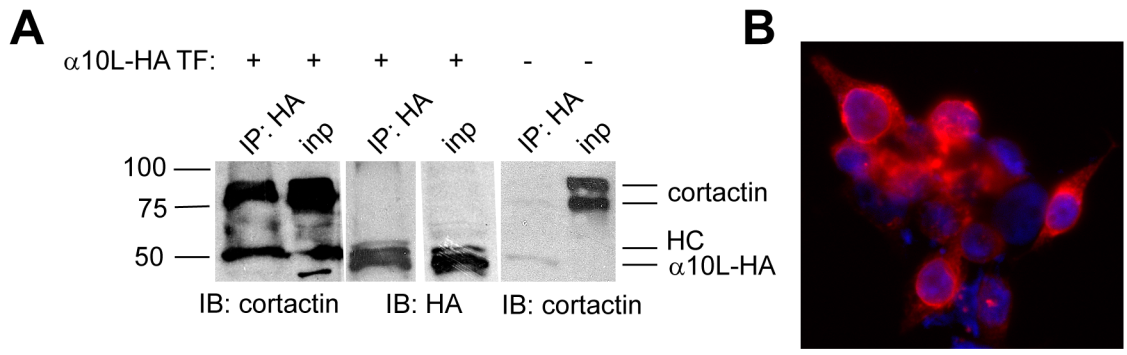

Figure 4.2: Co-immunoprecipitation of cortactin with the α10-nAChR cytoplasmic loop.
(A) Immunoprecipitation of the HA-tagged α10-nAChR loop construct (α10L-HA) from transfected HEK293 cells shows co-precipitation of endogenous cortactin (lane 1). Lane 3: re-blot of lane 1 showing precipitation of the α10L-HA construct. Negative control shows no cortactin co-precipitation with HA antibody from untransfected cell lysates (lanes 5,6). HC: antibody heavy chain. (B) Epifluorescence image of HEK293 cells transfected with the α10L-HA construct and labeled with anti-HA antibody (red) and DAPI nuclear counterstain (blue).

transfected cells with HA antibody showed that the construct was largely confined to perinuclear regions rather than to the surface membrane as expected (Figure 4.2b). Together, these preliminary studies show that cortactin and δ-catenin are present at postsynaptic sites in hair cells and suggest that cortactin may interact with the α10-nAChR cytoplasmic loop, supporting our model of cortactin and δ-catenin functions in efferent synapse assembly.

14-3-3 interacts with SK2 and the SK2-ARK splice variant

We also tested for interaction of SK2 channels with the small linker protein 14-3-3, based on the presence of six canonical 14-3-3 binding motifs at the tail of the SK2 cytoplasmic C-terminal. We found that a maltose binding protein (MBP)-tagged construct of the SK2 C-terminal interacts with GST-tagged 14-3-3ζ in recombinant peptide binding assays (Figure 4.3). This interaction was specific, as background levels of 14-3-3-GST co-precipitation with MBP alone were significantly lower than with SK2-MBP (Figure 4.3, lane 3), and GST alone did not interact with SK2-MBP (data not shown). We also tested for interaction of 14-3-3-GST with the SK2-ARK splice variant that, as we have demonstrated, differs from SK2 in function, localization, and protein interactions with α9/10-nAChRs and α-actinin-1. However, we found no difference between the two SK2 variants in interactions with 14-3-3.

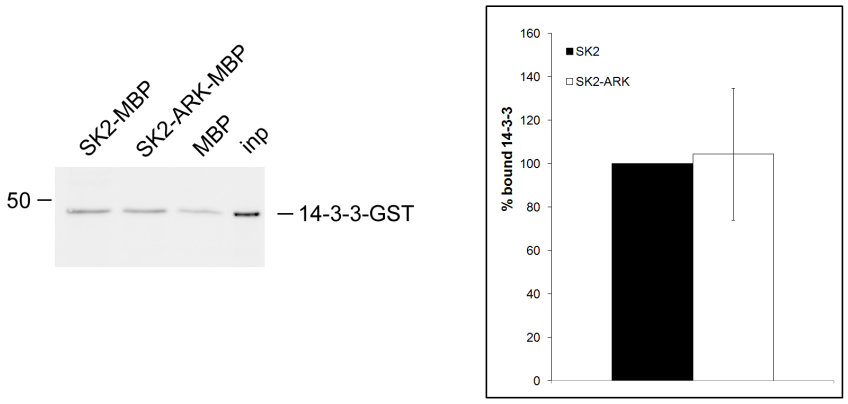

Figure 4.3: Interaction of 14-3-3 with SK2.
Direct interaction of GST-tagged 14-3-3ζ with the MBP-tagged SK2 and SK2-ARK C-terminal constructs. Negative controls indicate negligible nonspecific interactions with MBP (lane 3) or GST alone (not shown). Graph shows normalized band densities of co-precipitated 14-3-3-GST.

Discussion

In previous chapters, we have characterized the protein composition of the efferent postsynaptic site in cochlear hair cells and demonstrated that α9/10-nAChRs and SK2 channels physically interact to promote their functional coupling and efferent hair cell inhibition. Identification of the specific mechanisms and interactions that mediate the coupling of nAChRs and SK2 channels and their anchoring in the hair cell membrane will be key to our understanding of olivocochlear synapse assembly and function. The results presented here identify candidate adapter proteins for α10-nAChRs and SK2 channels and suggest roles for cortactin and 14-3-3 in the localization and functional coupling of α9/10-nAChRs and SK2 channels in hair cells.

We show that cortactin and its binding partner, δ-catenin, are concentrated at postsynaptic sites in chicken hair cells and present preliminary data suggesting that cortactin may interact with the α10-nAChR cytoplasmic loop. Mounting evidence suggests that the α10 subunit, though it cannot form functional homopentamers alone (Elgoyhen et al., 2001), is an essential regulatory subunit in α9/10-nAChR heteropentamers. Co-expression of α10 with α9 in *Xenopus* oocytes yields current amplitudes 100-fold higher than α9-nAChRs alone, with Ca^{2+} responses and desensitization kinetics that more closely resemble acetylcholine-evoked currents in hair cells (Elgoyhen et al., 2001). Acetylcholine-evoked currents in outer hair cells of α10-knockout mice are significantly reduced compared to wild-type littermates, suggesting that the function and/or membrane localization of the remaining α9-nAChR homopentamers is impaired in the

absence of the α10 subunit (Vetter et al., 2007). Our results suggest that interaction with cortactin could provide a mechanism by which α10 could mediate the localization of α9/10-nAChRs. In neurons, cortactin binds to the Shank postsynaptic density protein, providing a link between the postsynaptic density and the actin cytoskeleton that may couple synaptic activity to changes in local cytoskeletal structure (Hering and Sheng, 2003; Naisbitt et al., 1999). δ-catenin interacts with PSD-95, N-cadherin, and glutamate receptor-associated proteins in neurons, thereby anchoring glutamate receptors to adhesion complexes and to the postsynaptic scaffold (Silverman et al., 2007). Thus, interaction of α10-nAChRs with cortactin may promote postsynaptic anchoring of α9/10-nAChRs both through linkage to the actin cytoskeleton as well as to the postsynaptic scaffold through interaction with δ-catenin and S-SCAM. In future studies, it would be interesting to determine whether other neuronal postsynaptic scaffold and adhesion proteins such as PSD-95 and neuroligin are expressed at hair cell synapses and whether interactions of cortactin, δ-catenin, and S-SCAM with these proteins play a role in hair cell synapse development similar to their role at neuronal glutamatergic synapses. Interaction of cortactin with ion channels, including Kv1.2 and large conductance BK potassium channels, couples channels to the cortical actin network and also directly regulates channel function (Hattan et al., 2002; Tian et al., 2008). Thus, it is possible that association of α10-nAChR subunits with cortactin may modulate both the synaptic anchoring as well as the function of α9/10-nAChRs.

We have also identified 14-3-3 as a novel binding partner of SK2 channels. Previous work in our lab showing that 14-3-3 dimers link α3-nAChRs to APC in neurons (Rosenberg et al., 2008), together with our finding that the APC postsynaptic complex is conserved at the hair cell efferent synapse (see Chapter 2), suggests the possibility that 14-3-3 plays a similar role in hair cells, anchoring SK2 channels at the synapse via APC. However, 14-3-3 proteins play diverse roles in the regulation of channel trafficking and function; different 14-3-3 isoforms promote the surface membrane trafficking of TASK potassium channels (Rajan et al., 2002; Zuzarte et al., 2009), α4-nAChRs (Jeanclos et al., 2001), and NR2C-containing NMDA-Rs (Chen and Roche, 2009), block the functional heterodimerization of $GABA_B$Rs (Couve et al., 2001), and can directly regulate the functional properties of several different ion channels (Kagan et al., 2002; Li et al., 2006; Zhou et al., 1999). Hence, numerous possibilities exist regarding the role of 14-3-3 in SK2 channel localization and/or function in hair cells. Studies of SK2 channels in heterologous cells demonstrate that PKA-mediated phosphorylation of SK2 at three consecutive C-terminal serine residues, each of which is the central residue of a predicted 14-3-3 binding motif, triggers their removal from the cell membrane (Ren et al., 2006). Therefore, if 14-3-3 binding at these three phosphoserine residues constitutes a mechanism for phosphorylation-dependent channel trafficking, these results would suggest that interaction with 14-3-3 negatively regulates SK2 surface expression. Future studies will be required to determine which residues in the SK2 C-terminal are

required for 14-3-3 interaction and what how this interaction may affect SK2 channel surface expression and function.

Chapter 5

Discussion and Future Directions

Summary

Inhibition of hair cell activity by efferent olivocochlear synapses constitutes a critical feedback system that regulates hearing sensitivity and frequency selectivity, aids sound detection in background noise, and protects hair cells against noise overexposure and damage (for review, see (Elgoyhen et al., 2009). Hyperpolarization of hair cells and the suppression of their electromotile amplification processes in response to cholinergic signals depends on the functional coupling of α9/10-nAChRs to SK2 channels (Fuchs and Murrow, 1992a; Oliver et al., 2000). The mechanisms underlying the assembly of postsynaptic sites and the proper localization of α9/10-nAChRs and SK2 channels have previously been poorly understood. The work presented in this thesis provides new insights into the molecular structure of postsynaptic sites and mechanisms that regulate the localization and coupling of nAChRs and SK2 channels. We identify new protein components of the postsynaptic scaffold in hair cells. We show that a physical association between nAChRs and SK2 channels likely supports their functional coupling at synapses and show that this association is regulated by two interrelated mechanisms: alternative splicing of the SK2 channel, and synaptic Ca^{2+} signaling. Finally, we present preliminary data demonstrating interactions of α10-nAChRs and SK2 channels with adapter proteins that may regulate the synaptic localization and anchoring of nAChR-SK2 complexes.

The postsynaptic complex in hair cells

We have identified a postsynaptic protein complex in cochlear hair cells that may support the synaptic localization and retention of α9/10-nAChRs and their partner SK2 channels. APC, which plays a critical role in nicotinic receptor clustering in myotubes (Wang et al., 2003) and at both pre- and postsynaptic sites in neurons (Farias et al., 2007; Temburni et al., 2004), localizes to the synaptic region in chicken hair cells adjacent to synapsin-labeled presynaptic terminals. In chick peripheral neurons, APC facilitates the delivery of α3-containing nAChRs to the synapse by interacting with the microtubule binding protein EB1 to direct microtubule-based trafficking of nAChR to the developing synaptic region (Temburni et al., 2004). Our finding that EB1 localizes to the synaptic site in hair cells as well as in neurons suggest that APC and EB1 play a similar role in the targeting of α9/10-nAChRs and their associated SK2 channels to the synapse. APC and EB1 are also essential in neurons for the assembly of a postsynaptic complex composed of cytoskeletal and scaffolding proteins, including the cytoskeletal regulatory proteins MACF and IQGAP1, β-catenin, PSD-93, S-SCAM, and neuroligin. Disrupting APC-EB1 interaction reduces the synaptic levels of many proteins in the complex (Rosenberg et al., 2008; Rosenberg et al., 2010; Temburni et al., 2004). We show that MACF and S-SCAM demonstrate postsynaptic concentration in chick hair cells, further supporting the notion that a similar protein complex underlies synaptic assembly in neurons and in hair cells. Furthermore, immunofluorescence and Western blotting experiments indicate that the neural adhesion proteins neuroligin-1 and

N-cadherin, as well as β-catenin, which links the APC synaptic complex to N-cadherin in neurons, are expressed in the cochlea, suggesting that they are also included in the hair cell postsynaptic complex (Murthy et al., 2009b). Together, these results strongly suggest that the APC-centered postsynaptic complex originally identified in neurons is conserved in hair cells and may be important for the synaptic localization of α9/10-nAChRs.

Hair cells also show similarities to neurons in the transsynaptic regulation of presynaptic contacts. In neurons, postsynaptic APC-EB1 and β-catenin-S-SCAM interactions are important for normal presynaptic alignment and adhesion, as disruption of either interaction causes reductions in accumulation of presynaptic active zone proteins and abnormal terminal structure (Rosenberg et al., 2010). Other studies have shown that nAChRs themselves are also essential for normal synapse assembly, as deletion of α3-nAChRs in mice causes abnormal presynaptic terminal morphology and protein expression at superior cervical ganglion neuron synapses (Krishnaswamy and Cooper, 2009). Similarly, α9-nAChR knockout mice show significant upregulation of transsynaptic adhesion molecules and abnormal, hypertrophied synaptic boutons with altered expression of presynaptic vesicle and active zone proteins. Conversely, hair cells of mice expressing a functionally-enhanced α9-nAChR mutant show a significant increase in number of efferent bouton contacts (Murthy et al., 2009b). Thus, both APC and α9-nAChR-mediated synaptic activity likely contribute to the expression and localization of postsynaptic complex proteins and the regulation of efferent terminal development.

While the APC postsynaptic complex has now been demonstrated to support nAChR localization and synapse assembly in multiple systems and cells, it seems that specific linkages between the core complex and membrane receptors may vary with the cell type and/or nAChR subtype. For example, APC binds directly to β-nAChR subunits in muscle (Wang et al., 2003) but not to α3-nAChRs in neurons, which are instead linked to APC through 14-3-3 (Rosenberg et al., 2008; Temburni et al., 2004). Therefore, we sought to identify potential adapter proteins that could specifically anchor α9/10-nAChRs and SK2 channels to the core APC complex. Based on the presence of canonical protein interaction motifs in the intracellular domains of SK2 channels and the α10-nAChR subunit, we proposed 14-3-3 and cortactin, respectively, as adapter proteins. We also proposed α-actinin-1 as an SK2 adapter protein based on the role of α-actinin-2 in SK2 localization in cardiac muscle cells (Lu et al., 2009; Lu et al., 2007). Consistent with our predictions, we found that α-actinin-1, the predominant α-actinin isoform expressed in the chicken cochlea, and cortactin are localized to the postsynaptic region in chicken hair cells. δ-catenin, a scaffolding protein that interacts with cortactin and S-SCAM to support postsynaptic structure in neurons (Abu-Elneel et al., 2008; Ide et al., 1999; Martinez et al., 2003), also shows strong localization at the synapse. 14-3-3 appeared to be associated with presynaptic terminals, as indicated by strong co-localization with SV2 using an antibody against the 14-3-3β isoform. However, we found that 14-3-3ζ interacts directly with the C terminal of SK2 in recombinant peptide binding assays, though it has been suggested that 14-3-3 interactions may not be isoform-specific *in vitro*

(Aitken et al., 2002). Future studies will be required to determine which 14-3-3 isoforms are expressed in hair cells and interact with SK2 *in vivo.* The potential roles of 14-3-3, cortactin, and α-actinin-1 in nAChR and SK2 channel interactions and anchoring are discussed below.

Our immunolabeling studies, together with previous reports of adhesion protein expression in the cochlea (Murthy et al., 2009b), suggest the model of the postsynaptic complex in hair cells shown in Figure 5.1. In this model, APC assembles cytoskeletal regulators and scaffolding proteins to target α9/10-nAChR and SK2 channel delivery to the synaptic pole and promote their stable membrane retention through interactions with adapter proteins. It would be interesting in future studies to determine whether this complex also links to the

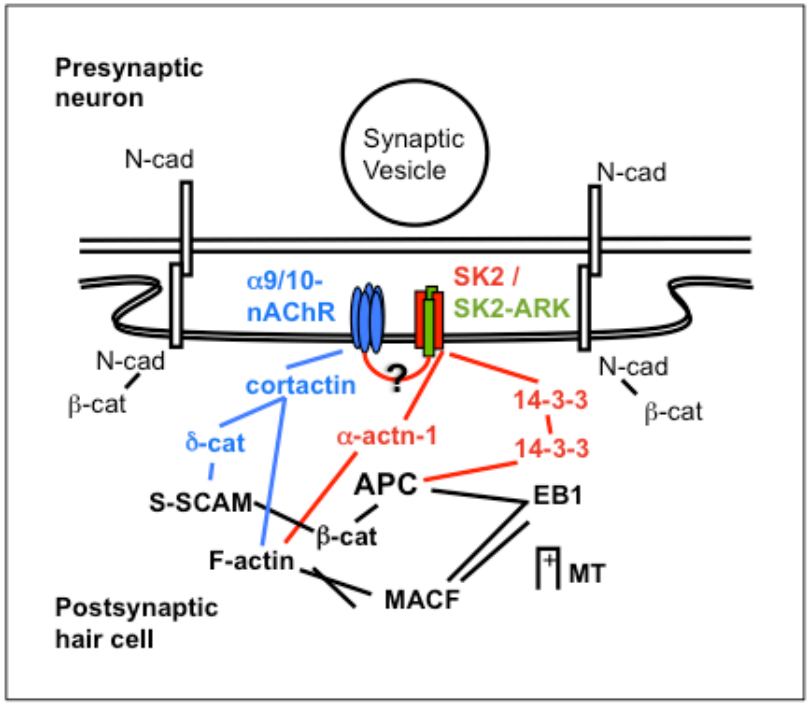

Figure 5.1: Molecular model of olivocochlear postsynaptic sites in hair cells.

subsynaptic cistern located in close proximity to the hair cell postsynaptic membrane (Cohen and Fermin, 1978; Grant et al., 2006; Saito, 1983). The enhancement of acetylcholine-evoked outward currents in hair cells by ryanodine receptor agonists suggests that ryanodine receptors may be somehow coupled to nAChRs to promote their fast activation by Ca^{2+} influx (Lioudyno et al., 2004). Thus, it is conceivable that the same postsynaptic complex directs the localization of α9/10-nAChRs in the surface membrane and ryanodine receptors in the nearby subsynaptic cistern membrane.

In addition to regulation of synaptic development in outer hair cells, APC could be important for the structure and function of other cell types in the cochlea. It would be useful in future studies to determine whether the transient efferent synapses and clusters of α9/10-nAChRs and SK2 channels that form in early postnatal inner hair cells utilize the same postsynaptic protein complex that we describe in outer hair cells and, if so, how the assembly and disassembly of the complex is regulated during the interaction and subsequent departure of the efferent terminals.

One of few prior studies of APC in the cochlea demonstrates that APC is expressed in pillar cells, one of several supporting cell types that participate in the structural organization of the organ of Corti (Mogensen et al., 2002). In these cells, APC associates with the plus ends of elongating microtubules during development and forms clusters at the basal pole of the cells. APC *Min* mice with heterozygous deletion of APC show fewer clustered microtubules in these supporting cells, suggesting that APC could be important for the development of

proper cell polarity and structure in the organ of Corti that supports normal motility and sound detection (Mogensen et al., 2002). Supporting cells in the organ of Corti perform multiple roles, including intercellular signaling to regulate hair cell differentiation (Kelley, 2006) and modulation of OHC electromotility (Yu and Zhao, 2009). A previous study showing that APC is required for AMPAR clustering at glutamatergic synapses in neurons (Shimomura et al., 2007) suggests the additional possibility that APC could regulate postsynaptic architecture or the clustering of AMPARs to support glutamatergic transmission of sound signals. Our lab has recently developed a CaMKII-mediated conditional APC knockout mouse with early postnatal deletion of APC from excitatory neurons. These mice demonstrate elevated hearing thresholds and aberrant patterns of IHC innervation by spiral ganglion neurons (Hickman et al., 2011; Liberman et al., 2011). Future studies of the APC cKO mice will likely address the specific roles of APC in the cochlea that subserve normal sound detection and synaptic transmission.

Functional coupling of α9/10-nAChRs and SK2 channels

Mechanism of interaction

The fast dynamics of functional coupling between α9/10-nAChRs and SK2 channels in response to acetylcholine suggest close co-localization of these two channels in the postsynaptic hair cell membrane. SK2 currents in hair cells following acetylcholine application occur on a time scale identical to that of isolated SK2 channels activated by fast, direct Ca^{2+} application. Furthermore,

SK2 channel activation in response to acetylcholine can be attenuated by BAPTA, a high-affinity Ca^{2+} chelator, but not by the lower-affinity chelator EGTA. These results indicate that saturating Ca^{2+} concentrations in the vicinity of the SK2 channel are reached within a millisecond of α9/10-nAChR activation, which in turn suggests that SK2 channels and nAChRs are localized within 10-20nm of one another (Fakler and Adelman, 2008; Oliver et al., 2000). The coincident development of nAChR and SK2 channel membrane clusters in developing IHCs, combined with the loss of functional α9/10-nAChR surface expression from hair cells of SK2-knockout mice, further imply that a physical linkage between α9/10 and SK2 promotes their close association and co-trafficking in hair cells (Kong et al., 2008; Murthy et al., 2009a; Roux et al., 2011). Our work confirms this theory, showing that tagged α9/10-nAChRs and SK2 channels co-immunoprecipitate from *Xenopus laevis* oocytes. It is not clear from these experiments whether SK2 binds directly to the α9 and/or α10-nAChR subunit or whether their interaction is mediated by intermediate proteins. Several previous studies have demonstrated that, though functional coupling occurs between α9/10-nAChRs and SK2 channels co-expressed in *Xenopus* oocytes, both the inward and outward components of the biphasic response to acetylcholine occur significantly more slowly than in hair cells, indicating that hair cell-specific mechanisms, perhaps post-translational modifications or interacting proteins, are necessary for the functional interaction and rapid IPSC dynamics of nAChRs and SK2 channels in hair cells (Nie et al., 2004; Oliver et al., 2001b). Thus, it seems likely that α9/10 and SK2 interact through other associated proteins.

Future studies should aim to identify these linking proteins. α-actinin-1 co-precipitated with SK2 from chicken cochlear lysates and when exogenously co-expressed with SK2 and α9/10-nAChRs in *Xenopus* oocytes, raising the possibility that α-actinin-1 may participate in their interaction. This notion is supported by the linkage of SK2 channels to their Ca^{2+} source in cardiac myocytes, $Ca_V1.3$ voltage-gated Ca^{2+} channels, by the muscle-specific α-actinin isoform, α-actinin-2 (Lu et al., 2007). On the other hand, if α-actinin-1 promotes the interaction between α9/10-nAChRs and SK2 channels, we would expect to see a reduced interaction of the SK2-ARK splice variant with α9/10 consistent with the observed decrease in interaction with α-actinin-1; instead, we find that SK2-ARK shows an increased interaction with α9/10-nAChRs, suggesting that their linkage may depend on proteins other than α-actinin-1.

Future studies should clarify these results and determine what role α-actinin-1 may serve in the coupling of α9/10-nAChRs and SK2 channels, perhaps by comparing levels of α9/10-nAChR co-precipitation with SK2 from oocytes with or without co-expression of α-actinin-1. Because we detected endogenous expression of α-actinin-1 in oocytes (not shown), we could also identify and mutate critical residues in the SK2 channel for α-actinin-1 interaction to determine whether interaction of α9/10-nAChRs with SK2 is affected by abolishment of SK2-α-actinin-1 binding. Two residues in the SK2 C-terminal have been identified that are critical for interaction with α-actinin-2 (Lu et al., 2009) (see Fig. 1.4), suggesting possible mutations sites to target in order to abolish

interaction with α-actinin-1. Our finding that the SK2-ARK splice variant shows reductions in α-actinin-1 binding in peptide binding assays and in oocytes suggests that the region of the splice insertion might also participate in a-actinin-1 binding. Consistent with this hypothesis, the ARK insertion is immediately downstream of a 5-residue sequence showing strong conservation with the α-actinin-1 binding domain in the NR1 NMDA subunit (Krupp et al., 1999). If co-precipitation of α9/10 with SK2 from oocytes is reduced by omission of α-actinin-1 or by an SK2 mutant with significantly reduced α-actinin-1 binding, this result would indicate that α-actinin-1 is important for α9/10-SK2 coupling.

If, however, α-actinin-1 is not the link between SK2 and α9/10, alternative candidates should be identified. Because many studies of endogenous nAChR interactions in the cochlea are precluded by the lack of specific antibodies against either α9 or α10 subunits, we might test *in vivo* interactions between α9/10-nAChRs and SK2 channels by affinity pull-down assays using bead-immobilized α9- or α10-nAChR recombinant peptide constructs incubated with cochlear protein lysates. Co-precipitation of SK2 could then be assayed by immunoblotting, and candidate linking proteins could be identified by immunoblotting or by 2-dimensional gel electrophoresis and mass spectrometry. Alternatively we might identify proteins that link α9/10-nAChRs to SK2 using yeast-two-hybrid screens to search for common binding partners of the intracellular domains of SK2 and either α9 or α10-nAChRs. Resulting proteins of interest could then be tested for interaction with SK2 and α9/10 in cochlear lysates, oocytes, and/or recombinant peptide assays.

Synaptic localization of α9/10-nAChRs and SK2 channels

Studies of hair cells in SK2 channel knockout animals were originally conducted with the intent of examining olivocochlear function in hair cells when cholinergic responses would theoretically, in the absence of SK2-mediated hyperpolarization, be converted from inhibition to excitation. Unexpectedly, however, no responses to either efferent fiber stimulation or exogenous acetylcholine application could be observed in SK2-knockout hair cells, despite normal mRNA levels of α9 and α10-nAChRs. Thus, SK2 channels are somehow necessary for the functional surface expression of α9/10-nAChRs, potentially by mediating the membrane localization of a pre-assembled complex of linked α9/10-nAChRs and SK2 channels (Kong et al., 2008; Murthy et al., 2009a).

In a more recent study, Roux et al (2011) tested cholinergic responses in inner hair cells of neonatal rats, which receive transient efferent innervation that is lost at the onset of hearing (Glowatzki and Fuchs, 2000; Katz et al., 2004). At P0, small inward currents could be observed in response to acetylcholine that were not coupled to SK2-mediated outward currents, indicating, in contrast to previous results, that α9/10-nAChRs are capable of reaching the surface membrane before the functional expression of SK2 channels. However, responses to efferent synaptic stimulation could not be detected until P1, when outward SK2-mediated currents were first observed. Immunofluorescent SK2 clusters and α-bungarotoxin-labeled α9/10-nAChR clusters were also first detected at P1. Progressive increases in SK2 clustering and SK2-mediated outward currents from P1 through P8 were closely paralleled by α9/10-nAChR

clusters and responsiveness of IHCs to synaptic signals. Overall, the coincidence of SK2 channel functional expression with nAChR clustering and sensitivity to synaptic input suggest that SK2 may mediate co-clustering with α9/10-nAChRs and that this clustering supports the ability of hair cells to respond to efferent input.

In agreement with these studies, we found that membrane expression levels of α9/10-nAChRs in surface biotinylation assays were correlated with that of SK2 channels. Surface-biotinylated nAChRs could be detected when expressed alone in oocytes, implying the existence of a membrane targeting mechanism for α9/10-nAChRs that is independent of SK2 channels. This result is consistent with the appearance of low-level α9/10-nAChR currents in P0 IHCs that lack detectable SK2 channel function (Roux et al., 2011). However, α9/10-nAChR surface expression in our experiments was increased by over twofold when co-expressed with SK2 channels, consistent with the progressive increases in nAChR currents and clusters that occur synchronously with increasing SK2 channel function in IHCs (Roux et al., 2011). Furthermore, co-expression of the SK2-ARK variant that showed significantly reduced membrane expression compared to SK2 also showed significantly decreased surface expression of α9/10-nAChRs. Together, our results demonstrate that SK2 channels significantly influence the localization of α9/10-nAChRs and support previous work indicating a dominant role for SK2 channels in the localization of the nAChR-SK2 complex. We did not test for changes in SK2 surface expression in the presence or absence of α9/10-nAChRs, which would indicate a reciprocal

influence of nAChRs on SK2 channel localization. However, hair cells of α9 and α10 knockout mice show little change in SK2 channel localization, indicating that proper SK2 channel localization can occur independently of nAChRs (Gomez-Casati et al., 2009; Vetter et al., 2007). Overall, our results and previous studies suggest a model in which the synaptic localization of α9/10-nAChRs depends largely on interaction with SK2 channels but may also be supported by mechanisms or protein interactions specific to nAChRs.

Regulation by Ca^{2+} signaling

We show that the association between α9/10-nAChRs and SK2 channels is regulated by Ca^{2+}, providing a possible mechanism for dynamic regulation of efferent transmission in hair cells. We found that chelation of intracellular Ca^{2+} by pre-incubation with BAPTA-AM and lysis in soluble BAPTA increased co-precipitation of α9/10-nAChRs and SK2 channels from *Xenopus* oocytes by twofold, suggesting that Ca^{2+} influx during synaptic activity might inhibit their interaction. This result raises interesting questions regarding the functional impact of Ca^{2+}-induced dissociation of the nAChR-SK2 channels from α9/10-nAChRs. One possibility is that inhibiting the physical association of SK2 channels from nAChRs would limit Ca^{2+} exposure and result in accelerated SK2 inactivation and attenuation of the IPSC. However, saturating Ca^{2+} transients in hair cells are evoked on a sub-millisecond time scale (Oliver et al., 2000) and dissipate over hundreds of milliseconds (Evans et al., 2000; Sridhar et al., 1997). Given the abundance of Ca^{2+} in the synaptic region, likely resulting both from

α9/10-nAChR-mediated Ca^{2+} influx and from Ca^{2+}-induced Ca^{2+} release (CICR) from subsynaptic stores, it seems unlikely that simply inhibiting the interaction between SK2 channels and α9/10-nAChRs within the synaptic membrane would significantly impact IPSC dynamics.

An alternative possibility is that Ca^{2+}-triggered dissociation of the nAChR-SK2 complex could allow the hair cell to regulate synaptic α9/10-nAChRs and SK2 channels independently of one another, possibly shaping IPSC dynamics and plasticity or modulating other downstream effects of efferent signaling. SK2 channels in hippocampal neurons, which are closely coupled to NMDARs, are selectively removed from the postsynaptic density during long-term potentiation, leaving NMDAR currents unchanged. This process is dependent on PKA phosphorylation of the SK2 C-terminal (Lin et al., 2008). Thus, it is conceivable that, following dissociation of SK2 channels from α9/10-nAChRs at the hair cell synapse, distinct signaling pathways or protein interactions could separately regulate their synaptic levels or activity to subserve different downstream effects. In addition to the frequency-dependent suppression of the cochlear amplifier by efferent synapse activation, cholinergic signaling in hair cells provides protection against noise-induced hair cell damage and hearing loss (Kujawa and Liberman, 1997; Reiter and Liberman, 1995). Resistance to noise damage is strongly correlated with α9-nAChR expression levels and function but is not enhanced in mice overexpressing SK2 channels, suggesting that α9/10-nAChR activation triggers downstream pathways to control noise protection that are independent of fast hyperpolarization through activation of SK2 channels (Maison et al., 2002;

Maison et al., 2007; Taranda et al., 2009b). Hence, it is possible that activity-induced dissociation of α9/10-nAChRs from SK2 channels could provide a means for hair cells to selectively modulate the different downstream effects of efferent signals: regulation of synaptic nAChR levels might subserve noise protection mechanisms, while separate mechanisms of SK2 channel regulation could modulate the strength or plasticity of hair cell hyperpolarization and suppression of electromechanical cochlear responses.

The response of the synapse to Ca^{2+} may be further modulated by expression of the SK2-ARK splice variant. SK2-ARK displayed an enhanced interaction with α9/10-nAChRs in oocytes that was not significantly altered by pre-incubation with BAPTA-AM, suggesting that α9/10-nAChRs may be less likely to dissociate from SK2-ARK-containing channels in response to synaptic Ca^{2+} influx.

Future studies should test these possibilities and further explore how α9/10-nAChRs and SK2 channels are affected by synaptic Ca^{2+} signaling. Our results demonstrate Ca^{2+}-mediated regulation of nAChR-SK2 interactions, but we have not yet tested the effects of Ca^{2+} on their surface expression or retention. One possible way to address this would be to modify our surface biotinylation and endocytosis assay to determine whether Ca^{2+} manipulation affects the surface expression or endocytosis rates of SK2 or SK2-ARK channels and tagged α9/10-nAChRs in *Xenopus* oocytes. The chicken α9 and α10-nAChR subunits used in our experiments were less efficiently expressed in oocytes compared to SK2 channels, making analysis of nAChR endocytosis rates difficult in our experiments; thus, in future experiments we might use mammalian α9 and α10-

nAChRs, which are expressed well in oocytes (M. McIntosh, personal communication). nAChR and SK2 or SK2-ARK membrane expression levels and endocytosis rates could be measured in oocytes pre-loaded with BAPTA-AM prior to surface biotinylation and compared to controls. Alternatively, oocytes could be exposed to acetylcholine following biotinylation to mimic synaptic activation and Ca^{2+} signaling. These experiments could help us to better understand the behavior of surface nAChRs and SK2 channels in response to Ca^{2+}. Altered rates of endocytosis in oocytes exposed to acetylcholine or pre-incubated with BAPTA-AM would support a model in which synaptic Ca^{2+} signaling in hair cells alters the stability and membrane retention of nAChRs and/or SK2 channels to regulate the postsynaptic effects of efferent feedback.

Regulation by SK2-ARK alternative splicing

In Chapter 2, we characterized the protein interaction properties, surface expression, and developmental profile of the SK2-ARK alternative splice variant. SK2-ARK was originally identified in short hair cells of postnatal chickens, and its properties and functional effects have previously been unknown. The most significant differences that we find between the chicken SK2-ARK variant and its ARK-lacking counterpart are its dramatically decreased surface membrane expression, its enhanced interaction with α9/10-nAChRs, and the lack of inhibition of this interaction by Ca^{2+}. These results suggest that expression of SK2-ARK and its putative co-assembly with SK2 subunits could affect the surface trafficking of assembled SK2 channel tetramers, its association with

α9/10-nAChRs, and the response of the complex to synaptic Ca^{2+} signals. We found a small reduction in the Ca^{2+}-sensitivity of SK2-ARK channel gating in inside-out patch-clamp recordings. Given the rapid, saturating increase in postsynaptic Ca^{2+} concentrations elicited by efferent synapse activity in hair cells (Oliver et al., 2000), it is unlikely that the small decrease in sensitivity of SK2-ARK to sub-micromolar Ca^{2+} concentrations would significantly impact synaptic function. However, these experiments do not rule out changes in single-channel potassium conductance or current-voltage relationship of SK2-ARK channels that could affect the magnitude and dynamics of efferent IPSCs in hair cells; additional experiments will be needed to further characterize these functional properties of SK2-ARK.

We also find that the expression of the SK2-ARK variant in the chicken cochlea increases during embryonic development, constituting approximately 35% of total SK2 transcripts immediately prior to hatching. Further experiments will be necessary to determine the functional consequences of SK2-ARK expression in the cochlea and specific roles in the development or function of olivocochlear synapses.

Importantly, preliminary results of recent RT-PCR experiments in our lab show that the SK2-ARK variant is expressed in the mouse hippocampus, indicating that the functional effects of SK2-ARK expression may be relevant in mammalian species (A. Pirone, unpublished observations). Upcoming experiments in the lab will determine whether SK2-ARK is expressed in the mouse cochlea. Future experiments should address the spatial and temporal

expression patterns of SK2-ARK in mouse and/or chicken cochleae. The development of an antibody to specifically recognize ARK-containing SK2 channels would be an extremely useful tool in these studies. An anti-ARK antibody would allow us to test SK2-ARK localization in the cochlea to determine whether it duplicates “total” SK2 labeling with existing antibodies that would recognize both splice variants. Complete overlap between total and SK2-ARK-specific labeling would suggest that either SK2 and SK2-ARK co-assemble, or if they do not, that their localization patterns are similar. The presence of SK2 immunolabeling that does not overlap with specific SK2-ARK labeling would indicate SK2 channels that localize separately from SK2-ARK-containing channels. Based on our results showing dramatically decreased SK2-ARK membrane expression in oocytes, we might test for SK2-ARK-specific immunolabeling in hair cells that is preferentially localized to the cytoplasm rather than the postsynaptic membrane or test for co-localization with endosomal or Golgi markers.

Immunolabeling experiments might not only determine whether SK2 and SK2-ARK show similar subcellular or membrane localization, but also test their expression patterns in different regions of the cochlea or at different stages of development. α9/10-nAChRs and SK2 channels show graded expression levels in hair cells along the length of the mammalian cochlea, reflecting different levels of efferent input to regions detecting low (apical) versus high (basal) frequencies (Johnson et al., 2011; Morley and Simmons, 2002; Simmons and Morley, 1998; Wersinger et al., 2010). Therefore it is possible that levels of SK2-ARK might

also vary along the length of the cochlea and contribute differently to efferent inhibition at different frequencies. RT-PCR and clone analysis using the same methods as in the studies described here could be used to quantitatively describe relative levels of SK2 and SK2-ARK expression throughout the cochlea and throughout development. Alternatively, synthesis of oligonucleotide probes specific to SK2 or SK2-ARK would allow quantification using real-time qRT-PCR.

α9/10-nAChRs and BK channels

A recent study of potassium channel expression and function in the rat cochlea has revealed a novel mechanism of efferent cholinergic signaling, in which α9/10-nAChRs are functionally coupled to large conductance Ca^{2+}-activated potassium (BK) channels in addition to the well-studied coupling between α9/10-nAChRs and SK2 channels (Wersinger et al., 2010). The relative involvement of SK2 channels and BK channels was found to vary in different tonotopic regions of the cochlea. BK channels expression in hair cells showed a gradient along the length of the cochlea, with the greatest expression in OHCs in the basal, high-frequency region of the cochlea and lowest expression in apical, low-frequency hair cells. SK2 channels, by contrast, were strongly expressed at efferent synapses in the middle turn of the cochlea but also showed synaptic expression in basal and apical OHCs. Acetylcholine-evoked potassium currents recorded from basal hair cells demonstrated little effect of SK2 channel inhibition by apamin, whereas BK channel inhibition by iberiotoxin significantly reduced current amplitude. Conversely, apical hair cell currents were completely blocked

by apamin but were unaffected by iberiotoxin. These results demonstrate that hair cells in different tonotopic regions of the mammalian cochlea utilize different Ca^{2+}-activated potassium channels to mediate efferent hair cell inhibition, with an apparent gradient from BK-mediated inhibition in basal, high-frequency OHCs to SK2-mediated inhibition in apical, low-frequency OHCs. This gradient in channel function, combined with the differing Ca^{2+} affinities of BK and SK2 channels, may allow hair cells to respond preferentially to weak or strong efferent stimulation depending on the Ca^{2+} sensitivity of the predominant potassium channel (Wersinger et al., 2010).

Based on these findings, it would be interesting in future experiments to explore the mechanisms underlying the coupling of α9/10-nAChRs to BK channels. Experiments similar to those described here for α9/10 and SK2 could be conducted with BK channels in order to explore parallels between BK and SK2 in their interactions with α9/10-nAChRs. For instance, we might co-express tagged α9/10-nAChRs with BK channels in *Xenopus* oocytes in order to determine whether they also interact with one another and whether BK channels might, like SK2, modulate the surface expression of α9/10-nAChRs. Based on these results, we might then attempt to determine whether coupling of nAChRs to BK channels versus SK2 channels occurs through similar interacting proteins.

Adapter proteins for α9/10-nAChRs and SK2 channels

The studies described in this thesis have identified a core protein complex at olivocochlear postsynaptic sites in hair cells and explored the mechanisms that

regulate the interaction and membrane localization of functionally coupled α9/10-nAChRs and SK2 channels. A third goal of our work was to identify adapter proteins that connect the membrane-bound nAChR-SK2 complex to the underlying protein scaffold. We have presented preliminary data showing that three proteins, α-actinin-1, 14-3-3, and cortactin, are strong candidates as adapter proteins that could mediate the anchorage of SK2 channels and α9/10-nAChRs to the core synaptic protein complex.

α-actinin-1

We show in Chapter 3 that SK2 channels in the chicken cochlea interact with α-actinin-1. This interaction is direct and is mediated by the C-terminal of SK2, as revealed by recombinant peptide binding assays. A probable function of α-actinin-1 interaction is to promote SK2 channel surface expression or stability by providing a link to the local actin cytoskeleton. In cardiac muscle and in heterologous cells, the muscle-specific α-actinin-2 is required for the surface expression of SK2 channels (Lu et al., 2009), likely due to cytoskeletal anchorage, as inhibiting actin polymerization with cytochalasin D blocked the enhancing effect of α-actinin-2 on SK2 current density in HEK293 cells (Lu et al., 2007). SK2 immunolabeling in the absence of α-actinin-2 was associated with early endosome markers, suggesting that α-actinin-2 mediates SK2 channel recycling by preventing exocytosis or enhancing re-insertion from recycling endosomes (Lu et al., 2009). Based on these results, we propose that α-actinin-1, the non-muscle α-actinin isoform that we identified in the chick cochlea,

promotes SK2 stability in the hair cell synaptic membrane. Consistent with this theory, we found that the SK2-ARK variant with reduced binding to α-actinin-1 demonstrated impaired surface expression in oocytes, though the relatively small change in α-actinin-1 binding of SK2-ARK suggests that other factors may contribute to the significant reduction that we observed in its surface levels compared to SK2.

The marked effects of Ca^{2+} and CaM on binding of α-actinin-1 to SK2 imply that α-actinin-1-mediated cytoskeletal anchoring may be regulated by synaptic activity in hair cells, providing a potential mechanism for activity-dependent modulation of SK2 membrane levels. Ca^{2+} and Ca^{2+}-CaM appear to exert opposing effects on α-actinin-1 and SK2: 1mM Ca^{2+} alone strongly potentiated interaction of α-actinin-1 with both SK2 and SK2-ARK in peptide binding assays, whereas Ca^{2+}-bound CaM inhibited the interaction. Competition between α-actinin-1 and Ca^{2+}-CaM also occurs for binding to NR1 NMDA receptor subunits, such that CaM displaces α-actinin-1 from NR1 in response to NMDAR-mediated Ca^{2+} influx (Krupp et al., 1999; Merrill et al., 2007). Two key differences between these results and ours are, first, that Ca^{2+}-CaM mediates NMDARs *inactivation* versus SK2 channel activation; and, second, that Ca^{2+} alone does not enhance the binding of α-actinin-1 to NR1 (Merrill et al., 2007). In our experiments, the significant enhancement by Ca^{2+} of α-actinin-1 binding to SK2, even when partially blocked by 10μM CaM, implies that the net effect of Ca^{2+} influx may be to stabilize rather than block the interaction of SK2 with α-actinin-1, which would thereby promote SK2 membrane anchoring and retention. However, we cannot

rule out a different balance of Ca^{2+}- versus Ca^{2+}-CaM-mediated effects at physiological concentrations of Ca^{2+} and CaM. Postsynaptic Ca^{2+} concentration in hair cells has been estimated to be 10μM or more following efferent synapse activation (Oliver et al., 2000), whereas CaM in mammalian OHCs has been reported to reach 600mmol/kg (Takahashi, 1989). It is possible that, under these conditions of lower Ca^{2+} and higher CaM concentrations compared to those in our experiments, displacement of α-actinin-1 from SK2 by CaM may predominate over the Ca^{2+}-mediated enhancement of α-actinin-1 binding and result in loss rather than strengthening of α-actinin-1-mediated cytoskeletal anchoring. It would be worthwhile to test this possibility in future experiments by repeating these peptide binding assays using smaller concentrations of Ca^{2+} and larger amounts of CaM.

14-3-3

We have demonstrated that the small linker protein 14-3-3 interacts directly with SK2 channels, consistent with sequence analyses predicting six 14-3-3 binding motifs at the end of the intracellular C-terminal. Interaction with 14-3-3 in peptide binding assays was similar between SK2 and the SK2-ARK variant. At cholinergic synapses in chick ciliary ganglion neurons, 14-3-3 binding is required for linkage of α3-nAChRs to APC; APC co-precipitates with α3-nAChRs from neurons and from heterologous cells, and this interaction is prevented by a mutation in the α3-nAChR that eliminates 14-3-3 binding (Rosenberg et al., 2008). The similarities in protein composition that we have described between

neuronal and hair cell nicotinic synapses support the possibility that 14-3-3 constitutes a link between membrane-bound receptors and the postsynaptic protein network in hair cells as it does in neurons, though for the partner SK2 channel rather than the α9/10-nAChRs.

Alternatively, binding of 14-3-3 to SK2 may also serve other functions. Phosphorylation by PKA of three serine residues within the predicted 14-3-3 binding motifs mediates activity-dependent SK2 endocytosis from glutamatergic synapses in hippocampal neurons, which enhances synaptic plasticity by removing the inhibitory effects of SK2 currents on LTP induction (Lin et al., 2008). Thus, it is plausible that, rather than stabilizing SK2 by anchorage to APC, binding of 14-3-3 to phosphorylated motifs could promote SK2 endocytosis, which could in turn dynamically modulate the strength of efferent inhibition.

A third possibility is that 14-3-3 could regulate SK2 membrane targeting by facilitating its assembly and/or exit from the endoplasmic reticulum (ER) by blocking retention signals, as has been demonstrated for multiple ion channels and receptors. The intracellular N-terminal of SK2 contains an RKR motif, which is a canonical ER retention signal. Several other potassium channels, including TASK potassium channels, ATP-sensitive potassium channels, and KCNK3 channels, also contain RKR or similar retention motifs, which direct protein localization or retrieval to the ER by interacting with COP coat proteins. Binding of 14-3-3 to these potassium channels blocks the binding of COP proteins to retention motifs, resulting in the disinhibition of forward cellular trafficking (Heusser et al., 2006; O'Kelly et al., 2002; Yuan et al., 2003; Zuzarte et al.,

2009). Though 14-3-3 binding motifs and RKR motifs overlap in some instances (Yuan et al., 2003), it is often an RKR motif in a separate channel subunit that is masked by 14-3-3 to allow exit from the ER, thus providing a mechanism by which 14-3-3 serves as a "sensor" for correctly assembled channel multimers (Heusser et al., 2006; O'Kelly et al., 2002). Based on these studies, it is possible that binding of 14-3-3 to the C-terminal of SK2, as we have shown, blocks N-terminal RKR motifs in adjacent subunits to promote the release of properly assembled SK2 channels from the ER. In support of this notion, complex interactions among the N- and C-termini of SK2 and the associated CK2-PP2A complex suggest a model in which the N- and C-termini of different SK2 subunits are brought into close proximity (Allen et al., 2007). Thus, such an arrangement could facilitate intra-subunit contacts between N-terminal RKR motifs and C-terminal-bound 14-3-3 proteins.

Cortactin

We have proposed that cortactin functions as an adapter protein for α9/10-nAChRs in the cochlea by binding to the α10-nAChR subunit and anchoring receptors to the postsynaptic protein complex and actin cytoskeleton. In support of this hypothesis, we have shown that cortactin and its neuronal binding partner, δ-catenin (Martinez et al., 2003), are concentrated at the synaptic pole in chick hair cells and co-localize with S-SCAM, which binds to δ-catenin in neurons (Ide et al., 1999). Preliminary immunoprecipitation experiments suggest that, consistent with the presence of canonical cortactin binding motifs in the α10-

nAChR cytoplasmic loop, cortactin co-precipitates with a tagged α10-nAChR loop construct from heterologous cells. Together, these results support the synaptic anchoring of α9/10-nAChRs by cortactin to the actin cytoskeleton and to the postsynaptic complex via δ-catenin and S-SCAM.

Although our results, together with previous studies, indicate that the SK2 channel plays a critical role in the surface expression and clustering of α9/10-nAChRs, it is also apparent that α9/10-nAChR-specific mechanisms independent of SK2 channels can support their surface expression, as suggested by the presence of small nAChR currents in immature hair cells before the appearance of functional SK2 channels (Dulon and Lenoir, 1996; Roux et al., 2011) and our observation of low levels of surface biotinylated α9/10-nAChRs in *Xenopus* oocytes. nAChR-specific localization mechanisms may depend on protein interactions of the α10 subunit, as α10 is critical for the functional surface expression of hair cell nAChRs (Elgoyhen et al., 2001; Oliver et al., 2001b; Vetter et al., 2007). Thus, cortactin interactions with α10 subunits could constitute a mechanism for the synaptic expression or stabilization of α9/10-nAChRs.

Future studies of adapter proteins

Together with the results presented here, prior studies of α-actinin-1, 14-3-3, and cortactin indicate that these adapter proteins are likely candidates to regulate the surface localization and anchoring of SK2 channels and α9/10-nAChRs. Future experiments should therefore closely examine the influence of the adapter proteins on the interactions and cellular localization of SK2 and α9/10.

Interactions of SK2 and α10-nAChRs with 14-3-3 and cortactin, respectively, should be tested *in vivo* by SK2 immunoprecipitation or affinity pull-down assays using an immobilized α10-nAChR peptide. Using these methods, we might also test for co-precipitation of other proteins, such as APC, δ-catenin, or S-SCAM, which would support our hypothesis that these proteins anchor SK2 channels and α9/10-nAChRs via 14-3-3 and cortactin.

To identify the roles of adapter proteins in SK2 channel and α9/10-nAChR cellular localization, future experiments might determine whether blocking their interactions alters SK2 and α9/10-nAChR surface trafficking or retention in heterologous cell expression systems. Critical residues for 14-3-3 and cortactin interactions with SK2 and α10-nAChRs, respectively, are suggested by the importance of the central serine or threonine residue in 14-3-3 binding motifs (Yaffe, 2002) and the central proline of cortactin-SH3 binding motifs (Daly, 2004). SK2 channels and α9/10-nAChRs with abolished 14-3-3, α-actinin-1, or cortactin binding could be tested in HEK293 cells or in *Xenopus* oocytes for altered surface expression or internalization rates using biotinylation assays or for altered localization using immunolabeling with subcellular markers. Another possibility would be to co-express SK2 channels with 14-3-3 scavenging peptides that reduce 14-3-3 protein availability and have been shown to affect the surface expression and function of potassium channels in heterologous cells (Heusser et al., 2006; Sottocornola et al., 2006). If SK2 or α9/10-nAChR membrane expression or retention in heterologous cells are affected by preventing interactions with α-actinin-1, 14-3-3, or cortactin, these results would support our

hypothesis that the adapter proteins are essential for regulating the synaptic localization of the α9/10-SK2 receptor complex in hair cells.

Concluding remarks

The work presented in this thesis provides new insights into the mechanisms that mediate the assembly and regulation of the unique nicotinic olivocochlear synapse in hair cells. Functional coupling between α9/10-nAChRs and SK2 channels at hair cell synapses is essential for efferent control of sound sensitivity and frequency selectivity. Cholinergic signaling is also important for reducing the susceptibility of the cochlea to damage by noise overexposure. Our results uncover new mechanisms that direct nAChR and SK2 channel membrane localization, stability, and functional coupling at postsynaptic sites. We describe a postsynaptic protein complex in hair cells that shares many common components with neuronal and neuromuscular nicotinic synapses and likely promotes the synaptic localization and anchoring of nAChRs and SK2 channels. We also demonstrate for the first time that SK2 channels and α9/10-nAChRs physically interact with one another to support their functional coupling, and we present evidence of novel, interrelated mechanisms that regulate their interactions and localization in hair cells. Alternative splicing of the SK2 channel, resulting in expression of the SK2-ARK variant during cochlear development, alters the interactions and membrane expression of SK2 and α9/10-nAChRs. We further show that Ca^{2+} signaling differentially alters the interactions of SK2 and SK2-ARK channels with α9/10-nAChRs. Ca^{2+} also regulates the interaction of SK2

channels with a newly identified binding partner, α-actinin-1, providing a possible mechanism for activity-dependent modulation of SK2 membrane anchorage. Finally, preliminary data indicate that 14-3-3 and cortactin are binding partners of SK2 channels and α10-nAChRs that are strong candidates to connect the SK2-nAChR membrane complex to the underlying postsynaptic scaffold and regulate its synaptic localization and stability. Taken together, our results reveal new proteins and mechanisms that may contribute to the development and function of olivocochlear synapses and suggest new directions for future studies of efferent synapse assembly and transmission.

Bibliography

Abu-Elneel K, Ochiishi T, Medina M, Remedi M, Gastaldi L, Caceres A, and Kosik KS (2008). A delta-catenin signaling pathway leading to dendritic protrusions. *J Biol Chem*. 283:32781-32791.

Aitken A, Baxter H, Dubois T, Clokie S, Mackie S, Mitchell K, Peden A, and Zemlickova E (2002). Specificity of 14-3-3 isoform dimer interactions and phosphorylation. *Biochemical Society transactions*. 30:351-360.

Akil O, Chang J, Hiel H, Kong JH, Yi E, Glowatzki E, and Lustig LR (2006). Progressive deafness and altered cochlear innervation in knock-out mice lacking prosaposin. *J Neurosci*. 26:13076-13088.

Allen D, Bond CT, Lujan R, Ballesteros-Merino C, Lin MT, Wang K, Klett N, Watanabe M, Shigemoto R, Stackman RW, Jr., Maylie J, and Adelman JP (2011). The SK2-long isoform directs synaptic localization and function of SK2-containing channels. *Nat Neurosci*. 14:744-749.

Allen D, Fakler B, Maylie J, and Adelman JP (2007). Organization and regulation of small conductance Ca2+-activated K+ channel multiprotein complexes. *J Neurosci*. 27:2369-2376.

Ashmore JF (1987). A fast motile response in guinea-pig outer hair cells: the cellular basis of the cochlear amplifier. *J Physiol*. 388:323-347.

Beggs AH, Byers TJ, Knoll JH, Boyce FM, Bruns GA, and Kunkel LM (1992). Cloning and characterization of two human skeletal muscle alpha-actinin genes located on chromosomes 1 and 11. *J Biol Chem*. 267:9281-9288.

Belyantseva IA, Adler HJ, Curi R, Frolenkov GI, and Kachar B (2000). Expression and localization of prestin and the sugar transporter GLUT-5 during development of electromotility in cochlear outer hair cells. *J Neurosci*. 20:RC116.

Benser ME, Marquis RE, and Hudspeth AJ (1996). Rapid, active hair bundle movements in hair cells from the bullfrog's sacculus. *J Neurosci*. 16:5629-5643.

Bildl W, Strassmaier T, Thurm H, Andersen J, Eble S, Oliver D, Knipper M, Mann M, Schulte U, Adelman JP, and Fakler B (2004). Protein kinase CK2 is coassembled with small conductance Ca(2+)-activated K+ channels and regulates channel gating. *Neuron*. 43:847-858.

Bond CT, Herson PS, Strassmaier T, Hammond R, Stackman R, Maylie J, and Adelman JP (2004). Small conductance Ca2+-activated K+ channel knock-out mice reveal the identity of calcium-dependent afterhyperpolarization currents. *J Neurosci*. 24:5301-5306.

Brix J, and Manley GA (1994). Mechanical and electromechanical properties of the stereovillar bundles of isolated and cultured hair cells of the chicken. *Hear Res*. 76:147-157.

Brown MC, and Nuttall AL (1984). Efferent control of cochlear inner hair cell responses in the guinea-pig. *J Physiol*. 354:625-646.

Brownell WE, Bader CR, Bertrand D, and de Ribaupierre Y (1985). Evoked mechanical responses of isolated cochlear outer hair cells. *Science*. 227:194-196.

Bruce LL, Christensen MA, and Warr WB (2000). Postnatal development of efferent synapses in the rat cochlea. *J Comp Neurol*. 423:532-548.

Campbell JP, and Henson MM (1988). Olivocochlear neurons in the brainstem of the mouse. *Hear Res*. 35:271-274.

Chan DK, and Hudspeth AJ (2005). Ca2+ current-driven nonlinear amplification by the mammalian cochlea in vitro. *Nat Neurosci*. 8:149-155.

Chen BS, and Roche KW (2009). Growth factor-dependent trafficking of cerebellar NMDA receptors via protein kinase B/Akt phosphorylation of NR2C. *Neuron*. 62:471-478.

Chen L, Sun W, and Salvi RJ (2001). Electrically evoked otoacoustic emissions from the chicken ear. *Hear Res*. 161:54-64.

Cohen GM, and Fermin CD (1978). The development of hair cells in the embryonic chick's basilar papilla. *Acta Otolaryngol*. 86:342-358.

Cooper NP, and Guinan JJ, Jr. (2003). Separate mechanical processes underlie fast and slow effects of medial olivocochlear efferent activity. *J Physiol*. 548:307-312.

Couve A, Kittler JT, Uren JM, Calver AR, Pangalos MN, Walsh FS, and Moss SJ (2001). Association of GABA(B) receptors and members of the 14-3-3 family of signaling proteins. *Mol Cell Neurosci*. 17:317-328.

Crawford AC, and Fettiplace R (1985). The mechanical properties of ciliary bundles of turtle cochlear hair cells. *J Physiol*. 364:359-379.

Dai Z, Luo X, Xie H, and Peng HB (2000). The actin-driven movement and formation of acetylcholine receptor clusters. *J Cell Biol*. 150:1321-1334.

Dallos P (1992). The active cochlea. *J Neurosci*. 12:4575-4585.

Dallos P, and Harris D (1978). Properties of auditory nerve responses in absence of outer hair cells. *J Neurophysiol*. 41:365-383.

Daly RJ (2004). Cortactin signalling and dynamic actin networks. *Biochem J*. 382:13-25.

Dulon D, and Lenoir M (1996). Cholinergic responses in developing outer hair cells of the rat cochlea. *Eur J Neurosci*. 8:1945-1952.

Elgoyhen AB, Johnson DS, Boulter J, Vetter DE, and Heinemann S (1994). Alpha 9: an acetylcholine receptor with novel pharmacological properties expressed in rat cochlear hair cells. *Cell*. 79:705-715.

Elgoyhen AB, Katz E, and Fuchs PA (2009). The nicotinic receptor of cochlear hair cells: a possible pharmacotherapeutic target? *Biochem Pharmacol*. 78:712-719.

Elgoyhen AB, Vetter DE, Katz E, Rothlin CV, Heinemann SF, and Boulter J (2001). alpha10: a determinant of nicotinic cholinergic receptor function in mammalian vestibular and cochlear mechanosensory hair cells. *Proc Natl Acad Sci U S A*. 98:3501-3506.

Emadi G, Richter CP, and Dallos P (2004). Stiffness of the gerbil basilar membrane: radial and longitudinal variations. *J Neurophysiol*. 91:474-488.

Evans MG, Lagostena L, Darbon P, and Mammano F (2000). Cholinergic control of membrane conductance and intracellular free Ca2+ in outer hair cells of the guinea pig cochlea. *Cell calcium*. 28:195-203.

Exley R, Moroni M, Sasdelli F, Houlihan LM, Lukas RJ, Sher E, Zwart R, and Bermudez I (2006). Chaperone protein 14-3-3 and protein kinase A increase the relative abundance of low agonist sensitivity human alpha 4 beta 2 nicotinic acetylcholine receptors in Xenopus oocytes. *J Neurochem*. 98:876-885.

Eybalin M (1993). Neurotransmitters and neuromodulators of the mammalian cochlea. *Physiological reviews*. 73:309-373.

Faber ES (2009). Functions and modulation of neuronal SK channels. *Cell Biochem Biophys*. 55:127-139.

Fakler B, and Adelman JP (2008). Control of K(Ca) channels by calcium nano/microdomains. *Neuron*. 59:873-881.

Farias GG, Valles AS, Colombres M, Godoy JA, Toledo EM, Lukas RJ, Barrantes FJ, and Inestrosa NC (2007). Wnt-7a induces presynaptic colocalization of alpha 7-nicotinic acetylcholine receptors and adenomatous polyposis coli in hippocampal neurons. *J Neurosci*. 27:5313-5325.

Fettiplace R, and Fuchs PA (1999). Mechanisms of hair cell tuning. *Annu Rev Physiol*. 61:809-834.

Fettiplace R, and Hackney CM (2006). The sensory and motor roles of auditory hair cells. *Nat Rev Neurosci*. 7:19-29.

Fischer FP (1992). Quantitative analysis of the innervation of the chicken basilar papilla. *Hear Res*. 61:167-178.

Fuchs PA, and Murrow BW (1992a). Cholinergic inhibition of short (outer) hair cells of the chick's cochlea. *J Neurosci*. 12:800-809.

Fuchs PA, and Murrow BW (1992b). A novel cholinergic receptor mediates inhibition of chick cochlear hair cells. *Proceedings. Biological sciences / The Royal Society*. 248:35-40.

Galambos R (1956). Suppression of auditory nerve activity by stimulation of efferent fibers to cochlea. *J Neurophysiol*. 19:424-437.

Glowatzki E, and Fuchs PA (2000). Cholinergic synaptic inhibition of inner hair cells in the neonatal mammalian cochlea. *Science*. 288:2366-2368.

Gomez-Casati ME, Wedemeyer C, Taranda J, Lipovsek M, Dalamon V, Elgoyhen AB, and Katz E (2009). Electrical properties and functional expression of ionic channels in cochlear inner hair cells of mice lacking the alpha10 nicotinic cholinergic receptor subunit. *J Assoc Res Otolaryngol*. 10:221-232.

Grant L, Slapnick S, Kennedy H, and Hackney C (2006). Ryanodine receptor localisation in the mammalian cochlea: an ultrastructural study. *Hear Res*. 219:101-109.

Hammond RS, Bond CT, Strassmaier T, Ngo-Anh TJ, Adelman JP, Maylie J, and Stackman RW (2006). Small-conductance Ca2+-activated K+ channel type 2 (SK2) modulates hippocampal learning, memory, and synaptic plasticity. *J Neurosci*. 26:1844-1853.

Harris M, Garcia-Caballero A, Stutts MJ, Firsov D, and Rossier BC (2008). Preferential assembly of epithelial sodium channel (ENaC) subunits in Xenopus oocytes: role of furin-mediated endogenous proteolysis. *J Biol Chem*. 283:7455-7463.

Hasson T, Heintzelman MB, Santos-Sacchi J, Corey DP, and Mooseker MS (1995). Expression in cochlea and retina of myosin VIIa, the gene product defective in Usher syndrome type 1B. *Proc Natl Acad Sci U S A*. 92:9815-9819.

Hattan D, Nesti E, Cachero TG, and Morielli AD (2002). Tyrosine phosphorylation of Kv1.2 modulates its interaction with the actin-binding protein cortactin. *J Biol Chem*. 277:38596-38606.

He DZ, Beisel KW, Chen L, Ding DL, Jia S, Fritzsch B, and Salvi R (2003). Chick hair cells do not exhibit voltage-dependent somatic motility. *J Physiol*. 546:511-520.

He DZ, and Dallos P (1999). Development of acetylcholine-induced responses in neonatal gerbil outer hair cells. *J Neurophysiol*. 81:1162-1170.

Hering H, and Sheng M (2003). Activity-dependent redistribution and essential role of cortactin in dendritic spine morphogenesis. *J Neurosci*. 23:11759-11769.

Heusser K, Yuan H, Neagoe I, Tarasov AI, Ashcroft FM, and Schwappach B (2006). Scavenging of 14-3-3 proteins reveals their involvement in the cell-surface transport of ATP-sensitive K+ channels. *J Cell Sci*. 119:4353-4363.

Hickman T, Gomez-Casati M, Corfas G, and Jacob M (2011). Adenomatous polyposis coli (APC) protein is required for normal hearing. Midwinter Meeting: Association for Research in Otolaryngology (Baltimore, MD).

Hiel H, Luebke AE, and Fuchs PA (2000). Cloning and expression of the alpha9 nicotinic acetylcholine receptor subunit in cochlear hair cells of the chick. *Brain Res*. 858:215-225.

Hill AV (1910). The possible effects of the aggregation of the molecules of haemoglobin on its dissociation curves. *J Physiol*. 40:iv-vii.

Hirao K, Hata Y, Ide N, Takeuchi M, Irie M, Yao I, Deguchi M, Toyoda A, Sudhof TC, and Takai Y (1998). A novel multiple PDZ domain-containing molecule interacting with N-methyl-D-aspartate receptors and neuronal cell adhesion proteins. *J Biol Chem*. 273:21105-21110.

Hirokawa N (1978a). Synaptogenesis in the basilar papilla of the chick. *J Neurocytol*. 7:283-300.

Hirokawa N (1978b). The ultrastructure of the basilar papilla of the chick. *J Comp Neurol*. 181:361-374.

Housley GD, Marcotti W, Navaratnam D, and Yamoah EN (2006). Hair cells--beyond the transducer. *The Journal of membrane biology*. 209:89-118.

Ide N, Hata Y, Deguchi M, Hirao K, Yao I, and Takai Y (1999). Interaction of S-SCAM with neural plakophilin-related Armadillo-repeat protein/delta-catenin. *Biochem Biophys Res Commun*. 256:456-461.

Iida J, Hirabayashi S, Sato Y, and Hata Y (2004). Synaptic scaffolding molecule is involved in the synaptic clustering of neuroligin. *Mol Cell Neurosci*. 27:497-508.

Jacob MH, and Berg DK (1983). The ultrastructural localization of alpha-bungarotoxin binding sites in relation to synapses on chick ciliary ganglion neurons. *J Neurosci*. 3:260-271.

Jeanclos EM, Lin L, Treuil MW, Rao J, DeCoster MA, and Anand R (2001). The chaperone protein 14-3-3eta interacts with the nicotinic acetylcholine receptor alpha 4 subunit. Evidence for a dynamic role in subunit stabilization. *J Biol Chem*. 276:28281-28290.

Johnson SL, Adelman JP, and Marcotti W (2007). Genetic deletion of SK2 channels in mouse inner hair cells prevents the developmental linearization in the Ca2+ dependence of exocytosis. *J Physiol*. 583:631-646.

Johnson SL, Eckrich T, Kuhn S, Zampini V, Franz C, Ranatunga KM, Roberts TP, Masetto S, Knipper M, Kros CJ, and Marcotti W (2011). Position-dependent patterning of spontaneous action potentials in immature cochlear inner hair cells. *Nat Neurosci*. 14:711-717.

Kagan A, Melman YF, Krumerman A, and McDonald TV (2002). 14-3-3 amplifies and prolongs adrenergic stimulation of HERG K+ channel activity. *Embo J*. 21:1889-1898.

Katz E, Elgoyhen AB, Gomez-Casati ME, Knipper M, Vetter DE, Fuchs PA, and Glowatzki E (2004). Developmental regulation of nicotinic synapses on cochlear inner hair cells. *J Neurosci*. 24:7814-7820.

Kawase T, Delgutte B, and Liberman MC (1993). Antimasking effects of the olivocochlear reflex. II. Enhancement of auditory-nerve response to masked tones. *J Neurophysiol*. 70:2533-2549.

Keen JE, Khawaled R, Farrens DL, Neelands T, Rivard A, Bond CT, Janowsky A, Fakler B, Adelman JP, and Maylie J (1999). Domains responsible for constitutive and Ca(2+)-dependent interactions between calmodulin and small conductance Ca(2+)-activated potassium channels. *J Neurosci*. 19:8830-8838.

Kelley MW (2006). Regulation of cell fate in the sensory epithelia of the inner ear. *Nat Rev Neurosci*. 7:837-849.

Kemp DT (1978). Stimulated acoustic emissions from within the human auditory system. *The Journal of the Acoustical Society of America*. 64:1386-1391.

Kennedy HJ, Crawford AC, and Fettiplace R (2005). Force generation by mammalian hair bundles supports a role in cochlear amplification. *Nature*. 433:880-883.

Kettembeil S, Manley GA, and Siegl E (1995). Distortion-product otoacoustic emissions and their anaesthesia sensitivity in the European starling and the chicken. *Hear Res*. 86:47-62.

Kohler M, Hirschberg B, Bond CT, Kinzie JM, Marrion NV, Maylie J, and Adelman JP (1996). Small-conductance, calcium-activated potassium channels from mammalian brain. *Science*. 273:1709-1714.

Kong JH, Adelman JP, and Fuchs PA (2008). Expression of the SK2 calcium-activated potassium channel is required for cholinergic function in mouse cochlear hair cells. *J Physiol*. 586:5471-5485.

Kracun S, Harkness PC, Gibb AJ, and Millar NS (2008). Influence of the M3-M4 intracellular domain upon nicotinic acetylcholine receptor assembly, targeting and function. *Br J Pharmacol*. 153:1474-1484.

Krishnaswamy A, and Cooper E (2009). An activity-dependent retrograde signal induces the expression of the high-affinity choline transporter in cholinergic neurons. *Neuron*. 61:272-286.

Krupp JJ, Vissel B, Thomas CG, Heinemann SF, and Westbrook GL (1999). Interactions of calmodulin and alpha-actinin with the NR1 subunit modulate Ca2+-dependent inactivation of NMDA receptors. *J Neurosci*. 19:1165-1178.

Kujawa SG, and Liberman MC (1997). Conditioning-related protection from acoustic injury: effects of chronic deefferentation and sham surgery. *J Neurophysiol*. 78:3095-3106.

Lee WS, Ngo-Anh TJ, Bruening-Wright A, Maylie J, and Adelman JP (2003). Small conductance Ca2+-activated K+ channels and calmodulin: cell surface expression and gating. *J Biol Chem*. 278:25940-25946.

Leung CL, Sun D, Zheng M, Knowles DR, and Liem RK (1999). Microtubule actin cross-linking factor (MACF): a hybrid of dystonin and dystrophin that can interact with the actin and microtubule cytoskeletons. *J Cell Biol*. 147:1275-1286.

Li Y, Atkin GM, Morales MM, Liu LQ, Tong M, and Duncan RK (2009). Developmental expression of BK channels in chick cochlear hair cells. *BMC Dev Biol*. 9:67.

Li Y, Wu Y, and Zhou Y (2006). Modulation of inactivation properties of CaV2.2 channels by 14-3-3 proteins. *Neuron*. 51:755-771.

Liberman LD, Wang H, and Liberman MC (2011). Opposing gradients of ribbon size and AMPA receptor expression underlie sensitivity differences among cochlear-nerve/hair-cell synapses. *J Neurosci*. 31:801-808.

Liberman MC, Gao J, He DZ, Wu X, Jia S, and Zuo J (2002). Prestin is required for electromotility of the outer hair cell and for the cochlear amplifier. *Nature*. 419:300-304.

Lin MT, Lujan R, Watanabe M, Adelman JP, and Maylie J (2008). SK2 channel plasticity contributes to LTP at Schaffer collateral-CA1 synapses. *Nat Neurosci*. 11:170-177.

Lin MT, Lujan R, Watanabe M, Frerking M, Maylie J, and Adelman JP (2010). Coupled activity-dependent trafficking of synaptic SK2 channels and AMPA receptors. *J Neurosci*. 30:11726-11734.

Lioudyno M, Hiel H, Kong JH, Katz E, Waldman E, Parameshwaran-Iyer S, Glowatzki E, and Fuchs PA (2004). A "synaptoplasmic cistern" mediates rapid inhibition of cochlear hair cells. *J Neurosci*. 24:11160-11164.

Lioudyno MI, Verbitsky M, Glowatzki E, Holt JC, Boulter J, Zadina JE, Elgoyhen AB, and Guth PS (2002). The alpha9/alpha10-containing nicotinic ACh receptor is directly modulated by opioid peptides, endomorphin-1, and dynorphin B, proposed efferent cotransmitters in the inner ear. *Mol Cell Neurosci*. 20:695-711.

Liu Y, and Brehm P (1993). Expression of subunit-omitted mouse nicotinic acetylcholine receptors in Xenopus laevis oocytes. *J Physiol*. 470:349-363.

Lu L, Timofeyev V, Li N, Rafizadeh S, Singapuri A, Harris TR, and Chiamvimonvat N (2009). Alpha-actinin2 cytoskeletal protein is required for the functional membrane localization of a Ca2+-activated K+ channel (SK2 channel). *Proc Natl Acad Sci U S A*. 106:18402-18407.

Lu L, Zhang Q, Timofeyev V, Zhang Z, Young JN, Shin HS, Knowlton AA, and Chiamvimonvat N (2007). Molecular coupling of a Ca2+-activated K+ channel to L-type Ca2+ channels via alpha-actinin2. *Circ Res*. 100:112-120.

Luebke AE, and Foster PK (2002). Variation in inter-animal susceptibility to noise damage is associated with alpha 9 acetylcholine receptor subunit expression level. *J Neurosci*. 22:4241-4247.

Madhavan R, Gong ZL, Ma JJ, Chan AW, and Peng HB (2009). The function of cortactin in the clustering of acetylcholine receptors at the vertebrate neuromuscular junction. *PLoS One*. 4:e8478.

Maison SF, Luebke AE, Liberman MC, and Zuo J (2002). Efferent protection from acoustic injury is mediated via alpha9 nicotinic acetylcholine receptors on outer hair cells. *J Neurosci*. 22:10838-10846.

Maison SF, Parker LL, Young L, Adelman JP, Zuo J, and Liberman MC (2007). Overexpression of SK2 channels enhances efferent suppression of cochlear

responses without enhancing noise resistance. *J Neurophysiol*. 97:2930-2936.

Manley GA, Gleich, O., Kaiser, A., Brix, J. (1989). Functional differentiation of sensory cells in the avian auditory periphery. *J Comp Physiol A Neuroethol Sens Neural Behav Physiol*. 164:289-296.

Marcotti W, Johnson SL, and Kros CJ (2004). A transiently expressed SK current sustains and modulates action potential activity in immature mouse inner hair cells. *J Physiol*. 560:691-708.

Martin AR, and Fuchs PA (1992). The dependence of calcium-activated potassium currents on membrane potential. *Proceedings. Biological sciences / The Royal Society*. 250:71-76.

Martinez MC, Ochiishi T, Majewski M, and Kosik KS (2003). Dual regulation of neuronal morphogenesis by a delta-catenin-cortactin complex and Rho. *J Cell Biol*. 162:99-111.

Matthews TM, Duncan RK, Zidanic M, Michael TH, and Fuchs PA (2005). Cloning and characterization of SK2 channel from chicken short hair cells. *J Comp Physiol A Neuroethol Sens Neural Behav Physiol*. 191:491-503.

McKillop WM, Barrett JW, Pasternak SH, Chan BM, and Dekaban GA (2009). The extracellular domain of CD11d regulates its cell surface expression. *Journal of leukocyte biology*. 86:851-862.

Merrill MA, Malik Z, Akyol Z, Bartos JA, Leonard AS, Hudmon A, Shea MA, and Hell JW (2007). Displacement of alpha-actinin from the NMDA receptor NR1 C0 domain By Ca2+/calmodulin promotes CaMKII binding. *Biochemistry*. 46:8485-8497.

Millake DB, Blanchard AD, Patel B, and Critchley DR (1989). The cDNA sequence of a human placental alpha-actinin. *Nucleic Acids Res*. 17:6725.

Mogensen MM, Tucker JB, Mackie JB, Prescott AR, and Nathke IS (2002). The adenomatous polyposis coli protein unambiguously localizes to microtubule plus ends and is involved in establishing parallel arrays of microtubule bundles in highly polarized epithelial cells. *J Cell Biol*. 157:1041-1048.

Morley BJ, and Simmons DD (2002). Developmental mRNA expression of the alpha10 nicotinic acetylcholine receptor subunit in the rat cochlea. *Brain research. Developmental brain research*. 139:87-96.

Murthy V, Maison SF, Taranda J, Haque N, Bond CT, Elgoyhen AB, Adelman JP, Liberman MC, and Vetter DE (2009a). SK2 channels are required for function and long-term survival of efferent synapses on mammalian outer hair cells. *Mol Cell Neurosci*. 40:39-49.

Murthy V, Taranda J, Elgoyhen AB, and Vetter DE (2009b). Activity of nAChRs containing alpha9 subunits modulates synapse stabilization via bidirectional signaling programs. *Dev Neurobiol*. 69:931-949.

Murugasu E, and Russell IJ (1996). The effect of efferent stimulation on basilar membrane displacement in the basal turn of the guinea pig cochlea. *J Neurosci*. 16:325-332.

Naisbitt S, Kim E, Tu JC, Xiao B, Sala C, Valtschanoff J, Weinberg RJ, Worley PF, and Sheng M (1999). Shank, a novel family of postsynaptic density proteins that binds to the NMDA receptor/PSD-95/GKAP complex and cortactin. *Neuron*. 23:569-582.

Nathke I (2006). Cytoskeleton out of the cupboard: colon cancer and cytoskeletal changes induced by loss of APC. *Nat Rev Cancer*. 6:967-974.

Ngo-Anh TJ, Bloodgood BL, Lin M, Sabatini BL, Maylie J, and Adelman JP (2005). SK channels and NMDA receptors form a Ca2+-mediated feedback loop in dendritic spines. *Nat Neurosci*. 8:642-649.

Nie L, Song H, Chen MF, Chiamvimonvat N, Beisel KW, Yamoah EN, and Vazquez AE (2004). Cloning and expression of a small-conductance Ca(2+)-activated K+ channel from the mouse cochlea: coexpression with alpha9/alpha10 acetylcholine receptors. *J Neurophysiol*. 91:1536-1544.

Nishimura W, Yao I, Iida J, Tanaka N, and Hata Y (2002). Interaction of synaptic scaffolding molecule and Beta -catenin. *J Neurosci*. 22:757-765.

Norris CH, and Guth PS (1974). The release of acetylcholine (ACH) by the crossed olivo-cochlear bundle (COCB). *Acta Otolaryngol*. 77:318-326.

O'Kelly I, Butler MH, Zilberberg N, and Goldstein SA (2002). Forward transport. 14-3-3 binding overcomes retention in endoplasmic reticulum by dibasic signals. *Cell*. 111:577-588.

Ofsie MS, Hennig AK, Messana EP, and Cotanche DA (1997). Sound damage and gentamicin treatment produce different patterns of damage to the efferent innervation of the chick cochlea. *Hear Res*. 113:207-223.

Oliver D, He DZ, Klocker N, Ludwig J, Schulte U, Waldegger S, Ruppersberg JP, Dallos P, and Fakler B (2001a). Intracellular anions as the voltage sensor of prestin, the outer hair cell motor protein. *Science*. 292:2340-2343.

Oliver D, Klocker N, Schuck J, Baukrowitz T, Ruppersberg JP, and Fakler B (2000). Gating of Ca2+-activated K+ channels controls fast inhibitory synaptic transmission at auditory outer hair cells. *Neuron*. 26:595-601.

Oliver D, Ludwig J, Reisinger E, Zoellner W, Ruppersberg JP, and Fakler B (2001b). Memantine inhibits efferent cholinergic transmission in the cochlea by blocking nicotinic acetylcholine receptors of outer hair cells. *Molecular pharmacology*. 60:183-189.

Osman AA, Schrader AD, Hawkes AJ, Akil O, Bergeron A, Lustig LR, and Simmons DD (2008). Muscle-like nicotinic receptor accessory molecules in sensory hair cells of the inner ear. *Mol Cell Neurosci*. 38:153-169.

Peng HB, Xie H, and Dai Z (1997). Association of cortactin with developing neuromuscular specializations. *J Neurocytol*. 26:637-650.

Plazas PV, Katz E, Gomez-Casati ME, Bouzat C, and Elgoyhen AB (2005). Stoichiometry of the alpha9alpha10 nicotinic cholinergic receptor. *J Neurosci*. 25:10905-10912.

Pujol R, and Carlier E (1982). Cochlear synaptogenesis after sectioning the efferent bundle. *Brain Res*. 255:151-154.

Rajan R (1990). Electrical stimulation of the inferior colliculus at low rates protects the cochlea from auditory desensitization. *Brain Res*. 506:192-204.

Rajan S, Preisig-Muller R, Wischmeyer E, Nehring R, Hanley PJ, Renigunta V, Musset B, Schlichthorl G, Derst C, Karschin A, and Daut J (2002). Interaction with 14-3-3 proteins promotes functional expression of the potassium channels TASK-1 and TASK-3. *J Physiol*. 545:13-26.

Rebillard M, and Pujol R (1983). Innervation of the chicken basilar papilla during its development. *Acta Otolaryngol*. 96:379-388.

Reiter ER, and Liberman MC (1995). Efferent-mediated protection from acoustic overexposure: relation to slow effects of olivocochlear stimulation. *J Neurophysiol*. 73:506-514.

Ren Y, Barnwell LF, Alexander JC, Lubin FD, Adelman JP, Pfaffinger PJ, Schrader LA, and Anderson AE (2006). Regulation of surface localization of the small conductance Ca2+-activated potassium channel, Sk2, through direct phosphorylation by cAMP-dependent protein kinase. *J Biol Chem*. 281:11769-11779.

Ricci AJ, Crawford AC, and Fettiplace R (2000). Active hair bundle motion linked to fast transducer adaptation in auditory hair cells. *J Neurosci*. 20:7131-7142.

Rosenberg MM, Yang F, Giovanni M, Mohn JL, Temburni MK, and Jacob MH (2008). Adenomatous polyposis coli plays a key role, in vivo, in coordinating assembly of the neuronal nicotinic postsynaptic complex. *Mol Cell Neurosci*. 38:138-152.

Rosenberg MM, Yang F, Mohn JL, Storer EK, and Jacob MH (2010). The postsynaptic adenomatous polyposis coli (APC) multiprotein complex is required for localizing neuroligin and neurexin to neuronal nicotinic synapses in vivo. *J Neurosci*. 30:11073-11085.

Roux I, Wersinger E, McIntosh JM, Fuchs PA, and Glowatzki E (2011). Onset of cholinergic efferent synaptic function in sensory hair cells of the rat cochlea. *J Neurosci*. 31:15092-15101.

Ryan A, and Dallos P (1975). Effect of absence of cochlear outer hair cells on behavioural auditory threshold. *Nature*. 253:44-46.

Sailer CA, Hu H, Kaufmann WA, Trieb M, Schwarzer C, Storm JF, and Knaus HG (2002). Regional differences in distribution and functional expression of small-conductance Ca2+-activated K+ channels in rat brain. *J Neurosci*. 22:9698-9707.

Sailer CA, Kaufmann WA, Marksteiner J, and Knaus HG (2004). Comparative immunohistochemical distribution of three small-conductance Ca2+-activated potassium channel subunits, SK1, SK2, and SK3 in mouse brain. *Mol Cell Neurosci*. 26:458-469.

Saito K (1980). Fine structure of the sensory epithelium of the guinea pig organ of Corti: afferent and efferent synapses of hair cells. *Journal of ultrastructure research*. 71:222-232.

Saito K (1983). Fine structure of the sensory epithelium of guinea-pig organ of Corti: subsurface cisternae and lamellar bodies in the outer hair cells. *Cell Tissue Res*. 229:467-481.

Schaechinger TJ, and Oliver D (2007). Nonmammalian orthologs of prestin (SLC26A5) are electrogenic divalent/chloride anion exchangers. *Proc Natl Acad Sci U S A*. 104:7693-7698.

Scheffer D, Sage C, Plazas PV, Huang M, Wedemeyer C, Zhang DS, Chen ZY, Elgoyhen AB, Corey DP, and Pingault V (2007). The alpha1 subunit of nicotinic acetylcholine receptors in the inner ear: transcriptional regulation by ATOH1 and co-expression with the gamma subunit in hair cells. *J Neurochem*. 103:2651-2664.

Schumacher MA, Rivard AF, Bachinger HP, and Adelman JP (2001). Structure of the gating domain of a Ca2+-activated K+ channel complexed with Ca2+/calmodulin. *Nature*. 410:1120-1124.

Shimomura A, Ohkuma M, Iizuka-Kogo A, Kohu K, Nomura R, Miyachi E, Akiyama T, and Senda T (2007). Requirement of the tumour suppressor APC for the clustering of PSD-95 and AMPA receptors in hippocampal neurons. *Eur J Neurosci*. 26:903-912.

Silverman JB, Restituito S, Lu W, Lee-Edwards L, Khatri L, and Ziff EB (2007). Synaptic anchorage of AMPA receptors by cadherins through neural plakophilin-related arm protein AMPA receptor-binding protein complexes. *J Neurosci*. 27:8505-8516.

Simmons DD, Mansdorf NB, and Kim JH (1996). Olivocochlear innervation of inner and outer hair cells during postnatal maturation: evidence for a waiting period. *J Comp Neurol*. 370:551-562.

Simmons DD, and Morley BJ (1998). Differential expression of the alpha 9 nicotinic acetylcholine receptor subunit in neonatal and adult cochlear hair cells. *Brain research. Molecular brain research*. 56:287-292.

Sjoblom B, Salmazo A, and Djinovic-Carugo K (2008). Alpha-actinin structure and regulation. *Cell Mol Life Sci*. 65:2688-2701.

Slep KC, Rogers SL, Elliott SL, Ohkura H, Kolodziej PA, and Vale RD (2005). Structural determinants for EB1-mediated recruitment of APC and spectraplakins to the microtubule plus end. *J Cell Biol*. 168:587-598.

Song L, and Santos-Sacchi J (2010). Conformational state-dependent anion binding in prestin: evidence for allosteric modulation. *Biophys J*. 98:371-376.

Sottocornola B, Visconti S, Orsi S, Gazzarrini S, Giacometti S, Olivari C, Camoni L, Aducci P, Marra M, Abenavoli A, Thiel G, and Moroni A (2006). The potassium channel KAT1 is activated by plant and animal 14-3-3 proteins. *J Biol Chem*. 281:35735-35741.

Sridhar TS, Brown MC, and Sewell WF (1997). Unique postsynaptic signaling at the hair cell efferent synapse permits calcium to evoke changes on two time scales. *J Neurosci*. 17:428-437.

Sridhar TS, Liberman MC, Brown MC, and Sewell WF (1995). A novel cholinergic "slow effect" of efferent stimulation on cochlear potentials in the guinea pig. *J Neurosci*. 15:3667-3678.

Stackman RW, Hammond RS, Linardatos E, Gerlach A, Maylie J, Adelman JP, and Tzounopoulos T (2002). Small conductance Ca2+-activated K+ channels modulate synaptic plasticity and memory encoding. *J Neurosci*. 22:10163-10171.

Stan A, Pielarski KN, Brigadski T, Wittenmayer N, Fedorchenko O, Gohla A, Lessmann V, Dresbach T, and Gottmann K (2010). Essential cooperation of N-cadherin and neuroligin-1 in the transsynaptic control of vesicle accumulation. *Proc Natl Acad Sci U S A*. 107:11116-11121.

Stocker M (2004). Ca(2+)-activated K+ channels: molecular determinants and function of the SK family. *Nat Rev Neurosci*. 5:758-770.

Stocker M, Krause M, and Pedarzani P (1999). An apamin-sensitive Ca2+-activated K+ current in hippocampal pyramidal neurons. *Proc Natl Acad Sci U S A*. 96:4662-4667.

Strassmaier T, Bond CT, Sailer CA, Knaus HG, Maylie J, and Adelman JP (2005). A novel isoform of SK2 assembles with other SK subunits in mouse brain. *J Biol Chem*. 280:21231-21236.

Su LK, Kinzler KW, Vogelstein B, Preisinger AC, Moser AR, Luongo C, Gould KA, and Dove WF (1992). Multiple intestinal neoplasia caused by a mutation in the murine homolog of the APC gene. *Science*. 256:668-670.

Sul B, and Iwasa KH (2009). Effectiveness of hair bundle motility as the cochlear amplifier. *Biophys J*. 97:2653-2663.

Sumita K, Sato Y, Iida J, Kawata A, Hamano M, Hirabayashi S, Ohno K, Peles E, and Hata Y (2007). Synaptic scaffolding molecule (S-SCAM) membrane-associated guanylate kinase with inverted organization (MAGI)-2 is associated with cell adhesion molecules at inhibitory synapses in rat hippocampal neurons. *J Neurochem*. 100:154-166.

Sziklai I, Szonyi M, and Dallos P (2001). Phosphorylation mediates the influence of acetylcholine upon outer hair cell electromotility. *Acta Otolaryngol*. 121:153-156.

Takahashi K, Thalmann, I., Thalmann, R. (1989). Very high levels of calmodulin (CAL) in outer hair cells (OHC) of organ of Corti (OC). *J. Acoust. Soc. Am.* 85:S31.

Takasaka T, and Smith CA (1971). The structure and innervation of the pigeon's basilar papilla. *Journal of ultrastructure research*. 35:20-65.

Tan X, Pecka JL, Tang J, Okoruwa OE, Zhang Q, Beisel KW, and He DZ (2011). From zebrafish to mammal: functional evolution of prestin, the motor protein of cochlear outer hair cells. *J Neurophysiol*. 105:36-44.

Tanaka K, and Smith CA (1978). Structure of the chicken's inner ear: SEM and TEM study. *Am J Anat*. 153:251.

Taranda J, Ballestero JA, Hiel H, de Souza FS, Wedemeyer C, Gomez-Casati ME, Lipovsek M, Vetter DE, Fuchs PA, Katz E, and Elgoyhen AB (2009a). Constitutive expression of the alpha10 nicotinic acetylcholine receptor subunit fails to maintain cholinergic responses in inner hair cells after the onset of hearing. *J Assoc Res Otolaryngol*. 10:397-406.

Taranda J, Maison SF, Ballestero JA, Katz E, Savino J, Vetter DE, Boulter J, Liberman MC, Fuchs PA, and Elgoyhen AB (2009b). A point mutation in the

hair cell nicotinic cholinergic receptor prolongs cochlear inhibition and enhances noise protection. *PLoS biology*. 7:e18.

Temburni MK, Rosenberg MM, Pathak N, McConnell R, and Jacob MH (2004). Neuronal nicotinic synapse assembly requires the adenomatous polyposis coli tumor suppressor protein. *J Neurosci*. 24:6776-6784.

Tian L, Chen L, McClafferty H, Sailer CA, Ruth P, Knaus HG, and Shipston MJ (2006). A noncanonical SH3 domain binding motif links BK channels to the actin cytoskeleton via the SH3 adapter cortactin. *Faseb J*. 20:2588-2590.

Tian L, McClafferty H, Chen L, and Shipston MJ (2008). Reversible tyrosine protein phosphorylation regulates large conductance voltage- and calcium-activated potassium channels via cortactin. *J Biol Chem*. 283:3067-3076.

Tritsch NX, and Bergles DE (2010). Developmental regulation of spontaneous activity in the Mammalian cochlea. *J Neurosci*. 30:1539-1550.

Tsen G, Williams B, Allaire P, Zhou YD, Ikonomov O, Kondova I, and Jacob MH (2000). Receptors with opposing functions are in postsynaptic microdomains under one presynaptic terminal. *Nat Neurosci*. 3:126-132.

Uziel A, Romand R, and Marot M (1981). Development of cochlear potentials in rats. *Audiology : official organ of the International Society of Audiology*. 20:89-100.

Verbitsky M, Rothlin CV, Katz E, and Elgoyhen AB (2000). Mixed nicotinic-muscarinic properties of the alpha9 nicotinic cholinergic receptor. *Neuropharmacology*. 39:2515-2524.

Vetter DE, Katz E, Maison SF, Taranda J, Turcan S, Ballestero J, Liberman MC, Elgoyhen AB, and Boulter J (2007). The alpha10 nicotinic acetylcholine receptor subunit is required for normal synaptic function and integrity of the olivocochlear system. *Proc Natl Acad Sci U S A*. 104:20594-20599.

Vetter DE, Liberman MC, Mann J, Barhanin J, Boulter J, Brown MC, Saffiote-Kolman J, Heinemann SF, and Elgoyhen AB (1999). Role of alpha9 nicotinic ACh receptor subunits in the development and function of cochlear efferent innervation. *Neuron*. 23:93-103.

Waites GT, Graham IR, Jackson P, Millake DB, Patel B, Blanchard AD, Weller PA, Eperon IC, and Critchley DR (1992). Mutually exclusive splicing of calcium-binding domain exons in chick alpha-actinin. *J Biol Chem*. 267:6263-6271.

Walsh EJ, McGee J, McFadden SL, and Liberman MC (1998). Long-term effects of sectioning the olivocochlear bundle in neonatal cats. *J Neurosci*. 18:3859-3869.

Wang C, Wang HG, Xie H, and Pitt GS (2008). Ca2+/CaM controls Ca2+-dependent inactivation of NMDA receptors by dimerizing the NR1 C termini. *J Neurosci*. 28:1865-1870.

Wang J, Jing Z, Zhang L, Zhou G, Braun J, Yao Y, and Wang ZZ (2003). Regulation of acetylcholine receptor clustering by the tumor suppressor APC. *Nat Neurosci*. 6:1017-1018.

Warr WB, and Guinan JJ, Jr. (1979). Efferent innervation of the organ of corti: two separate systems. *Brain Res*. 173:152-155.

Watanabe T, Wang S, Noritake J, Sato K, Fukata M, Takefuji M, Nakagawa M, Izumi N, Akiyama T, and Kaibuchi K (2004). Interaction with IQGAP1 links APC to Rac1, Cdc42, and actin filaments during cell polarization and migration. *Developmental cell*. 7:871-883.

Weaver AM, Karginov AV, Kinley AW, Weed SA, Li Y, Parsons JT, and Cooper JA (2001). Cortactin promotes and stabilizes Arp2/3-induced actin filament network formation. *Curr Biol*. 11:370-374.

Wen Y, Eng CH, Schmoranzer J, Cabrera-Poch N, Morris EJ, Chen M, Wallar BJ, Alberts AS, and Gundersen GG (2004). EB1 and APC bind to mDia to stabilize microtubules downstream of Rho and promote cell migration. *Nat Cell Biol*. 6:820-830.

Wersinger E, and Fuchs PA (2010). Modulation of hair cell efferents. *Hear Res*.

Wersinger E, McLean WJ, Fuchs PA, and Pyott SJ (2010). BK channels mediate cholinergic inhibition of high frequency cochlear hair cells. *PLoS One*. 5:e13836.

Whitehead MC, and Morest DK (1985). The development of innervation patterns in the avian cochlea. *Neuroscience*. 14:255-276.

Williams BM, Temburni MK, Levey MS, Bertrand S, Bertrand D, and Jacob MH (1998). The long internal loop of the alpha 3 subunit targets nAChRs to subdomains within individual synapses on neurons in vivo. *Nat Neurosci*. 1:557-562.

Wilson JP (1980). Evidence for a cochlear origin for acoustic re-emissions, threshold fine-structure and tonal tinnitus. *Hear Res*. 2:233-252.

Winslow RL, and Sachs MB (1987). Effect of electrical stimulation of the crossed olivocochlear bundle on auditory nerve response to tones in noise. *J Neurophysiol*. 57:1002-1021.

Xia XM, Fakler B, Rivard A, Wayman G, Johnson-Pais T, Keen JE, Ishii T, Hirschberg B, Bond CT, Lutsenko S, Maylie J, and Adelman JP (1998).

Mechanism of calcium gating in small-conductance calcium-activated potassium channels. *Nature*. 395:503-507.

Xu Y, Tuteja D, Zhang Z, Xu D, Zhang Y, Rodriguez J, Nie L, Tuxson HR, Young JN, Glatter KA, Vazquez AE, Yamoah EN, and Chiamvimonvat N (2003). Molecular identification and functional roles of a Ca(2+)-activated K+ channel in human and mouse hearts. *J Biol Chem*. 278:49085-49094.

Yaffe MB (2002). How do 14-3-3 proteins work?-- Gatekeeper phosphorylation and the molecular anvil hypothesis. *FEBS letters*. 513:53-57.

Yanai H, Satoh K, Matsumine A, and Akiyama T (2000). The colorectal tumour suppressor APC is present in the NMDA-receptor-PSD-95 complex in the brain. *Genes Cells*. 5:815-822.

Yu N, and Zhao HB (2009). Modulation of outer hair cell electromotility by cochlear supporting cells and gap junctions. *PLoS One*. 4:e7923.

Yuan H, Michelsen K, and Schwappach B (2003). 14-3-3 dimers probe the assembly status of multimeric membrane proteins. *Curr Biol*. 13:638-646.

Yuhas WA, and Fuchs PA (1999). Apamin-sensitive, small-conductance, calcium-activated potassium channels mediate cholinergic inhibition of chick auditory hair cells. *Journal of comparative physiology. A, Sensory, neural, and behavioral physiology*. 185:455-462.

Zhang M, Kalinec GM, Urrutia R, Billadeau DD, and Kalinec F (2003). ROCK-dependent and ROCK-independent control of cochlear outer hair cell electromotility. *J Biol Chem*. 278:35644-35650.

Zheng J, Shen W, He DZ, Long KB, Madison LD, and Dallos P (2000). Prestin is the motor protein of cochlear outer hair cells. *Nature*. 405:149-155.

Zheng XY, Henderson D, Hu BH, Ding DL, and McFadden SL (1997a). The influence of the cochlear efferent system on chronic acoustic trauma. *Hear Res*. 107:147-159.

Zheng XY, Henderson D, McFadden SL, and Hu BH (1997b). The role of the cochlear efferent system in acquired resistance to noise-induced hearing loss. *Hear Res*. 104:191-203.

Zhou Y, Schopperle WM, Murrey H, Jaramillo A, Dagan D, Griffith LC, and Levitan IB (1999). A dynamically regulated 14-3-3, Slob, and Slowpoke potassium channel complex in Drosophila presynaptic nerve terminals. *Neuron*. 22:809-818.

Zidanic M (2002). Cholinergic innervation of the chick basilar papilla. *J Comp Neurol*. 445:159-175.

Zorrilla de San Martin J, Ballestero J, Katz E, Elgoyhen AB, and Fuchs PA (2007). Ryanodine is a positive modulator of acetylcholine receptor gating in cochlear hair cells. *J Assoc Res Otolaryngol*. 8:474-483.

Zuzarte M, Heusser K, Renigunta V, Schlichthorl G, Rinne S, Wischmeyer E, Daut J, Schwappach B, and Preisig-Muller R (2009). Intracellular traffic of the K+ channels TASK-1 and TASK-3: role of N- and C-terminal sorting signals and interaction with 14-3-3 proteins. *J Physiol*. 587:929-952.